

Liquid Chromatography: Injection Broadening in Ion Chromatography and Retention Properties  
of a New Hydrophilic Interaction Liquid Chromatography Stationary Phase

by

Ya Zhang

A thesis submitted in partial fulfillment of the requirements for the degree of

Master of Science

Department of Chemistry  
University of Alberta

© Ya Zhang, 2014

## **ABSTRACT**

Ion Chromatography (IC) is a powerful technique in the separation and analysis of inorganic ions and small charged organic molecules. Meanwhile, Hydrophilic Interaction Liquid Chromatography (HILIC) enables the separation of polar hydrophilic compounds. Although their retention mechanisms are different, the same goal applies. Chromatographers want a fast and thorough separation. This thesis focuses on improving separations in both modes.

Injection solvent mismatch in Reversed Phase Liquid Chromatography (RPLC) leads to peak broadening and even distortion. In this thesis, systematic studies on IC columns showed that the characteristics of injection solvent mismatch broadening are very different than in RPLC. Also, IC is much more tolerant to high matrix concentration. The sensitivity parameter for evaluating RPLC injection solvent response was applied in the IC column studied for the comparison and can be further used in evaluating other IC columns. In modern IC, suppressors are widely used. Injection system peaks are usually neglected because they are eliminated by the suppressor. However this thesis showed that the system peak strongly affects the nearby analyte peak shape and retention.

Porous Graphitic Carbon (PGC) is popular in some RPLC applications due to its excellent pH and temperature stability. This stability would also be attractive

for HILIC applications. However, the hydrophobic character of PGC makes it incompatible with HILIC separations. In this thesis, PGC was converted into a hydrophilic phase by attaching acetanilide to the surface. The new Amide-PGC shows unique selectivity among 37 stationary phases under HILIC mode. The thesis demonstrates its potential in separating nucleobases, carboxylic acids and pharmaceuticals. Retention is shown to be due to both HILIC partitioning and adsorption on the PGC surface.

In summary, this thesis improves liquid chromatography in two aspects: IC separations through an understanding of injection broadening; and HILIC through the development of a new stationary phase which enables unique HILIC selectivity.

## **PREFACE**

The experiments in Chapter 2 and 3 were designed by myself with the advice from my supervisor Prof. C. A. Lucy. C. D. Iverson contributed to the PGC separation understanding part in Chapter 3. I was responsible for conducting experiments, collecting results, data analysis, and manuscript composition. Prof. C. A. Lucy was involved in chapter revision.

Chapter 2 has been submitted as “Effect of injection matrix concentration on peak shape and separation efficiency in ion chromatography” by Y. Zhang and C. A. Lucy to Journal of Chromatography A.

## **ACKNOWLEDGEMENTS**

I would like to thank my supervisor, Dr. Charles A. Lucy, for his guidance, patience and encouragement in my research in the University of Alberta. The advices on research as well as career planning are very useful.

I also want to thank my lab mates for their help. Dr. M. F. Wahab helped me a lot with IC instrument while Dr. M. E. A. Ibrahim helped me with the HILIC instrument. I want to thanks Chad Iverson for his help in the HILIC stationary phase synthesis. Thanks also to Di Wu and Lei Pei for a good time in the lab. Finally thank you to my committee, for your guidance during my degree and on my thesis: Dr. James Harynuk, Dr. Michael J. Serpe and Dr. John C. Vederas.

The funding is from Natural Sciences and Engineering Research Council of Canada (NSERC), Dionex (Thermo Fisher) and the University of Alberta. I am grateful for the help from the machine shop, glass shop, Analytical and Instrumentation Lab, and IT support.

Thank you to my families for the emotional support and encouragement. Xiaoyu, Dalin and Hao, you are the reason why I want to be a better me.

# TABLE OF CONTENTS

<b>CHAPTER ONE: Introduction</b> .....	1
1.1 Motivation and Thesis Overview .....	1
1.2 Basic Chromatography .....	3
1.2.1 Chromatographic Parameters .....	5
1.3 Peak Broadening.....	10
1.3.1 Van Deemter Equation .....	11
1.3.2 Extra Column Band Broadening .....	16
1.4 Ion Chromatography.....	22
1.4.1 Instrumentation.....	23
1.4.2 Ion Exchange Separation Principles.....	27
1.5 Hydrophilic Interaction Liquid Chromatography.....	28
1.5.1 Principle of Retention.....	30
1.5.2 Stationary Phase Types .....	31
1.6 Overview of Thesis Chapters .....	34
1.7 References .....	35
<b>CHAPTER TWO: Injection Matrix Effects on Separation in Ion Chromatography</b> .....	40

2.1 Introduction .....	40
2.2 Experimental .....	42
2.2.1 Instrumentation.....	42
2.2.2 Chemicals .....	43
2.2.3 Solution Preparation .....	44
2.3 Data Analysis Method .....	45
2.3.1 RPLC Data Analysis Method .....	45
2.3.2 Statistical Moment Analysis.....	45
2.4 Results .....	47
2.4.1 Injection Solvent Effects in RPLC .....	47
2.4.2 Injected eluent effects in IC.....	56
2.5 Discussion .....	65
2.6 Conclusions .....	71
2.7 References .....	72
<b>CHAPTER THREE: Amide Carbon HILIC Stationary Phase .....</b>	<b>76</b>
3.1 Introduction .....	76
3.2 Experimental .....	79
3.2.1 Chemicals .....	79
3.2.2 Apparatus.....	82

3.2.3 Synthesis of Amide-PGC Stationary Phase.....	83
3.2.4 Column Packing and Treatment.....	87
3.2.5 Standard, Sample and Eluent Preparation.....	89
3.3 Results and Discussion.....	91
3.3.1 Surface Characterization of Amide-PGC.....	95
3.3.2 HILIC Behavior of Amide-PGC.....	99
3.3.3 Organic Acids Separation.....	102
3.3.4 Selectivity Plot.....	105
3.3.5 Mechanism of HILIC Retention on Amide-PGC.....	113
3.3.6 Attenuated RPLC Separation.....	115
3.4 Conclusions.....	118
3.5 References.....	118
<b>CHAPTER FOUR: Conclusions.....</b>	<b>123</b>
4.1 Conclusions and Perspectives.....	123
4.2 References.....	125

## LIST OF FIGURES

1.1	Schematic of an HPLC system	4
1.2	Sample Chromatogram	6
1.3	Asymmetry measurement	9
1.4	Eddy diffusion broadening	12
1.5	van Deemter plot of plate height vs linear velocity	15
1.6	Volume and mass overloading effects due to injection	18
1.7	Schematic viscous fingering effect	20
1.8	Representative Ion Chromatography (IC) system	24
1.9	Suppressor scheme	26
1.10	Scheme of HILIC interactions	29
2.1	Effects of injection solvent on RPLC separations	48
2.2	Effects of injection solvent on the retention times of RPLC analytes	49
2.3	Effects of injection solvent on the efficiencies of RPLC analytes	51
2.4	Effects of injection solvent on the asymmetries of RPLC analytes	52
2.5	Effects of injection matrix concentration on the IC separations	57
2.6	Effects of injection matrix concentration on the center of gravities of IC analytes	59

2.7	Effects of injection matrix concentration on the variances of IC analytes	60
2.8	Effects of injection matrix concentration on the efficiencies of IC analytes	61
2.9	Effects of injection matrix concentration on the asymmetries of IC analytes	62
2.10	Injection system peaks under different injection matrix concentration conditions	69
3.1	Synthetic route for Amide-PGC stationary phase	84
3.2	Apparatus for removing un-modified PGC particles	86
3.3	Column packing apparatus	88
3.4	Scheme for synthesizing Amide-PGC via diazonium reaction	92
3.5	Comparison of PGC and Amide-PGC on wettability	93
3.6	High resolution O <sub>1s</sub> XPS spectrum of the Amide-PGC phase	97
3.7	Separations of uracil, cytosine and thymidine on the Amide-PGC column	99
3.8	Retention factor of uracil, cytosine and thymidine on the Amide-PGC as a function of %ACN	100
3.9	Comparison of the separation of six aromatic carboxylic acids on eight commercial columns and two homemade HILIC carbon columns	102
3.10	Hydrophilicity vs. ion exchange selectivity plot	105
3.11	Retention mechanism study	113
3.12	Attenuated RPLC separations	116

## LIST OF TABLES

1.1	Chemical structures of selected types of HILIC stationary phase	33
2.1	Measured sensitivity for the ACE 5C18 RPLC column	55
2.2	Measured sensitivity for AS 23 anion exchange column	65
3.1	Structures of compounds used in Chapter 3	80
3.2	Elemental analysis of PGC and Amide-PGC	95
3.3	X-Ray Photoelectron Spectroscopy of Amide-PGC	96
3.4	Characteristics of HILIC columns characterized	106

## LIST OF ABBREVIATIONS AND SYMBOLS

ACN	Acetonitrile
$A_s$	Asymmetry
A term	Multiple paths broadening
AU	Absorbance units
BEH	Ethylene bridged hybrids
B term	Longitudinal diffusion
BTMA	Benzyltrimethylammonium ion
C	Concentration
$^{\circ}\text{C}$	Celsius
C term	Mass transfer resistance
$D_M$	Diffusion coefficient in the mobile phase
$D_S$	Diffusion coefficient in the stationary phase
$d_c$	diameter of the channels in the packed column
$d_p$	Particle diameter
$E^{y-}$	Anion with y- charge
ERLIC	Electrostatic Repulsion Hydrophilic Interaction Liquid Chromatography
H	Plate height

h	hour(s)
HILIC	Hydrophilic interaction liquid chromatography
HPLC	High performance liquid chromatography
$h_p$	Peak height
i	Current
$i_m$	Analyte i in the mobile phase
$i_s$	Analyte i in the stationary phase
IC	Ion chromatography
i.d.	Inner diameter
k	Retention factor
L	Column length
LC	Liquid chromatography
m	Weight
mM	Millimolar
min	minute(s)
mA	Milliampere
N	Plate number
NPLC	Normal phase liquid chromatography

Pa	Pascal
PEEK	Polyether ether ketone
PGC	Porous graphitic carbon
PREG	Polar retention effect on graphite
psi	Pounds per square inch
Q	Effective column capacity
$R_s$	Resolution
RPLC	Reversed phase liquid chromatography
$t_R$	Retention time
$t_0$	Dead time
U	Voltage
u	Linear velocity
UHMWPE	Ultrahigh molecular weight polyethylene
UV	Ultraviolet
$V_s$	Volume of stationary phase
$V_m$	Volume of mobile phase inside the column
$W_b$	Baseline width
$W_h$	Half height width

$\mu\text{m}$	Micrometer(s)
$\alpha$	Selectivity
$\lambda$	Packing factor
$\sigma$	Conductivity
$\sigma^2$	Peak variance
$\gamma$	Obstruction factor
$\varphi$	Volume fraction of strong eluent

# **CHAPTER ONE: Introduction**

## **1.1 Motivation and Thesis Overview**

Liquid chromatography (LC) was first introduced by Tswett in 1903 [1]. After 63 years development, Horvath et al. [2] introduced High Performance Liquid Chromatography (HPLC). An HPLC column is packed with small microparticles. HPLC instrumentation uses a high pressure pump to force eluent through the column. Each analyte interacts differently with the packed material, resulting in the separation. HPLC is a powerful separation technique which has been widely used in separating complicated mixtures [3-6]. There are many modes of liquid chromatography. Reversed Phase Liquid Chromatography (RPLC) is the most widely used one for separating non-polar to moderately polar analytes [7]. Normal Phase Liquid Chromatography (NPLC) is mainly used for separating polar analytes which have limited water-solubility [8]. Hydrophilic Interaction Liquid Chromatography (HILIC) is excellent in separating polar compounds which dissolve in water [5,9]. Ion-Exchange Chromatography (IC) is for the separation of inorganic and small organic ions [6].

No matter which type of liquid chromatography is chosen for a separation, the ultimate goal is the same: the fast separation of as many components as possible. The sample usually contains many analytes. Each analyte component is retained

on the column in a characteristic time. The overall time required for a separation depends on how long these components spend in the column. For identification and quantification these components must be separated from each other. Thus, method development and new stationary phase development are critical in to achieving fast and complete separations.

In this thesis, Chapter 2 investigates the injection matrix effect on ion chromatographic (IC) separations. Real samples may contain high concentrations of interfering matrix ions. Many IC protocols recommend diluting the sample to deal with high matrix concentration [10]. The dilution step takes time and sacrifices analyte signal. Chapter 2 investigates the effect of sample matrix (carbonate) on injection induced broadening. Chapter 2 provides a guide for the degree of dilution needed prior to IC analysis. The time required for sample pre-treatment will be saved.

Unique selectivity is another desire for liquid chromatographic separation. All analytes cannot be separated on one universal column. Using the right column for sample analysis is very important. Different stationary phases provide different selectivity. Chapter 3 discusses the development of a new porous graphitic carbon (PGC) based amide stationary phase for HILIC separations. The Amide-PGC provides unique selectivity relative to other HILIC stationary phases.

Chapter 4 summarizes the improvement this thesis made on separations and future perspectives.

## 1.2 Basic Chromatography

The interactions between analytes and the mobile phase and those between analytes and the stationary phase are the foundation for the theory of chromatographic separations. The mobile phase, also called the eluent, refers to a fluid which carries the sample through the column. In liquid chromatography the stationary phase is most commonly a packed particle bed. Different analytes have different affinities with the mobile phase. They also have different affinities for the stationary phase. These affinities include but are not limited to: partitioning; adsorption; ion exchange, etc. The analyte which has greater affinity for the stationary phase is eluted out of the column later.

**Fig. 1.1** shows the basic components of an HPLC system. The mobile phase (eluent) is pumped by a high pressure pump into the column. The injection valve is used to inject a fixed volume (e.g., 20  $\mu\text{L}$ ) of sample solution into the mobile phase. The injection can be done either manually or by autosampler (not shown here). Manual injection uses a handheld syringe to fill the injection loop. An autosampler uses robotics to inject sample solutions in a precise and reproducible volume [11]. The column contains the stationary phase packing. It is where the

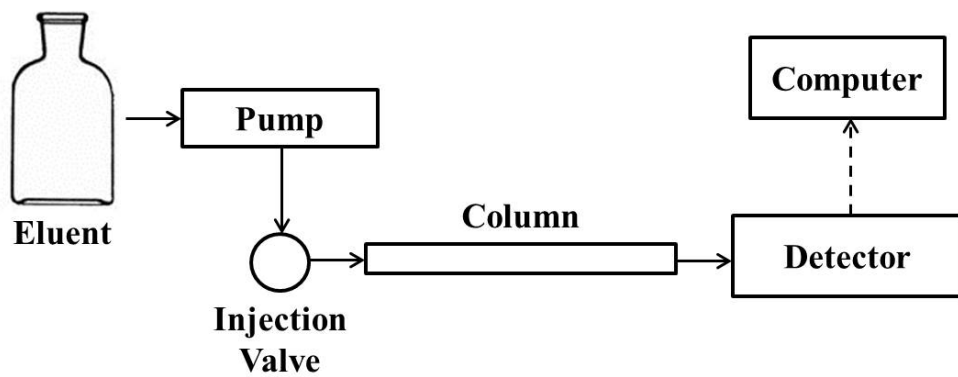


**Figure 1.1** Schematic of an HPLC system. Adapted from [12].

analytes separate due to their interactions with the mobile phase and stationary phase. The detector detects the separated analytes after they come out of column. In Chapter 2, conductivity will be used for detection and in Chapter 3 I use UV absorbance. The computer receives and collects the signal from the detector, and is used to analyze the data.

### 1.2.1 Chromatographic Parameters [11,12]

The thermodynamic equilibrium of an analyte between the mobile phase and the stationary phase is the fundamental principle of separation. Within the column analyte  $i$  will be distributed between the two phases.  $i_m$  refers the portion of analyte in the mobile phase ( $m$ ) whereas  $i_s$  refers to the portion inside the stationary phase ( $s$ ). The equilibrium is expressed as:

$$i_m \rightleftharpoons i_s \quad (1.1)$$

The retention factor ( $k_i$ ) is defined as the mole ratio of analyte  $i$  in the stationary phase vs. that in the mobile phase:

$$k_i = \frac{C_s V_s}{C_m V_m} \quad (1.2)$$

where  $C_s$  is the concentration of analyte in the stationary phase and  $C_m$  is the concentration of analyte in the mobile phase.  $V_s$  is the volume of stationary phase and  $V_m$  is the volume of mobile phase inside the column.

As shown in **Fig. 1.2**, retention time  $t_R$  is the time the analyte spends in the

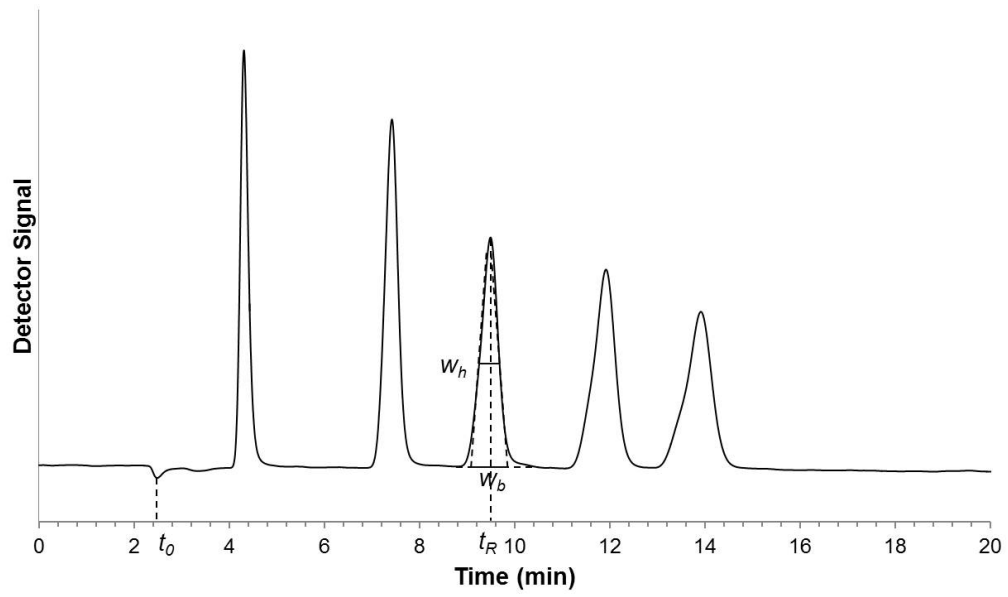


**Figure 1.2** Sample chromatogram. Adapted from [12].

column. The dead time  $t_0$  is the time required for a non-retained component to pass through the column. Thus, the retention factor can be expressed as:

$$k_i = \frac{t_R - t_0}{t_0} \quad (1.3)$$

The peaks in **Fig. 1.2** are different in sharpness. Efficiency or theoretical plate number ( $N$ ) is used to define the sharpness of an analyte peak. Assuming the peak is Gaussian, we have:

$$N = 5.54 \left( \frac{t_R}{W_h} \right)^2 = 16 \left( \frac{t_R}{W_b} \right)^2 \quad (1.4)$$

where  $W_h$  is the width at half height and  $W_b$  is the baseline width.

The number of theoretical plates depends on the column length. Plate height ( $H$ ) is used to eliminate the column length effect:

$$H = \frac{L}{N} \quad (1.5)$$

where  $L$  is the column length.

When dealing with multiple analytes, the separation factor ( $\alpha$ ) is used to describe the relative retention between two analytes. Assuming analyte  $j$  is more retained than analyte  $i$ , we have:

$$\alpha_{i,j} = \frac{k_j}{k_i} \quad (1.6)$$

Another parameter to deal with the separation power is resolution ( $R_S$ ):

$$R_S = \frac{t_{R,j} - t_{R,i}}{W_{b,AVG}} \quad (1.7)$$

where  $W_{b,AVG}$  is the average baseline width of two peaks.

Resolution can also be expressed as:

$$R_S = \left(\frac{\sqrt{N}}{4}\right) \left(\frac{k}{1+k}\right) \left(\frac{\alpha-1}{\alpha}\right) \quad (1.8)$$

where  $N$  is the efficiency,  $k$  is the retention factor and  $\alpha$  is the separation factor.

According to **Eq. 1.8**, we know that there are three ways to improve the resolution.

$R_S$  is proportional to the square root of  $N$ , which is related to the quality of the packing of the column, the stationary phase particle size and the flow rate.

Retention factor varies with analyte, and can be controlled by changing the eluent concentration or nature. If  $k = 0$ , the analyte elutes at the dead time. Under such

circumstances,  $R_S$  is zero, indicating that there is no separation. The term

$k/(k + 1)$  in **Eq. 1.8** will reach its maximum limit of 1 when  $k$  is very large,

however, at the cost of long separation times. Therefore it is recommended that

the retention range be  $0.5 < k < 10$ , as a compromise between resolution and

analysis time. Selectivity  $\alpha$  depends on the stationary phase chemistry and the

eluent type.

Not all analyte peaks are Gaussian. The asymmetry factor  $A_S$  is a parameter for evaluating whether the peak is symmetrical, tailing or fronting:

$$A_S = \frac{B}{A} \quad (1.9)$$

where  $A$  and  $B$  are the widths measured at 10% of peak height ( $h_p$ ) as shown in

**Fig. 1.3**. If the asymmetry factor is 1, the peak is symmetrical, but may not be

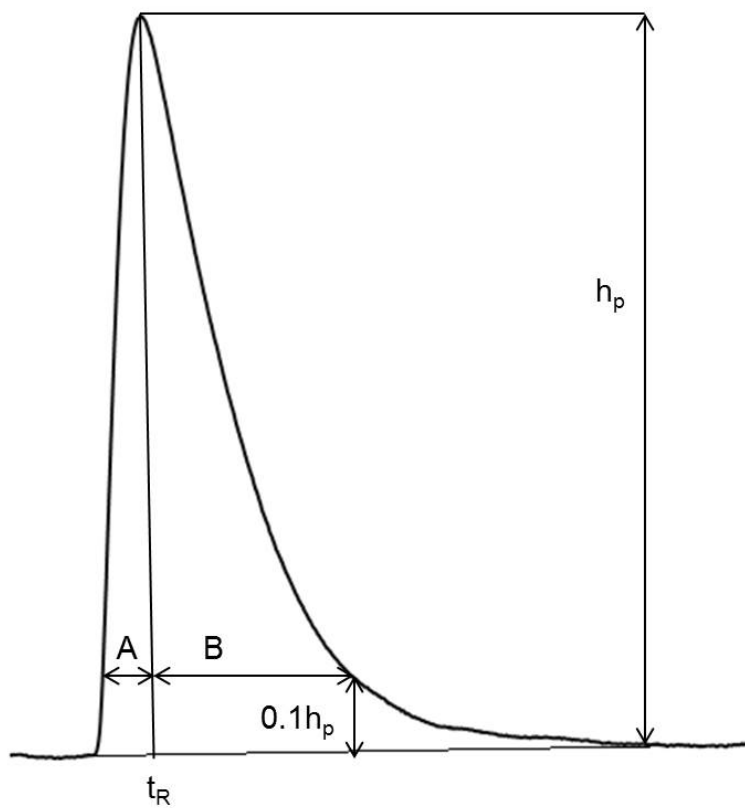


**Figure 1.3** Asymmetry measurement. Adapted from [11].

Gaussian. An asymmetry factor greater than 1 means the peak is tailing, while an  $A_S$  smaller than 1 refers to a fronting peak.

Under statistical moment analysis [13], asymmetry can also be defined by the nonparametric term:

$$A = \frac{\mu_1 - t_R}{\sqrt{\bar{\mu}_2}} \quad (1.10)$$

where  $\mu_1$  is the first statistical moment which is the peak centre of gravity,  $t_R$  is the retention time (peak maxima) of the current peak, and  $\bar{\mu}_2$  is the second centralized statistical moment which represents the peak variance. The parameter  $A$  is positive if the peak is tailing and negative if the peak is fronting (details in **Section 2.3.2**).

### 1.3 Peak Broadening

Ideally, after the separation inside the column, the resultant peaks should be very sharp. However, during and after injection of sample solution, band broadening happens, which results in peak broadening as shown in **Fig. 1.2**.

The statistical variance ( $\sigma^2$ ) of a peak is commonly used to describe the dispersion of a peak. A separation without any broadening has a zero variance.

Plate height ( $H$ ) can also be expressed as [12]:

$$H = \frac{\sigma^2}{L} \quad (1.11)$$

where  $L$  is the column length.

The smaller the variance is, the smaller the plate height. And eventually, the separation efficiency ( $N$ ) is bigger, meaning a sharp peak.

### 1.3.1 Van Deemter Equation

Van Deemter et al. [14] introduced the van Deemter equation to mathematically represent and summarize the three factors which cause band broadening inside the column. The three factors are: eddy diffusion ( $A$  term); longitudinal diffusion ( $B$  term); and resistance to mass transfer ( $C$  term). The plate height can be expressed as:

$$H = A + \frac{B}{u} + Cu \quad (1.12)$$

where  $u$  is the linear velocity of the mobile phase.

Eddy diffusion ( $A$ -term) describes the broadening caused by different flow paths of analyte molecules travelling along the column. As shown in **Fig 1.4**, analytes may follow paths through the column that are of different lengths. These different lengths lead to different times for individual analyte molecules to be eluted. Finally, different elution time results in band broadening.

The eddy diffusion is independent of flow rate. It depends on the packing factor ( $\lambda$ ) and particle size ( $d_p$ ), and is independent of linear velocity, as shown in **Eq. 1.12**.

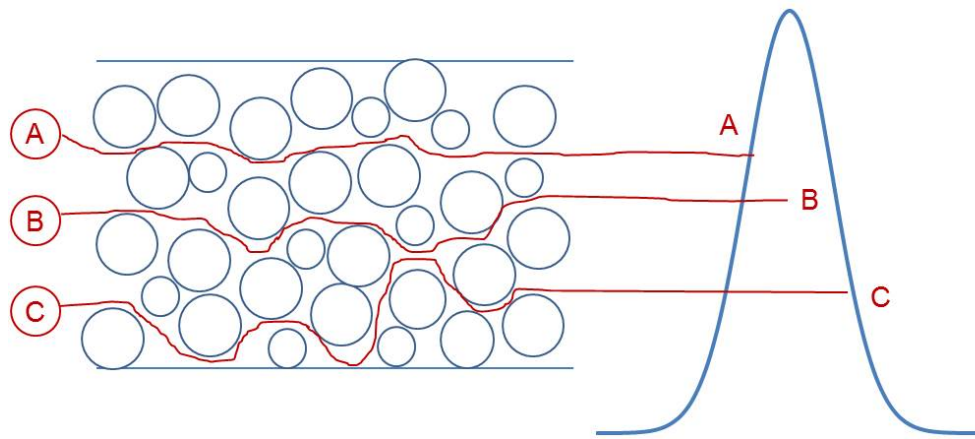


**Figure 1.4** Eddy diffusion band broadening. Adapted from [12].

$$A = 2\lambda d_p \quad (1.13)$$

A better-packed column has a smaller  $\lambda$ . The packing factor  $\lambda$  determines how different the possible flow paths are. If the column is so well packed such that all the paths are nearly the same, then the packing factor is minimized but will not reach zero [15]. Simulations have shown that packing geometry also affects the performance of ordered packed beds in simulation [15]. Smaller particles allow more path choices for analytes to select as they pass through the column. Sampling more paths averages out the differences in the individual paths. However, smaller particles are more difficult to pack and can be less uniform in size distribution, resulting in an increase in  $\lambda$ . Also small particles require high pressure for the HPLC system.

Longitudinal diffusion (*B*-term) is caused by the random thermal motion of molecules which causes molecules to move from regions of high concentration to low concentration. Only the diffusion happens along the mobile phase flow direction can be tracked by the detector. The longer time the analyte spends in the mobile phase, the more time longitudinal diffusion is allowed to occur. Thus, longitudinal diffusion is inversely proportional to the linear velocity. The *B*-term parameter is defined as:

$$B = 2\gamma D_M \quad (1.14)$$

where  $\gamma$  is the obstruction factor and  $D_M$  is the diffusion coefficient in the mobile phase. Longitudinal diffusion is less significant in HPLC than gas chromatography because diffusion coefficients in liquids are very low compared to those in gases due to the high viscosity of liquids compared to gases.

Mass transfer resistance broadening ( $C$ -term) is related with the finite time necessary for analyte to move into and out of the stationary phase. Analyte molecules in the stationary phase are not moving while the analyte molecules in the mobile phase have moved ahead of those in the stationary phase. The overall analyte zone is broadened, resulting in band broadening. Higher linear velocity or low analyte diffusion aggravate the broadening. Higher linear velocity allows less time for the mass transfer equilibrium to occur. So the  $C$ -term is proportional to the linear velocity. The  $C$  parameter is the sum of [16]:

$$C = C_S + C_M \quad (1.15)$$

$$C_S \propto \frac{d_p^2}{D_S} \quad (1.16)$$

$$C_M \propto \frac{d_c^2}{D_M} \quad (1.17)$$

where  $d_p$  is the diameter of the porous particle;  $d_c$  is the diameter of the channels in the packed column;  $D_S$  is the diffusion coefficient within the pores of the particles and  $D_M$  is the diffusion coefficient in the mobile phase [17,18].

**Fig. 1.5** represents the total broadening caused by the above three factors. The

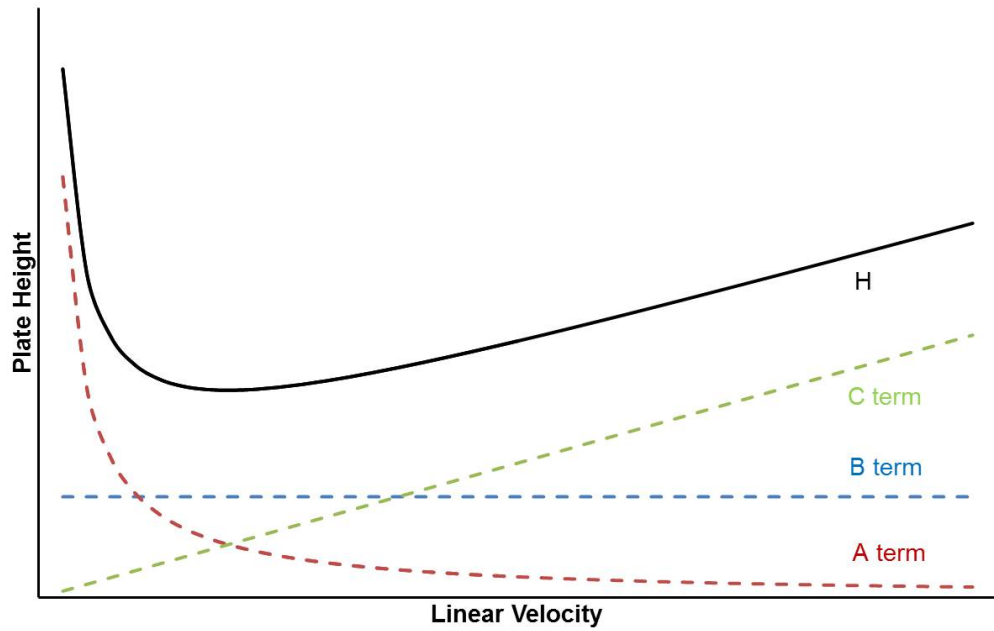


**Figure 1.5** van Deemter plot of plate height vs. linear velocity. Adapted from [12].

plate height decreases as the linear velocity increases until it reaches the optimal velocity. Since separation efficiency is inversely proportional to the plate height for a certain column length  $L$  as described in **Eq. 1.10**, highest efficiency is achieved at the optimal linear velocity. Above the optimal velocity, the plate height is  $C$ -term dominated and increases with increasing linear velocity. To minimize the analysis time, HPLC systems are typically operated above the optimum linear velocity (i.e., in the  $C$ -term dominated regime). Hence much of the recent HPLC research and instrument development has focused on development of smaller particle stationary phases and instruments that can withstand the resultant higher back pressures.

### **1.3.2 Extra Column Band Broadening**

Besides the band broadening inside the column as discussed in **Section 1.3.1**, extra column band broadening also contributes to the peak broadening in real analyses. Recent years have seen dramatic improvements in column efficiency, e.g. through the use of smaller ( $< 2 \mu\text{m}$ ) particles. However, to fully take advantage of the improved column efficiency, extra column broadening must be minimized. The actual peak broadening measured in terms of a statistical variance ( $\sigma_{observed}^2$ ) is the sum of different variance contributions.

$$\sigma_{observed}^2 = \sigma_{column}^2 + \sigma_{tubing}^2 + \sigma_{inj}^2 + \sigma_{detector}^2 \quad (1.17)$$

where  $\sigma_{column}^2$  is the column variance arising from the van Deemter equation (**Eq. 1.11**);  $\sigma_{tubing}^2$  is the connecting tubing variance;  $\sigma_{inj}^2$  is the variance originated from injection and  $\sigma_{detector}^2$  is the variance caused by detector.

Connecting tubing can be modeled as an unretentive open tubular chromatographic column. Therefore assuming  $k = 0$  in **Eq. 1.16**, we have:

$$C_M = \frac{d_c^2}{96D_M} \quad (1.18)$$

$$C_M = H_M = \frac{\sigma^2}{L} \quad (1.19)$$

$$\sigma_{tubing}^2 = \frac{d_c^2 L_{tubing}}{96D_M} \quad (1.20)$$

So the connecting tubing should be narrow and short to eliminate the tubing broadening. Also gaps in the fittings and connections need to be avoided, as they would cause an abrupt increase in  $d_c$  within the flow path.

The injection broadening refers to the broadening caused by injection volume (volume overloading), injected amount of analytes (mass overloading) and the injection solvent used in dissolving analyte sample [19]. In **Fig. 1.6 (a)**, as the injected volume of analyte solution increases (under conditions where the amount of analyte does not saturate the stationary phase), the peak broadens symmetrically to a greater retention time, and eventually has a flat top [20]. Mass overloading means a highly concentrated analyte solution is injected which causes

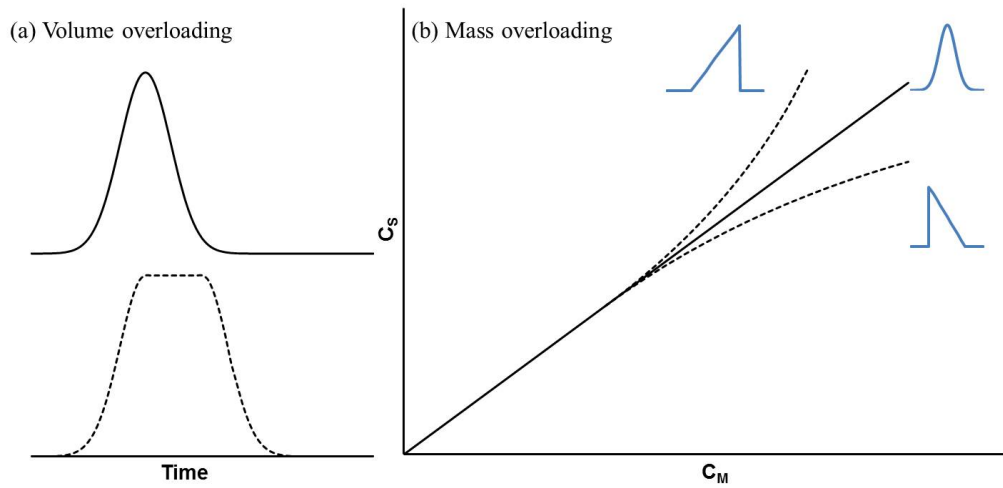


**Figure 1.6** Volume and mass overloading effects due to injection. Adapted from [12].

that sorption isotherm to exhibit non-linear behavior. As shown in **Fig. 1.6 (b)**, if the isotherm is concave, the analyte's tendency to stay in the stationary phase increases with concentration. In this case, the highest concentration part of the peak lags behind resulting in a triangular "fronting peak". If the isotherm is convex, the analyte will stay in the mobile phase more as the concentration increases, such that the highest concentration part of the peak elutes faster than the low concentration part, giving a "tailing peak". Tailing is most common in RPLC [21-23], but both fronting and tailing behavior are observed in ion chromatography and HILIC [24,25]. In this thesis, injection conditions are controlled so as to avoid both volume overload and mass overload.

The injection solvent viscosity mismatch causes distorted peak shapes. Hydrodynamic instability happens at the boundary between the injection solvent and the eluent due to viscosity mismatch as shown in **Fig 1.7**. This instability causes peak distortion, especially in early eluting peaks [26,27]. Injection solvent strength mismatch gives rise to broadened peaks. The strength mismatch broadening is caused by injecting a stronger solvent than the eluent. Upon injection, the localized retention factor of the analyte is smaller than that in the eluent due to the stronger injection solvent. As a consequence, analyte within the injection band travels faster than analyte in the regular mobile phase. This causes

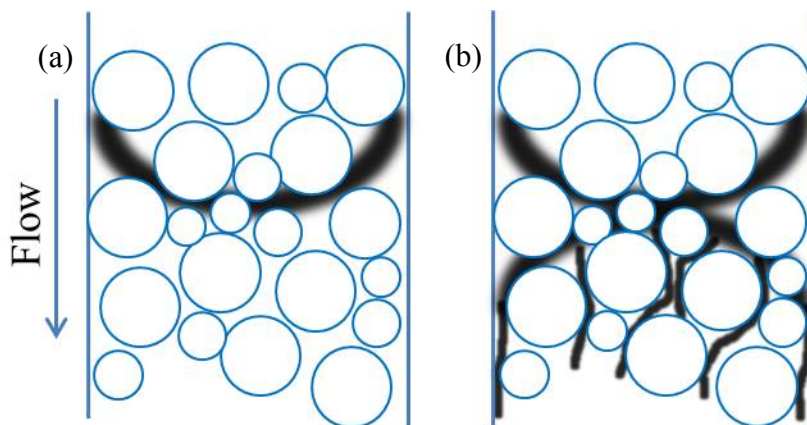


**Figure 1.7** Schematic of viscous fingering effect: (a) normal injection band profile whose viscosity is the same as eluent; (b) viscous fingering as the result of a less viscous injection band entering a more viscous eluent. Adapted from [28].

broadening of the peak. The elution velocity of the injected solvent band differs from that of the analyte. Thus, the two bands become separated as they pass down the column and so the effect on the localized analyte retention factor dissipates gradually [29,30]. Injection solvent strength mismatch has been studied in detail in RPLC [31]. However, the effect has received little attention in other modes of LC such as IC. In Chapter 2 I investigate injection solvent broadening in IC.

Detector broadening arises from two aspects: finite detector cell volume which causes actual peak broadening or distortion and detector time constant which distorts the observed peak [32,33]. The detector cell usually has a short cylindrical shape, which can be regarded as an open tube with small length to diameter ratio. Such dimensions give rise to dispersion due to the parabolic Newtonian flow. The parabolic flow broadening can be lessened by designing the way inlet and outlet are connected to the cell to create a secondary flow. Dilution inside the cell should also be considered because the detector reads the average concentration of analyte inside the cell. If the cell volume is too large, two close peaks may be in the cell at the same time, and would appear as only a single peak. So small cell volumes are preferred [34,35]. Usually, the detector cell should be less than 10% of a typical eluted peak volume.

Detector time constant is defined as the time required for the electronics to

reach 0.632 of the maximum response [18]. The signal at time  $t$  is the convolution of the actual peak signal with the detector exponential response. This results in a broadened and tailed peak. Shorter detector time constants improve the peak shape at the cost of higher background noise levels [34,36].

Rearranging **Eq. 1.3** and **1.4**, we have:

$$W_b = 4N^{-0.5}t_0(1 + k) \quad (1.21)$$

Assuming  $N$  is constant for every analyte, early eluting peaks are narrower (i.e.,  $\sigma_{column}^2$  in **Eq. 1.17** is smaller). Thus, the relative contribution from extra column broadening is higher for the early eluting peaks. As such, chromatographers are trained to monitor these early peaks to detect evidence of extra column band broadening. However, as I will show in Chapter 2, there are conditions where later eluting peaks may be most impacted by effects such as injection solvent broadening.

#### **1.4 Ion Chromatography**

Ion Chromatography (IC) is a powerful separation technique for the analysis of inorganic ions, peptides, small nucleotides and amino acids. In 1975, Small et al. [37] invented ion exchange chromatography using suppressed conductivity as the detection method. After that, IC gradually gained in popularity as a method to

determine trace (ppm to ppb) concentrations of inorganic ions and small organic ions [38-40]. The stationary phase of IC consists of particles possessing ionic sites. There are two types of IC, namely cation and anion exchange chromatography. Cation exchange chromatography has anionic exchange sites for the retention of cations. While anion exchange chromatography contains cationic exchange sites on the stationary phase for interacting with anions. Since anion exchange chromatography is used in this thesis, we will use it to demonstrate the IC mechanism and instrumentation.

#### **1.4.1 Instrumentation**

**Fig. 1.8** shows the components of an IC instrument. The pump, injection and column parts are similar to HPLC but due to the alkaline nature of IC eluents are constructed of polyether ether ketone (PEEK) material. The use of PEEK also avoids any metal contamination which could bind to the ion exchange column and cause spurious conductivity peaks. Alkaline mobile phase such as hydroxide, carbonate and bicarbonate are typically used to be compatible with the suppressed conductivity detection (see below). An on-line eluent generator is often used to generate hydroxide, carbonate, and carbonate/bicarbonate (combined with electrolytic pH modifier) eluent via electro-dialytic process [41]. The on-line

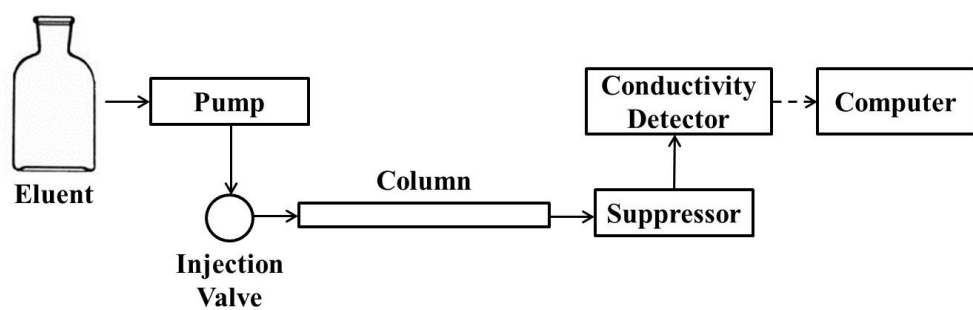


**Figure 1.8** Representative ion chromatography (IC) system. Adapted from [40].

eluent generator is not shown in **Fig. 1.8** because it is not related to the research in this thesis. As mentioned in **Fig. 1.8**, the stationary phase must possess cationic sites for ionic interaction with analyte anions (e.g.,  $F^-$ ,  $Cl^-$ ,  $SO_4^{2-}$ , etc.). The anion exchange site is usually a hydrophilic quaternary ammonium functional group.

Due to the highly basic nature of these mobile phases, polymeric resin substrate must be used rather than silica, the common stationary phase substrate for HPLC [42,43].

The suppressor in **Fig. 1.8** reduces the background conductivity signal from the eluent by converting it to water (low conductance) or carbonic acid (weak acid, low conductance). An anion exchange suppressor (**Fig. 1.9**) contains cation exchange membranes, with eluent (e.g.,  $Na^+OH^-$  or  $2Na^+CO_3^{2-}$ ) on one side and a source of  $H^+$  (e.g., sulfuric acid or electrolysis) on the other side. The cation exchange membrane only permits cations to pass through.  $H^+$  is generated electrolytically at the anode.  $Na^+$  is replaced by  $H^+$  via diffusion through the cation exchange membrane. In the eluent stream the  $H^+$  reacts with eluent  $OH^-$  or  $CO_3^{2-}$  to form water or carbonic acid which have low conductance.  $H^+$  will also replace the analyte counter cation, e.g.  $Na^+$ , which has a moderate conductance, 50.1  $Scm^2/mol$ . Since  $H^+$  cation has a high conductance (349.8  $Scm^2/mol$ ), the analyte conductivity signal for strong acid anions (e.g.,  $Cl^-$ ,  $NO_3^-$ ) is enhanced.

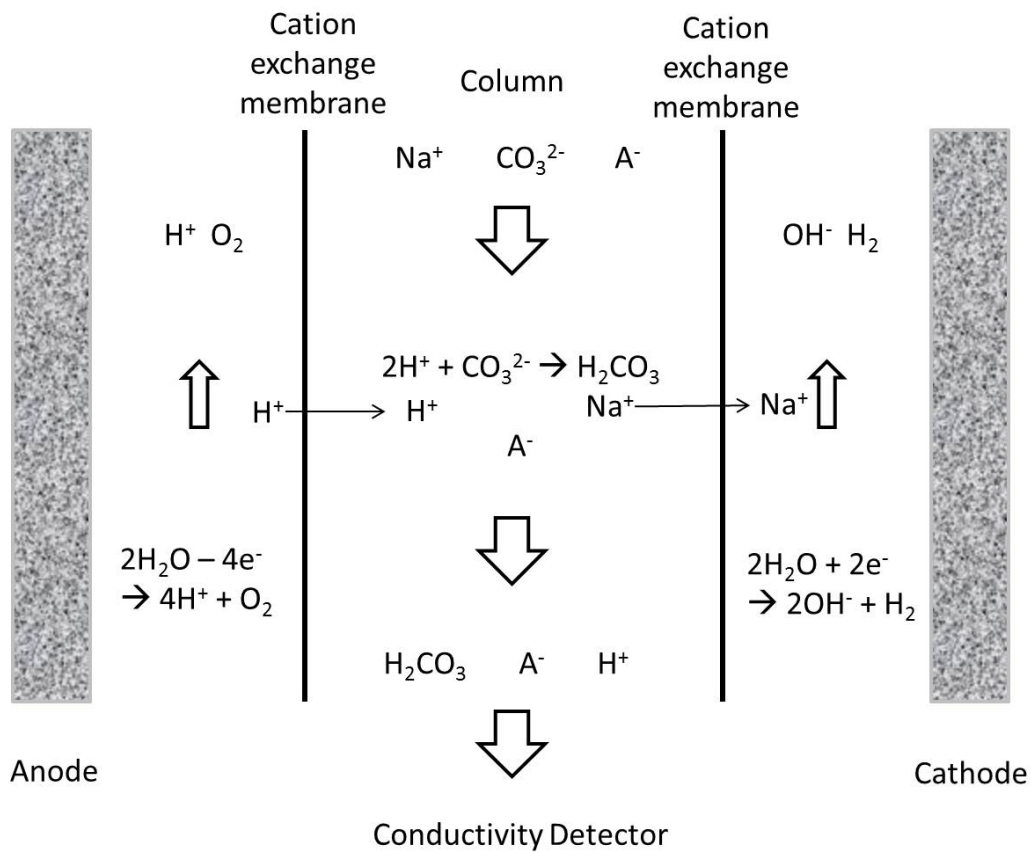


**Figure 1.9** Suppressor scheme. Sodium hydroxide is the eluent. A<sup>-</sup> is the analyte ion with counter ion Na<sup>+</sup>. Adapted from [40].

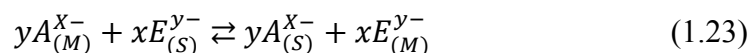
UV detector is quite often used in HPLC but few ions are UV-absorbing. Conductivity detection is commonly used in IC detection because all ions are conducting. The conductivity of solution depends on the concentration, ion types (conductance) and temperature. The eluent solution carrying analyte ions flow through detector cell where a potential is applied between two oppositely placed electrodes. Current  $i$  is monitored as a function of time. For conductivity ( $\sigma$ ), we have:

$$\sigma = \frac{i}{U} \quad (1.22)$$

where  $U$  is the applied voltage and  $i$  is the measured current. Conductivity can be calculated then. The conducting analyte ion as well as counter ion  $H^+$ , give a peak signal response. By protonating the eluent anion, the background conductivity has been suppressed.

### 1.4.2 Ion Exchange Separation Principles

The ion exchange equilibrium between an analyte ion with the stationary phase and an eluent ion with the stationary phase is [40]:



where  $A^x$  is the analyte ion with  $x$  charge and  $E^{y-}$  is the eluent ion with  $y$  charge.

The subscript  $M$  means in the mobile phase, whereas the subscript  $S$  means the ion

is associated with the stationary phase.

The retention factor of  $A^{x-}$  can be expressed as:

$$\log k_A = \frac{1}{y} \log(K_{A,E}) + \frac{x}{y} \log\left(\frac{Q}{y}\right) + \log\left(\frac{w_R}{V_m}\right) - \frac{x}{y} \log [E_m^{y-}] \quad (1.24)$$

where  $K_{A,E}$  is the ion-exchange selectivity constant of the analyte ion over the eluent ion;  $Q$  is the effective column capacity;  $w_R$  is the weight of resin (stationary phase); and  $V_m$  is the dead time volume of the column. For a given column, **Eq. 1.24** can be simplified as:

$$\log k_A = \text{const} - \frac{x}{y} \log [E_m^{y-}] \quad (1.25)$$

From **Eq. 1.24**,  $\log k_A$  is in linear relationship with the logarithm of  $[E_m^{y-}]$ .

### 1.5 Hydrophilic Interaction Liquid Chromatography

Hydrophilic Interaction Liquid Chromatography (HILIC) was first defined by Alpert [44] in 1990 for the separation of peptides, nucleic acid and other polar analytes. Since then, HILIC has gained popularity for three reasons: enabling the retention of polar compounds such as pharmaceuticals; water compatibility; and compatible with mass spectroscopy (MS) system due to high %ACN used as the eluent.

In HILIC the stationary phase is polar and hydrophilic, whereas the aqueous mobile phase is less polar with a high %ACN. As the eluent travels through the

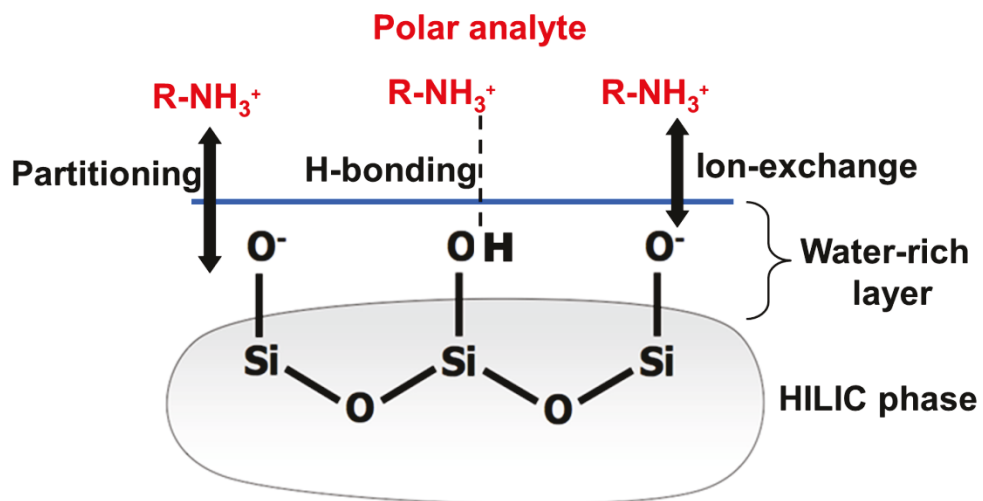


**Figure 1.10** Scheme of HILIC interactions. Adapted from Reference [45] with permission of Dr. Mohammed E.A. Ibrahim.

column, a stagnant water rich layer forms on surface of the stationary phase (**Fig. 1.10**). The more hydrophilic the stationary phase is, the thicker formed water layer [46]. Contrary to RPLC, the elution order of HILIC is from least polar to more polar. A more hydrophilic stationary phase results in longer HILIC retention time.

As shown in **Fig. 1.10**, partitioning of analytes between the ACN rich mobile phase and water layer is essential for HILIC separation. Besides the partitioning mechanism, other interactions such as hydrogen bonding, adsorption and ion exchange also affect the retention [47,48].

### 1.5.1 Principle of Retention

Compared with ACN, water is the stronger eluent. The retention time decreases as %ACN decreases. Usually, %ACN should be more than 60% for the HILIC separation. This phenomenon is different from RPLC where retention time increases as %ACN decreases. Assuming the retention of an analyte only originates from partitioning in water-rich layer, we have the linear strength model which is similar to RPLC:

$$\log k = \log k_0 - S\varphi \quad (1.26)$$

where  $k$  is the retention of analyte molecule,  $k_0$  is the retention of analyte molecule in the weakest eluent (usually ACN without water),  $S$  is a constant and  $\varphi$  is the

percent of water in the eluent.

However, as mentioned above, other interactions such as hydrogen bonding might also contribute the retention mechanism. **Eq. 1.26** only applies when other interactions are negligible in relation to partitioning. If other interactions play a significant role in HILIC retention, HILIC may display adsorption type retention behavior [9].

### **1.5.2 Stationary Phase Types**

Many different categories of HILIC stationary phase have been developed [9,45,49]. They can be classified as: underivatized silica; neutral silica; zwitterionic silica; positively and negatively charged silica, and finally non-silica.

Underivatized silica refers to bare silica columns. The silanol group on the silica surface is hydrated by the HILIC eluent to form the stagnant water rich layer. Based on the surface chemistry, underivatized silica can be grouped as: type-A silica (acidic due to metal contamination); type-B silica (less acidic, no metal contamination) and type-C (Si-H instead of Si-OH on surface). It can also be sorted as totally porous; superficially porous; monolithic and Ethylene Bridged Hybrids (BEH) based on the silica structure.

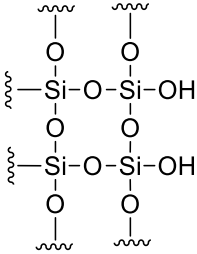
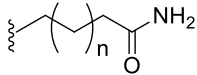
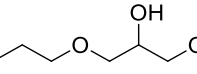
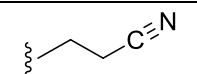
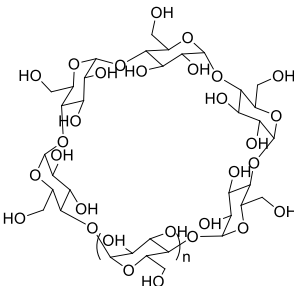
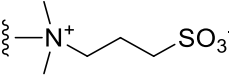
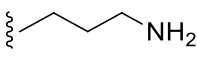
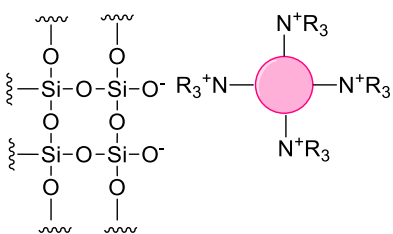
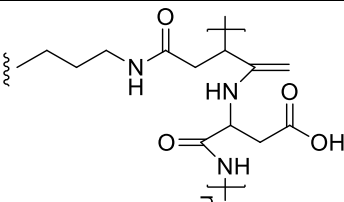
Neutral derivatized silica consists of amide-, diol-, cyano- and

cyclodextrin-modified silica stationary phase. A typical amide-silica HILIC column is TSK gel Amide-80 in which the amide group is connected to the silica support through a short alkyl chain. Amide phases have dipole and hydrogen bond accepting character. As shown in **Table 1.1**, a diol functionality has a hydrophilic hydroxyl group, which has a dipole and hydrogen bond donating and accepting character. A cross-linked diol phase provides better stability under acidic conditions due to suppressed hydrolysis. In addition, cross-linked diol phase shows HILIC/RPLC mode separation depending on the %ACN [50]. Cyano stationary phases lacks mechanical stability [20]. It also shows low retention in HILIC mode as some hydrophilic analytes such as cytosine eluted faster than hydrophobic dead time marker toluene [47], and so is not discussed further. Cyclodextrin can be regarded as toroid whose outside is hydrophilic while inside is hydrophobic because of the sugar unit arrangement. In addition to HILIC retention, cyclodextrin phases also exhibit chiral separation ability [51].

Zwitterionic refers to stationary phases which contain both basic quaternary ammonium and acidic sulfonic sites [52,53]. Usually, sulfoalkylbetaine is linked to the silica surface for zwitterionic stationary phase. Such phases behave essentially as hydrophilic neutral HILIC phases [48].

Aminopropyl and polycationic latex coatings can provide positive charge on

**Table 1.1** Chemical structures of selected types of HILIC stationary phase

Type	Functionalities	Surface chemical structure
Underivatized silica	Silica	
Neutral Silica	Amide	
	Diol	
	Cyano	
	Cyclodextrin	
Zwitterionic	Sulfoalkylbetaine	
Positively Charged	Aminopropyl	
	Polycationic latex	
Negatively Charged	poly(aspartic acid)	

silica. Polysuccinimide modification makes negatively charged silica surface. The aminopropyl stationary phase has been widely used in HILIC for a variety of applications [54,55]. However, it exhibits irreversible adsorption and unstable attachment to the silica [56,57]. Monolith silica coated with polycationic latex enables fast separations [58]. In addition, the positive charge provides Electrostatic Repulsion Hydrophilic Interaction Liquid Chromatographic (ERLIC) separation for amino acids [58]. Polysuccinimide based silica can either be used directly as a HILIC stationary phase or after further modification to other stationary phases such as poly(aspartic acid) which acts as weak cation exchanger [59].

## **1.6 Overview of Thesis Chapters**

This thesis explores the separation potential of liquid chromatography. Chapter Two investigates the injection matrix effect on ion chromatography separations. The results are statistically analyzed and compared with injection solvent effect in RPLC. It provides a practical suggestion on sample preparation which may save analysts sample preparation time. In Chapter three, a new class of HILIC stationary phase is synthesized. It is characterized by elemental analysis and X-ray Photoelectron Spectroscopy (XPS). Its separation ability is compared

with other HILIC stationary phases. The graphitic porous carbon based stationary phase has unique selectivity. Finally, Chapter Four summarizes the thesis as well as discusses future work.

### 1.7 References

- [1] K. Sakodyns, *J. Chromatogr.* 73 (1972) 303.
- [2] C.G. Horvath, S.R. Lipsky, *Nature* 211 (1966) 748.
- [3] J.M. Peng, J.E. Elias, C.C. Thoreen, L.J. Licklider, S.P. Gygi, *Journal of Proteome Research* 2 (2003) 43.
- [4] M.J. Motilva, A. Serra, A. Macia, *J. Chromatogr. A* 1292 (2013) 66.
- [5] B. Buszewski, S. Noga, *Anal. Bioanal. Chem.* 402 (2012) 231.
- [6] P.R. Haddad, P.N. Nesterenko, W. Buchberger, *J. Chromatogr. A* 1184 (2008) 456.
- [7] J.L. Rafferty, L. Zhang, J.I. Siepmann, M.R. Schure, *Anal. Chem.* 79 (2007) 6551.
- [8] H. Kazoka, *J. Chromatogr. A* 942 (2002) 1.
- [9] P. Hemstrom, K. Irgum, *J. Sep. Sci.* 29 (2006) 1784.
- [10] P.R. Haddad, P. Doble, M. Macka, *J. Chromatogr. A* 856 (1999) 145.
- [11] L.R. Snyder, J.J. Kirkland, J.W. Dolan, *Introduction to Modern Liquid*

Chromatography, 3rd ed., Wiley, Hoboken, 2010.

- [12] D.C. Harris, Quantitative Chemical Analysis, 7th ed., W.H. Freeman and Co., New York, 2007.
- [13] C.F. Poole, The Essence of Chromatography, Elsevier, Amsterdam, 2003, p 49.
- [14] J.J. van Deemter, F.J. Zuiderweg, A. Klinkenberg, Chemical Engineering Science 5 (1956) 271.
- [15] M.R. Schure, R.S. Maier, D.M. Kroll, H.T. Davis, J. Chromatogr. A 1031 (2004) 79.
- [16] G. Desmet, K. Broeckhoven, Anal. Chem. 80 (2008) 8076.
- [17] S.J. Hawkes, J. Chem. Educ. 60 (1983) 393.
- [18] J.M. Miller, Chromatography: Concepts and Contrasts, Wiley, Hoboken, 2005.
- [19] J.W. Dolan, LC-GC North America 23 (2005) 738.
- [20] U.D. Neue, HPLC Columns: Theory, Technology, and Practice, Wiley-VCH, New York, 1997.
- [21] J. Dai, P.W. Carr, D.V. McCalley, J. Chromatogr. A 1216 (2009) 2474.
- [22] D.V. McCalley, J. Chromatogr. A 793 (1998) 31.
- [23] T. Fornstedt, G. Guiochon, Anal. Chem. 66 (1994) 2116.

- [24] D.V. McCalley, *J. Chromatogr. A* 1217 (2010) 858.
- [25] D.V. McCalley, *J. Chromatogr. A* 1171 (2007) 46.
- [26] G. Rousseaux, A. De Wit, M. Martin, *J. Chromatogr. A* 1149 (2007) 254.
- [27] G. Rousseaux, M. Martin, A. De Wit, *J. Chromatogr. A* 1218 (2011) 8353.
- [28] H.J. Catchpole, R. Andrew Shalliker, G.R. Dennis, G. Guiochon, *J. Chromatogr. A* 1117 (2006) 137.
- [29] S. Keunchkarian, M. Reta, L. Romero, C. Castells, *J. Chromatogr. A* 1119 (2006) 20.
- [30] B. Alsehli, J.W. Dolan, *LC-GC North America* 30 (2012) 898.
- [31] B.J. VanMiddlesworth, J.G. Dorsey, *J. Chromatogr. A* 1236 (2012) 77.
- [32] R.P.W. Scott, *Liquid Chromatography Detectors*, Elsevier, Amsterdam, 1986.
- [33] T. Hanai, *HPLC, a practical guide*, Royal Society of Chemistry, Cambridge, 1999.
- [34] F. Gritti, C.A. Sanchez, T. Farkas, G. Guiochon, *J. Chromatogr. A* 1217 (2010) 3000.
- [35] F. Gritti, G. Guiochon, *J. Chromatogr. A* 1218 (2011) 4632.
- [36] C.A. Lucy, K.K.C. Yeung, X.J. Peng, D.D.Y. Chen, *LC GC* 16 (1998) 26.
- [37] H. Small, T.S. Stevens, W.C. Bauman, *Anal. Chem.* 47 (1975) 1801.

- [38] K. Tian, P.K. Dasgupta, T.A. Anderson, *Anal. Chem.* 75 (2003) 701.
- [39] V. Ruiz-Calero, L. Puignou, M.T. Galceran, M. Diez, *J. Chromatogr. A* 775 (1997) 91.
- [40] J. Weiss, *Handbook of Ion Chromatography*, Wiley-VCH, Weinheim, 2004.
- [41] M. Swartz, *LC-GC North America* 28 (2010) 530.
- [42] C. Pohl, *LC-GC North America* 24 (2006) 32.
- [43] C.A. Pohl, J.R. Stillian, P.E. Jackson, *J. Chromatogr. A* 789 (1997) 29.
- [44] A.J. Alpert, *J. Chromatogr.* 499 (1990) 177.
- [45] M.E.A. Ibrahim, in PhD thesis, Department of Chemistry, University of Alberta, Edmonton, Alberta, Canada, 2014.
- [46] M.E.A. Ibrahim, C.A. Lucy, in B.A. Olsen, B.W. Pack (Editors), *Hydrophilic Interaction Chromatography: a Guide for Practitioners*, John Wiley & Sons Inc., Hoboken, 2013.
- [47] N.P. Dinh, T. Jonsson, K. Irgum, *J. Chromatogr. A* 1218 (2011) 5880.
- [48] M.E.A. Ibrahim, Y. Liu, C.A. Lucy, *J. Chromatogr. A* 1260 (2012) 126.
- [49] P. Jandera, *Analytica Chimica Acta* 692 (2011) 1.
- [50] P. Jandera, T. Hajek, V. Skerikova, J. Soukup, *J. Sep. Sci.* 33 (2010) 841.
- [51] Z.M. Guo, Y. Jin, T. Liang, Y.F. Liu, Q. Xu, X.M. Liang, A.W. Lei, J.

Chromatogr. A 1216 (2009) 257.

- [52] W. Jiang, K. Irgum, *Anal. Chem.* 73 (2001) 1993.
- [53] W. Jiang, K. Irgum, *Anal. Chem.* 71 (1999) 333.
- [54] J.C. Valette, C. Demesmay, J.L. Rocca, E. Verdon, *Chromatographia* 59 (2004) 55.
- [55] D. Singer, J. Kuhlmann, M. Muschket, R. Hoffmann, *Anal. Chem.* 82 (2010) 6409.
- [56] B.A. Olsen, *J. Chromatogr. A* 913 (2001) 113.
- [57] M. Lafosse, B. Herbreteau, M. Dreux, L. Morinallory, *J. Chromatogr.* 472 (1989) 209.
- [58] M.E.A. Ibrahim, T. Zhou, C.A. Lucy, *J. Sep. Sci.* 33 (2010) 773.
- [59] A.J. Alpert, *J. Chromatogr.* 266 (1983) 23.

# **CHAPTER TWO: Injection Matrix Effects on Separation in Ion Chromatography<sup>1</sup>**

## **2.1 Introduction**

Recent years have seen dramatic advances in the speed and efficiency achievable in reversed phase liquid chromatography (RPLC) [1] and ion chromatography (IC) [2]. However to fully realize the benefits offered by these column improvements, broadening due to extra column components must be minimized [3,4]. Much of the discussion of extra column broadening has focused on the effect of connecting tubing [4-6], detector volume [4,6], and the injection volume [6-8]. Less attention has focused on the detrimental effects that can be caused by the injection solvent [3,9]. In RPLC, samples should be dissolved in the mobile phase or a weaker solvent. Injecting samples that are dissolved in stronger solvents leads to retention time changes, peak broadening and even peak distortions such as flat or split peaks [3,10-12]. If a large volume containing a high concentration of strong solvent is injected, a second peak may even appear on the front of the analyte peak [13]. Similar injection broadening has been reported in Hydrophilic Interaction Liquid Chromatography (HILIC) [14].

Alternately, the sample may be dissolved in a different solvent than the

---

<sup>1</sup> A version of this chapter has been submitted to *Journal of Chromatography A* as Y. Zhang and C.A. Lucy, Injection Matrix Effects on Separation in Ion Chromatography.

mobile phase. In such cases, both the elution strength and the viscosity of the injected solvent can affect chromatographic performance. When the solvent has a different viscosity from the mobile phase, hydrodynamic instability at the boundary between the injected solvent and eluent causes peak distortion, particularly of the early eluting analytes [15,16]. The viscous fingering effects on band shape become dramatic as injection volume increases.

A number of practices can help chromatographers avoid injection-induced artifacts. For instance it is recommended that the sample solvent from any pre-treatment steps such as extraction be evaporated off and the sample be re-dissolved in the mobile phase [17,18]. Alternately if possible, the sample should be dissolved in a solvent that is a weaker eluent than the mobile phase. This enables focusing of the sample at the head of the column [3]. Sometimes the sample may not be soluble or may decompose if it is stored in the mobile phase for a long time. In such cases, other suitable organic solvents might be useful [19]. Using sample diluents that are water-immiscible and elute after the analyte peaks can minimize peak distortion and broadening [20,21]. Finally, the use of small injection volumes minimizes injection-induced broadening [22], but at the expense of signal intensity. With such a myriad of options, it can be difficult to select the most appropriate injection procedure. To address this, VanMiddlesworth

and Dorsey developed a *sensitivity parameter*,  $s$ , that quantifies how the column responds to a change in the injection solvent composition [9].

IC plays a significant role in the separation and analysis of inorganic ions [23] and small organic molecules [24,25]. Many IC protocols call for samples containing high concentrations of matrix ions to be diluted (*dilute and shoot sample prep*) [26]. This step both increases the sample preparation time and sacrifices analyte signal.

However, there is little research in the effect of concentrated eluent on the injection induced broadening in Ion Chromatography (IC). In this chapter, we monitor how the retention and peak shape of  $F^-$ ,  $Cl^-$ ,  $NO_2^-$ ,  $Br^-$ ,  $NO_3^-$  and  $SO_4^{2-}$  are affected by the presence of a concentrated  $HCO_3^-/CO_3^{2-}$  eluent/matrix. The use of concentrated eluent as the matrix enables subsequent suppression of the matrix peak, which allows direct investigation of the changes in analyte peak shape and location. We also quantitatively evaluate the impact of matrix concentration on IC separation efficiencies via the sensitivity parameter [9].

## **2.2 Experimental**

### **2.2.1 Instrumentation**

The IC chromatography system was a Dionex ICS-2000 (Thermo Scientific,

Sunnyvale, CA, USA) equipped with a 20  $\mu\text{L}$  injection loop (unless otherwise noted), a 4 mm ASRS-300 electrolytic suppressor and a Dionex ED-40 electrochemical conductivity detector. Separations were performed at 1.0 mL/min and 25  $^{\circ}\text{C}$  on a Dionex IonPac AS23 anion-exchange column (250 mm  $\times$  4 mm i.d., 6.0  $\mu\text{m}$ ) with data acquisition at 50 Hz. IC data was collected and analyzed using Chromeleon<sup>TM</sup> 6.80 software (Dionex, part of Thermo Scientific, Sunnyvale, CA, USA).

The RPLC system consisted of: a 709 dual-piston pump (Metrohm, Herisau, Switzerland); a 6-port Rheodyne model 8125 (Rheodyne, Cotati, CA, USA) injection valve equipped with a 20  $\mu\text{L}$  loop; ACE 5C18 column (5 cm  $\times$  4.6 mm i.d., 5  $\mu\text{m}$ ; Advanced Chromatography Technologies Ltd, Aberdeen, Scotland) at ambient temperature and a Lambda-Max Model 481 LC spectrometer (Waters, Milford, MA, USA) set at 215 nm. Data were collected at 20 Hz using a Dionex advanced computer interface with Dionex PeakNet 5.2 software.

### **2.2.2 Chemicals**

All water used was purified to  $\geq 17.8 \text{ M}\Omega\text{-cm}$  using a Barnstead E-pure ultrapure water purification system (Dubuque, IA, USA). All reagents were reagent grade or better. The IC eluent was prepared from anhydrous sodium

carbonate ( $\text{Na}_2\text{CO}_3$ ) and sodium bicarbonate ( $\text{NaHCO}_3$ ) from Caledon Laboratories Ltd. (Georgetown, ON, Canada). Sodium chloride ( $\text{NaCl}$ ) and sodium nitrate ( $\text{NaNO}_3$ ) were from EMD Chemicals Inc. (Darmstadt, Germany). Sodium bromide ( $\text{NaBr}$ ), sodium fluoride ( $\text{NaF}$ ), sodium nitrite ( $\text{NaNO}_2$ ), sodium sulfate ( $\text{Na}_2\text{SO}_4$ ), benzyl alcohol, acetophenone, benzene and o-xylene were from Sigma-Aldrich (St. Louis, MO, USA).

Acetonitrile (Optima grade), toluene and formic acid were from Thermo Fisher Scientific (Fair Lawn, NJ, USA).

### **2.2.3 Solution Preparation**

Stock IC matrix solution (0.500 M  $\text{Na}_2\text{CO}_3$  and 0.0500 M  $\text{NaHCO}_3$ ) was prepared by dissolving  $\text{Na}_2\text{CO}_3$  and  $\text{NaHCO}_3$  in 20 mL purified water, sonicating and then diluting to 50 mL in a volumetric flask. The mobile phase for IC was prepared by pipetting 5 mL of above stock matrix solution and then diluted to 1 L. The eluent was vacuum degassed before use, as well as degassed on-line.

Stock IC analyte solutions were prepared individually by dissolving  $\text{NaF}$ ,  $\text{NaCl}$ ,  $\text{NaNO}_2$ ,  $\text{NaBr}$ ,  $\text{NaNO}_3$  and  $\text{Na}_2\text{SO}_4$  in 100 mL water to 0.100 M. Individual analyte solutions were prepared by mixing the respective stock analyte solution with various volumes of the stock matrix solution and bringing to volume (25 mL)

with purified water.

The RPLC mobile phase was prepared by adding 96  $\mu\text{L}$  of  $\text{HCOOH}$  in 100 mL of 30% ACN. The eluent was vacuum degassed. Stock RPLC analyte solutions were prepared by dissolving benzyl alcohol, acetophenone, benzene, toluene, o-xylene in 25 mL ACN to 0.05 M. Individual analyte solutions were prepared by mixing the respective stock analyte solution with different percent of ACN for the desired injection solvent composition.

## **2.3 Data Analysis Method**

### **2.3.1 RPLC Data Analysis Method**

The RPLC data was analyzed by traditional chromatographic parameters such as retention time, as discussed in **Section 1.2.1**.

### **2.3.2 Statistical Moment Analysis [27,28]**

For the IC data, the first and second statistical moments and peak asymmetry were calculated using Chromeleon<sup>TM</sup> 6.80 software. All data are the average of three replicate injections ( $\text{SO}_4^{2-}$  result is based on one or two injection). Statistical moment analysis method is based on the actual statistical distribution of the data points collected rather than assuming an idealized peak shape. Statistical moment

analysis is used in this paper due to the distorted peaks observed at high matrix concentrations.

The zeroth moment ( $\mu_0$ ) is the peak area and the first moment ( $\mu_1$ ) is the center of gravity of the peak by integration,

$$\text{Zero moment: } \mu_0 = \int f(t)dt \quad (2.1)$$

$$\text{First moment: } \mu_1 = \frac{\int t*f(t)dt}{\mu_0} \quad (2.2)$$

where  $t$  is the time in minutes and  $f(t)$  is the baseline-corrected conductivity signal over time. The first moment is referred to as the averaged retention time in the Chromeleon software.

The second moment centralized statistical moment ( $\bar{\mu}_2$ ) is the retention time variance.

$$\bar{\mu}_2 = \frac{\int (t-\mu_1)^2*f(t)dt}{\mu_0} \quad (2.3)$$

Peak efficiencies were calculated from the first moment and second centralized moment:

$$N = \frac{\mu_1^2}{\bar{\mu}_2} \quad (2.4)$$

The non-parametric peak asymmetry ( $A$ ) is defined as:

$$A = \frac{\mu_1 - t_R}{\sqrt{\bar{\mu}_2}} \quad (2.5)$$

where  $t_R$  is the retention time (peak maxima) of the current peak. The parameter  $A$  is positive if the peak is tailing, and negative if the peak is fronting.

## 2.4 Results

This chapter explores the effect of concentrated matrix within injected samples on the peak shapes observed for trace analytes in ion chromatography (IC). To put the behavior in context, a brief review of injection solvent effects in reversed phase liquid chromatography (RPLC) will be presented.

### 2.4.1 Injection Solvent Effects in RPLC

Peak distortion and extra broadening can occur if the analytes are injected in a solvent that is a stronger mobile phase or of different viscosity than the eluent [3,10-13,15,16]. This phenomenon has been well established in RPLC. **Fig. 2.1** shows the RPLC separation of aromatic compounds. The retention factors of these analytes range from 1.5 to 52 with the 30% ACN mobile phase. The %ACN values indicated in **Fig. 2.1** are the injected solvent for each separation.

When the analyte is dissolved in the mobile phase (30% ACN) (lower chromatogram in **Fig. 2.1**) the peaks are Gaussian and show high efficiency ( $N=1700-3400$ ). Early eluting peaks (benzyl alcohol and acetophenone) display some peak tailing due to extra-column band broadening [29].

As the injection solvent strength increases, there is little change in the retention time of the peaks (**Fig. 2.2**), consistent with ref. [9]. The injection

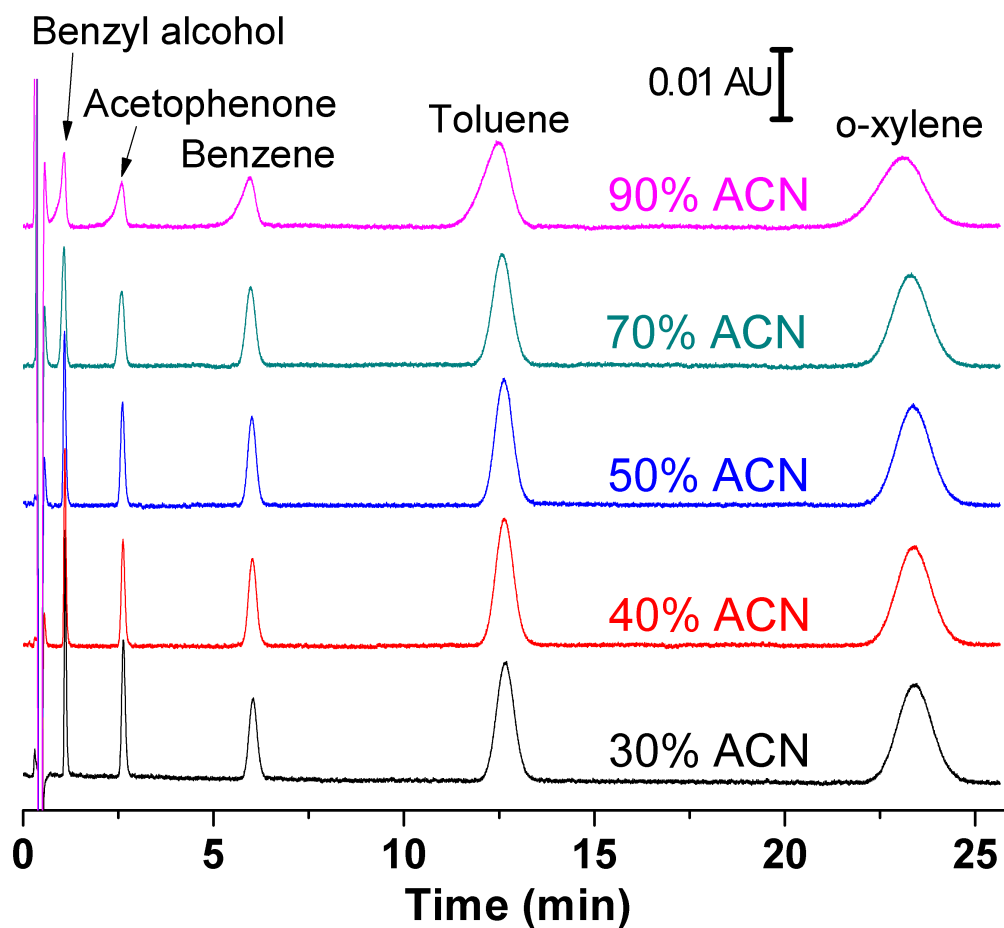


**Figure 2.1** Effects of injection solvent on RPLC separations. Conditions: ACE 5C18 column (5 cm × 4.6 mm i.d., 5 μm); 1 mL/min 30% ACN with 25 mM formic acid buffer in ambient temperature; analytes: 0.016 – 0.11 mM of benzyl alcohol, acetophenone, benzene, toluene and o-xylene; 20 μL of sample in the solvent indicated; UV detection at 215 nm. Chromatograms are offset for clarity.

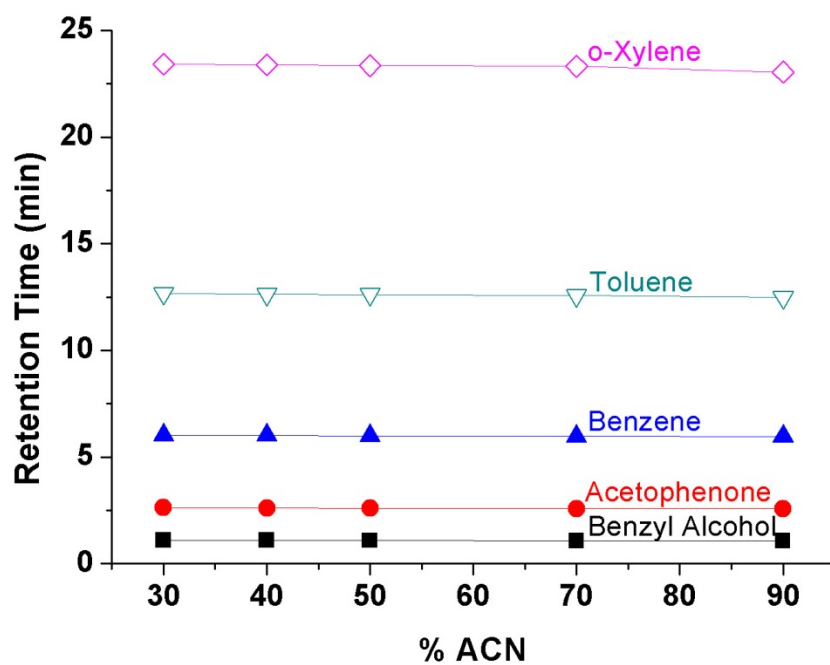


**Figure 2.2** Effects of injection solvent on the retention times of RPLC analytes.

Conditions are the same as in **Fig. 2.1**.

solvent most significantly affects the efficiency (almost exclusively due to increased peak width) and asymmetry of the peaks (**Figs. 2.3 and 2.4**) [9]. **Fig. 2.1** and **Fig. 2.3** show that the peak distortion increases as the difference in solvent strength between the injection solvent and eluent increases. The general trend of increased fronting with increased injection solvent strength is consistent with past work, although the precise peak asymmetry observed varied between different RPLC columns [9]. In **Fig. 2.1**, the two early eluting analytes are the first to exhibit peak broadening and fronting. These peaks are initially tailing in 30%ACN injection solvent due to extra column broadening. But as the injection solvent mismatch becomes more severe, the resultant fronting overwhelms the extra column tailing effects. Only at the highest injection solvent strengths ( $\geq 70\%$  ACN) do the later eluting peaks (toluene and o-xylene) exhibit injection-induced broadening.

Injection of a high %ACN, introduces a zone at the head of the column where the localized retention factor ( $k_{local}$ ) is much lower than that under typical eluent conditions (e.g.,  $k_{eluent}$  with 30% ACN eluent in **Fig. 2.1**). The localized strong eluent band then travels down the column at a velocity based on the retention characteristics of the strong eluent component. So long as the analyte remains in the eluent band, it experiences lower retention than it would in the eluent ( $k_{local} <$

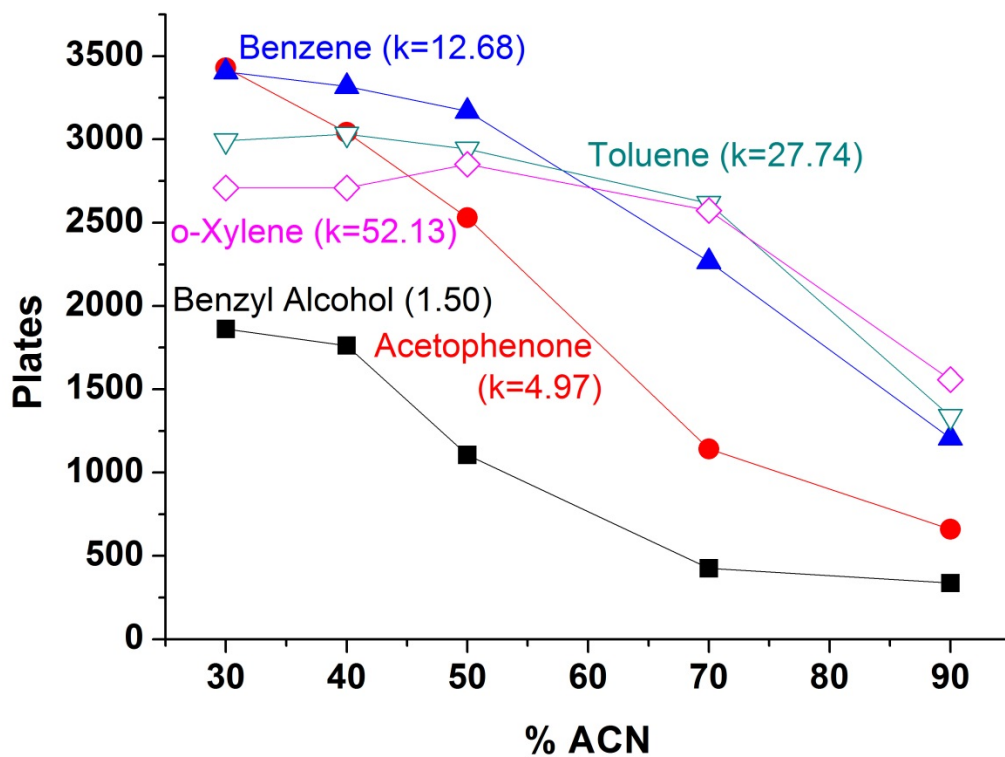


**Figure 2.3** Effects of injection solvent on the efficiencies of RPLC analytes.

Conditions are the same as in **Fig. 2.1**.

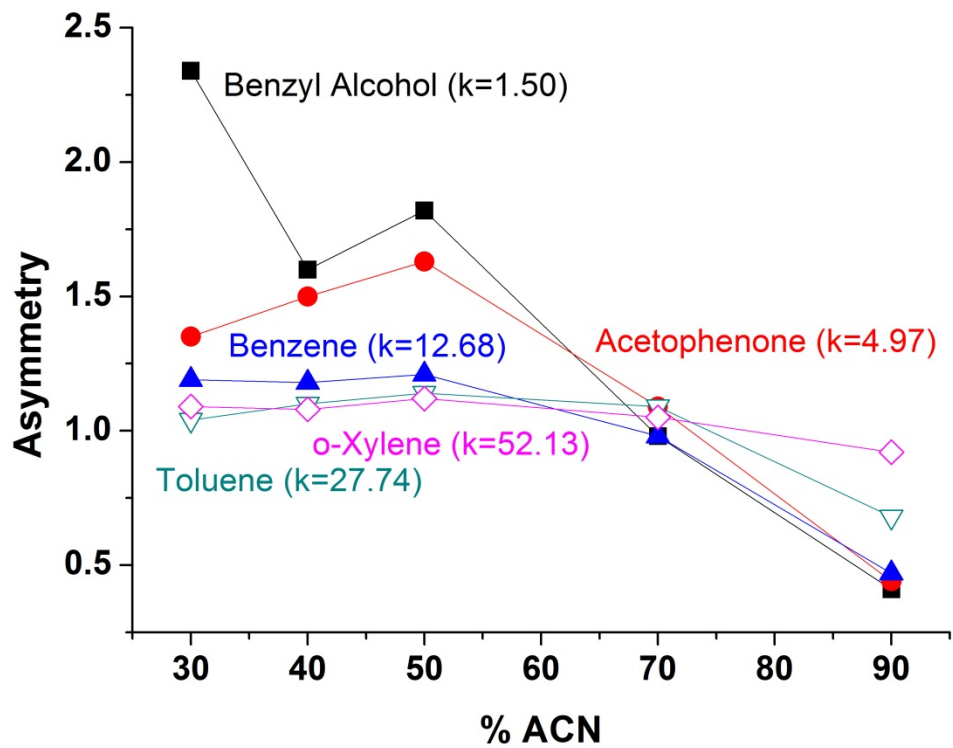


**Figure 2.4** Effects of injection solvent on the asymmetries of RPLC analytes.

Conditions are the same as in **Fig. 2.1**.

$k_{\text{eluent}}$ ). In RPLC, the strong eluent (e.g., ACN) is weaker retained than most analytes. Thus the injection solvent zone will migrate down the column faster than the analyte bands. Strongly retained analytes such as toluene and o-xylene quickly lag behind the injection solvent band, and so are less affected by the injection solvent (**Fig. 2.1**). The early eluting analytes travel at only a slightly slower velocity than the injected solvent band. Thus the weakly retained analytes spend more time co-migrating with the band of injected strong solvent [11,21], and so are most affected by the injected solvent in RPLC.

When the injection solvent is stronger than the eluent in RPLC, its effect on early eluting peak is to broaden and front the peak [9,30]. The ACN zone elutes faster than the analyte band. Thus as the analyte and solvent band become resolved on column, the front of the each analyte band will reside in an ACN-richer zone than the back of the analyte band. Since analytes move faster in stronger eluent, the front of the analyte band moves faster than its back, causing a broadened and fronting peak.

To quantitatively evaluate the impact of the injected solvent on the separation, VanMiddlesworth and Dorsey introduced the sensitivity parameter ( $s$ ) [9]:

$$s = \frac{\sum_{n=1}^i (N_{\text{measured},n} / N_{\text{ideal},n})}{i} \quad (2.6)$$

where  $N_{\text{measured}, n}$  is the measured efficiency upon injection in a certain matrix,

$N_{\text{ideal}}$  is the optimum efficiency (i.e., that observed when the sample is dissolved in the eluent), and  $i$  is the number of different injection solvents studied.

The sensitivity parameter  $s$  reflects how a column responds to an injection solvent change. The closer the measured efficiency is to the ideal efficiency ( $s=1$ ), the better the column tolerates the injected matrix/solvent. By measuring efficiencies at a variety of matrix concentrations ( $n=1$  to  $i$  in **Eq. 2.6**), an average value of  $s$  is obtained that is indicative of the column, rather than a specific matrix concentration. If  $s$  is near to 1, the column is well able to tolerate the injected solvent range tested. Thus injection of samples in solvents within that range will not negatively affect the separation. In such a case, it is not necessary to dilute the sample prior to injection. In contrast, if  $s$  is quite low, (i.e. near 0), then small differences in the injected matrix cause great changes in the observed efficiencies. In such cases, the samples should be diluted or treated with other methods to eliminate the injection solvent effect. VanMiddlesworth and Dorsey observed  $s$  values ranging from 0.55 to  $\sim 1$  in their study of injection solvent effects in RPLC separation [9].

**Table 2.1** summarizes the measured sensitivity for the ACE 5C18 studied in **Fig. 2.1**. The magnitude of the injection sensitivity in **Table 2.1** are in good agreement with the values observed by VanMiddlesworth and Dorsey [9].

**Table 2.1** Measured sensitivity for the ACE 5C18 RPLC column.<sup>a</sup>

Analyte	k	s
Benzyl alcohol	1.50	0.59
Acetophenone	4.97	0.63
benzene	12.69	0.78
toluene	27.74	0.86
o-xylene	52.13	0.92

- a. Conditions: ACE 5C18 (5 cm × 4.6 mm i.d., 5 μm); eluent, 1 mL/min 30% ACN; 20 μL of sample in the solvent indicated; analytes, 0.016 mM benzyl alcohol, 0.016 mM acetophenone, 0.11 mM benzene, 0.10 mM toluene, 0.098 mM o-xylene; column temp., 25 °C; detection, 215 nm.

**Table 2.1** also shows that the sensitivity is inversely dependent on the retention factor. As noted in **Fig. 2.2**, retention time is only weakly affected by the injection solvent. Rather the injection solvent predominantly impacts the efficiency by broadening the peak (**Fig. 2.3**), with more retained peaks showing less change in their peak width. These observations are also consistent with the work of VanMiddlesworth and Dorsey [9].

Injection volume has also been shown to impact solvent strength injection broadening in RPLC [5,8,22]. Injection of larger volumes causes greater broadening [5,8,22]. This is reflected by lower sensitivity *s* with increased injection volume [9].

### 2.4.2 Injected eluent effects in IC

**Fig. 2.5** shows the effect of injecting samples dissolved in a greater carbonate/bicarbonate concentration than the eluent (2.5 mM Na<sub>2</sub>CO<sub>3</sub> and 0.25 mM NaHCO<sub>3</sub>). The strongly retained sulfate (~30.5 min) is excluded from **Fig. 2.5** to enable visualization of the effect of injection matrix on the earlier eluting peaks. Injecting analyte anions which are either in pure water (black trace in **Fig. 2.5**) or in the eluent yields high efficiency and symmetrical peaks. As in RPLC (**Fig. 2.1**), injection of analyte in a stronger eluent results in peak broadening.

When a smaller injection volume (10 µL vs. 20 µL) was used, the injection induced broadening was much more subdued than observed in **Fig. 2.5**. Conversely when 25 µL samples were injected, the same general trends were observed but the distortions were greater resulting in loss of resolution between Br<sup>-</sup> and NO<sub>3</sub><sup>-</sup>. The effect of injection volume is consistent with the dependence previously reported for RPLC [5,8,22], and so was not studied further. Twenty µL is used in our studies, as that is the commonly used injection volume in IC. A few differences from the injection-induced broadening in RPLC are immediately apparent. First, comparing the red (25/2.5 mM Na<sub>2</sub>CO<sub>3</sub>/NaHCO<sub>3</sub>) and black (2.5/0.25 mM Na<sub>2</sub>CO<sub>3</sub>/NaHCO<sub>3</sub>) chromatograms in **Fig. 2.5** indicates that the injection of a ten-fold more concentrated eluent than the mobile phase causes

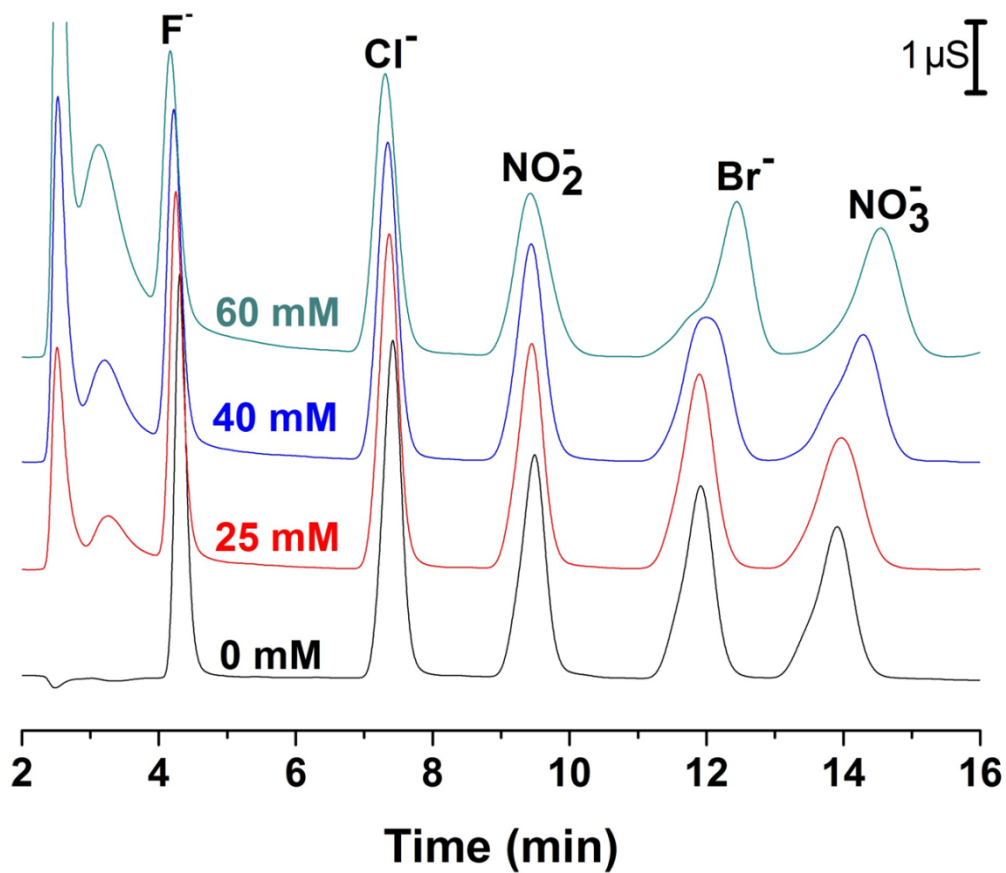


**Figure 2.5** Effect of injection matrix concentration on IC separations. Conditions: Dionex AS23 column (250 × 4 mm i.d., 6 μm); 1 mL/min of 2.5 mM Na<sub>2</sub>CO<sub>3</sub> and 0.25 mM NaHCO<sub>3</sub> in 25 °C; analytes: 0.5 mM of NaF, NaCl, NaNO<sub>2</sub>, NaBr, NaNO<sub>3</sub> in the injection matrix indicated (25 mM means 25/2.5 mM CO<sub>3</sub><sup>2-</sup>/HCO<sub>3</sub><sup>-</sup>); 20 μL of injection.

minimal broadening. This is in contrast to RPLC, where in **Fig. 2.1** injection of *triple* the mobile phase composition (30% ACN to 90% ACN injection sample solvent) resulted in noticeable broadening for all analyte peaks.

Second, the  $\text{Br}^-$  and  $\text{NO}_3^-$  peaks in **Fig. 2.5** are more affected than the earlier eluted anions by the injection solvent, whereas in RPLC the least retained peaks (benzyl alcohol and acetophenone in **Fig. 2.1**) were most affected. When the matrix concentration was  $>40/4$  mM  $\text{Na}_2\text{CO}_3/\text{NaHCO}_3$ , the  $\text{NO}_2^-$ ,  $\text{Br}^-$  and  $\text{NO}_3^-$  initially broaden, and then exhibit asymmetry. Further, under severe matrix injection the  $\text{NO}_3^-$  exhibits a small shoulder along the peak front (e.g., green  $\text{NO}_3^-$  injected in  $40/4$  mM  $\text{Na}_2\text{CO}_3/\text{NaHCO}_3$ ). In contrast, the injected matrix has little effect on the strongly retained  $\text{SO}_4^{2-}$  (**Fig. 2.6-2.9**).

**Fig. 2.6** shows the effect of the injected matrix concentration on the first moment (i.e., center of gravity) of the analyte anions.  $\text{F}^-$ ,  $\text{Cl}^-$  and  $\text{NO}_2^-$  are essentially unaffected. The first moment for  $\text{Br}^-$  increased slightly while that of  $\text{NO}_3^-$  increased more noticeably with increasing injected eluent concentration. The center of gravity of  $\text{SO}_4^{2-}$  decreased slightly with increasing injected eluent concentration. Thus, retention times were almost unaffected even when the injection solvent was 10-fold of eluent concentration, and so retention time is still effective at identifying analytes. The minimal effect of injection solvent on the

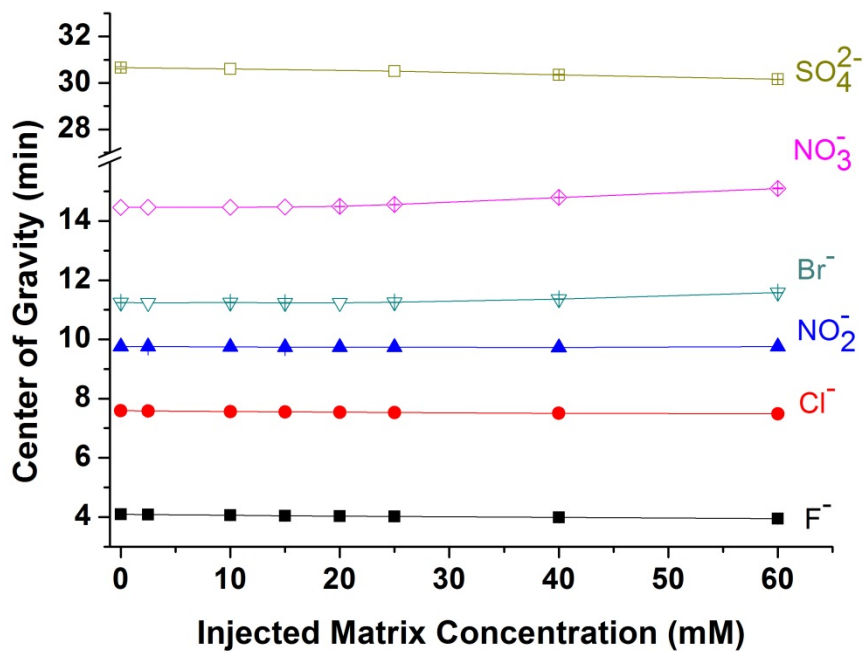


**Figure 2.6** Effects of injection matrix concentration on the center of gravities of IC analytes. Conditions are the same as in **Fig. 2.5**.

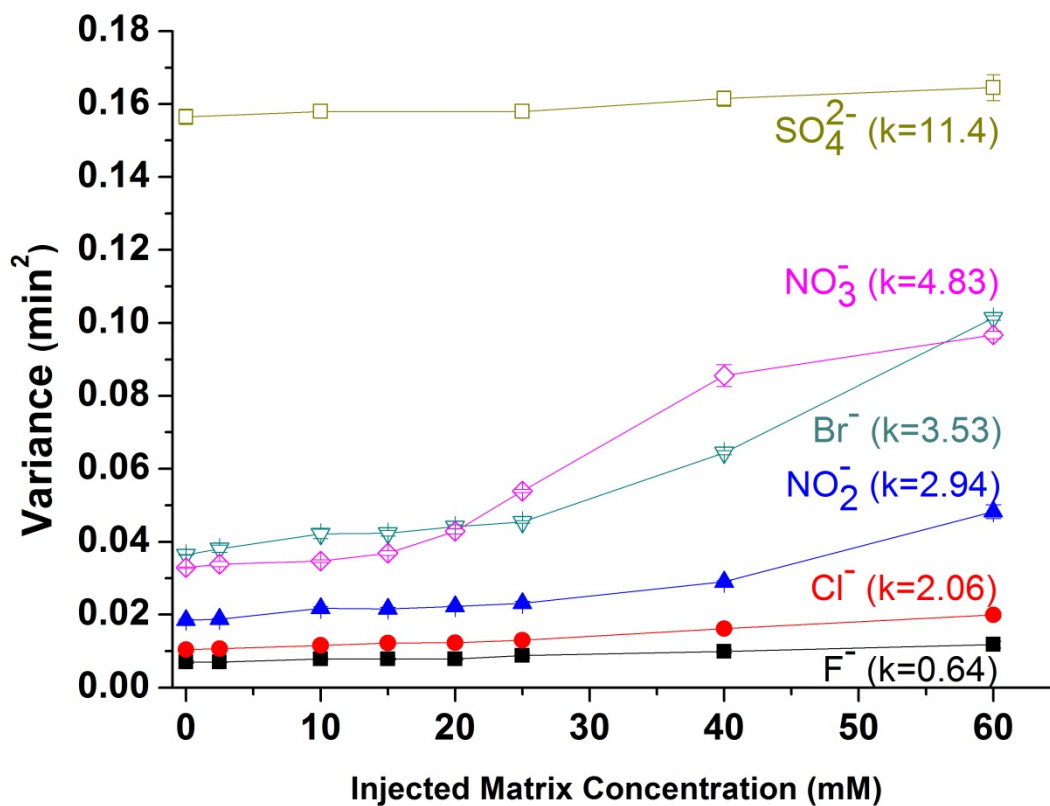


**Figure 2.7** Effects of injection matrix concentration on the variances of IC analytes. Conditions are the same as in **Fig. 2.5**.

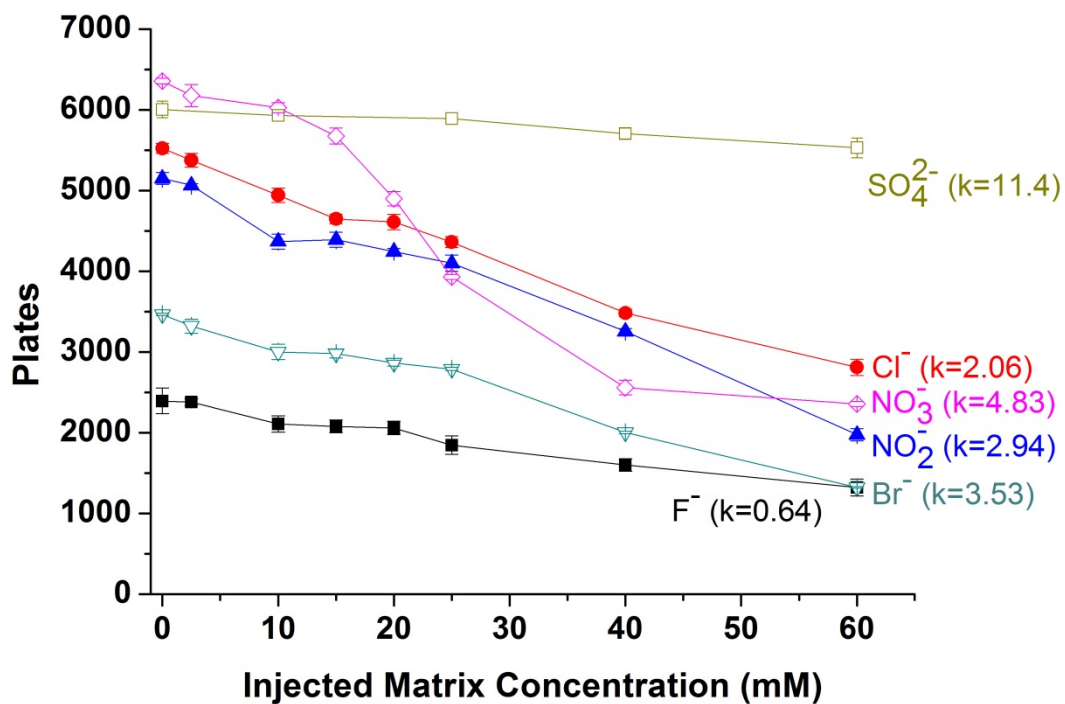


**Figure 2.8** Effects of injection matrix concentration on the efficiencies of IC analytes. Conditions are the same as in **Fig. 2.5**.

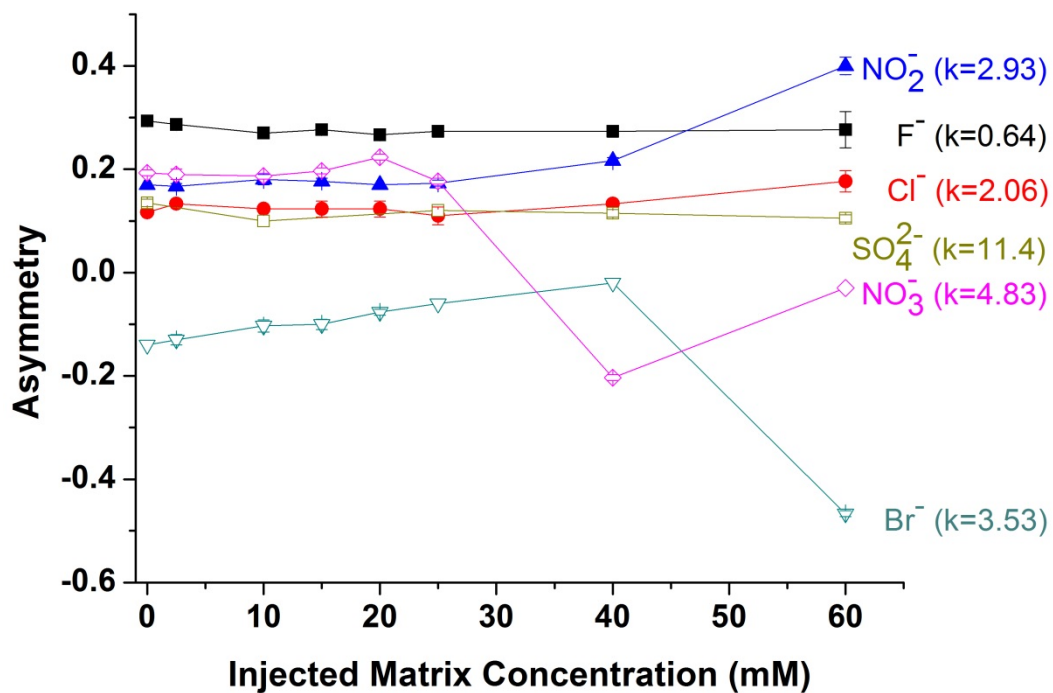


**Figure 2.9** Effects of injection matrix concentration on the asymmetries of IC analytes. Conditions are the same as in **Fig. 2.5**.

retention time is consistent with behavior in RPLC [9], albeit much greater magnitude of mismatch is tolerated in IC than RPLC.

**Fig. 2.7** shows the effect of the injected matrix concentration on the second centralized moment (i.e., variance) of the analyte anions. The change in peak width is predominantly responsible for the change in efficiency (**Fig. 2.8**), as the change in retention time is minimal (**Fig. 2.6**). Below ~10 mM matrix (4×[eluent]), efficiency shows little dependence on matrix concentration. From 10 ~ 25 mM matrix, the efficiencies for the less retained anions (F<sup>-</sup>, Cl<sup>-</sup>, NO<sub>2</sub><sup>-</sup> and Br<sup>-</sup>) were essentially unaffected, but that of NO<sub>3</sub><sup>-</sup> decreased significantly. When more concentrated matrix was injected, the separation efficiencies for the five earlier eluting anions in **Fig. 2.8** decreased substantially, while that of SO<sub>4</sub><sup>2-</sup> only decreased slightly. Nonetheless, Br<sup>-</sup> and NO<sub>3</sub><sup>-</sup> still were near-baseline resolved even when 60 mM matrix was injected (24×[eluent]).

**Fig. 2.9** shows the effect of the injected matrix concentration on the asymmetry  $A$  (**Eq. 2.5**) of the analyte anions. If  $A$  is positive, the peak is tailing. If  $A$  is negative, the peak is fronting. The asymmetry of early eluting F<sup>-</sup> was unaffected by the increases in the injection matrix concentration. As the retention factor increased from Cl<sup>-</sup> to NO<sub>2</sub><sup>-</sup> the injected matrix caused increasing tailing. In contrast, the next most retained Br<sup>-</sup> and NO<sub>3</sub><sup>-</sup> peaks become more fronted with

higher matrix concentration injection. Finally, the latest eluting ( $\text{SO}_4^{2-}$ ) peak was essentially unaffected by the injected matrix. Note, at 60 mM injected matrix, the  $\text{NO}_3^-$  peak exhibited a shoulder (**Fig. 2.5**), which made the asymmetry measure less fronted.

For almost all RPLC columns studied [9], the injection solvent mismatch caused all peaks to become increasingly fronted, no matter what their retention time. Comparing **Fig. 2.4** with **Fig. 2.9**, the asymmetry of early eluted peaks in RPLC are more susceptible to injection solvent broadening, whereas mid retained peaks are more susceptible in IC separations. As will be discussed in **Section 2.5**, the susceptibility of these peaks is due to their proximity to a system peak.

To quantitatively evaluate the impact of the inject matrix, we can use the sensitivity parameter of VanMiddlesworth and Dorsey [9], as was done for RPLC in **Section 2.4.1**. In **Table 2.2**, the Dionex AS 23 column was evaluated over the injected carbonate/bicarbonate matrix range from 0 to 60 mM. Within the 0 ~ 25 mM matrix range, the sensitivities of the six ions determined using **Eq. 2.6** were near 1 (~0.9), indicating that the separation of all anions on the AS 23 column is very tolerant to this injected matrix. Comparing the RPLC results in **Table 2.1**, early eluted analytes have lower sensitivity. In IC separation, it is the peak which is closer to second system peak that has low sensitivity. This will be discussed

further in **Section 2.5**.

When the matrix is concentrated (25-60 mM), all anions exhibit lower  $s$ , indicating less tolerance to the injected matrix. Moreover, the sensitivity was lowest for the  $\text{Br}^-$  and  $\text{NO}_3^-$  anions. Thus the sensitivity parameter reflects the same trends evident in the peak distortions evident in **Fig. 2.8**. That is that intermediate peaks within the IC chromatogram are most impacted by the injected matrix.

**Table 2.2** Measured injection sensitivity for AS 23 anion exchange column.<sup>a</sup>

Analyte	$\text{F}^-$	$\text{Cl}^-$	$\text{NO}_2^-$	$\text{Br}^-$	$\text{NO}_3^-$	$\text{SO}_4^{2-}$
<b>k</b>	0.64	2.06	2.94	3.53	4.83	11.4
<b>s (0 ~ 25 mM)</b>	0.90	0.89	0.88	0.89	0.87	0.97
<b>s (25 ~ 60 mM)</b>	0.66	0.64	0.60	0.59	0.46	0.97

a. Conditions: as in **Fig. 2.5**. Values based on triplicate injections of matrix concentrations of 0, 2.5, 10, 15, 20, 25, 40 and 60 mM, except for sulfate which are based on duplicate injections of 0, 2.5, 10, 25, 40 and 60 mM matrix.

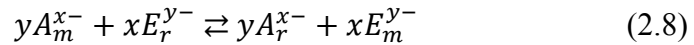
## 2.5 Discussion

There are two primary causes for the difference in injection-induced broadening between RPLC (**Fig. 2.1**) and IC (**Fig. 2.5**). First is the fundamental retention behavior. RPLC's partition-based retention can be approximated by the Linear Solvent Strength (LSS) model [31,32]:

$$\log k = \log k_w - S\varphi \quad (2.7)$$

where  $k$  is the retention factor;  $k_w$  is the value of  $k$  when 100% water is the mobile phase;  $\varphi$  is the volume fraction of organic solvent in the binary mobile phase; and  $S$  is a condition specific constant.

In contrast, retention in IC is governed by [33,34]:



where  $A^{x-}$  is the analyte ion with  $x$  charge and  $E^{y-}$  is the eluent ion with  $y$  charge. The subscript  $m$  means in the mobile phase whereas subscript  $r$  means the ion is associated with the resin (stationary phase). The retention factor of  $A^{x-}$  can be expressed as:

$$\log k_A = \frac{1}{y} \log(K_{A,E}) + \frac{x}{y} \log\left(\frac{Q}{y}\right) + \log\left(\frac{w_r}{V_m}\right) - \frac{x}{y} \log[E_m^{y-}] \quad (2.9)$$

where  $K_{A,E}$  is the ion-exchange selectivity constant of the analyte ion over the eluent ion;  $Q$  is the effective column capacity;  $w_r$  is the weight of resin (stationary phase); and  $V_m$  is the dead volume of the column. For a given column, **Eq. 2.9** can be simplified as:

$$\log k_A = \text{const} - \frac{x}{y} \log[E_m^{y-}] \quad (2.10)$$

The fundamental difference between **Eq. 2.7** and **2.10** is that in partitioning (RPLC) the log retention factor depends directly on the [eluent]. In contrast, in IC the  $\log k$  depends on the log [eluent]. Thus, the effect of eluent on retention factor

is mathematically more dramatic in RPLC than IC.

The second difference between RPLC and IC that impacts the injection-induced broadening is the retention of the strong eluent component. Like analytes, mobile phase components interact with the stationary phase and have a characteristic retention time. Generally, mobile phase components are selected such that they do not cause a detector response. Hence, no peak is observed at the retention time of the mobile phase component, but baseline disturbances known as *system peaks* may be observed [35-37]. The nearer an analyte peak elutes to system peak; the more it may be distorted [38,39].

In RPLC, ACN is weakly retained and elutes near the dead time [20,22]. Early eluting peaks are close to this system peak. Thus, weakly retained analytes move down the column at near the same velocity as the injected ACN band, and thus are most affected when the sample contains high concentrations of ACN [3,19,20,22]. In contrast, strongly retained compounds move down the column slower than the ACN band, and so are soon removed from the influence of the ACN band. Thus, strongly retained peaks are not affected by the ACN injection. Alternately, if the sample contains a more strongly retained solvent (e.g., tetrahydrofuran), the analytes that elute nearest the solvent retention time exhibit the most distorted peaks [21].

In IC two sets of system peaks are observed [36,37,40]. In **Fig. 2.10**, the first set of IC system peaks appear near the void volume at 2.3 and 3.1 min. Injection of deionized water gave negative dips at these times whereas higher matrix concentrations than the eluent gave positive peaks (**Fig. 2.10a**). The peak at 2.31 min is due to water dip and excluded sample cations [35,36,40,41]. The second peak at ~3 min has been attributed to “compensating effect” of the first dip [36].

The second set of system peaks associated with the  $\text{CO}_3^{2-}/\text{HCO}_3^-$  eluent appeared as baseline disruptions centered at 18.5 min injected (**Fig. 2.10**). Injection of deionized water (black trace) gave a dip followed by a positive peak, while injection of more concentrated  $\text{CO}_3^{2-}/\text{HCO}_3^-$  resulted in a positive/negative profile. The transition in the profile of the second system peak occurred when the injection matrix was the same as the eluent composition. **Fig. 2.10b** shows that it is the concentration of  $\text{CO}_3^{2-}$  that governs the second set of system peaks (**Fig. 2.10b**). This is consistent with past simulations and experiments on system peaks arising from dibasic acid ( $\text{HB}^-$  and  $\text{B}^{2-}$ ) eluents [37].

In **Fig. 2.5**, the analyte peaks ( $\text{Br}^-$  and  $\text{NO}_3^-$ ) near the second system peak are most distorted when high  $\text{CO}_3^{2-}/\text{HCO}_3^-$  matrix is injected [35]. Weakly retained ions such as  $\text{F}^-$  and strongly retained ions such as  $\text{SO}_4^{2-}$  ( $t_R \sim 30$  min, not shown in figure) were not affected. This behavior is analogous to that observed in RPLC

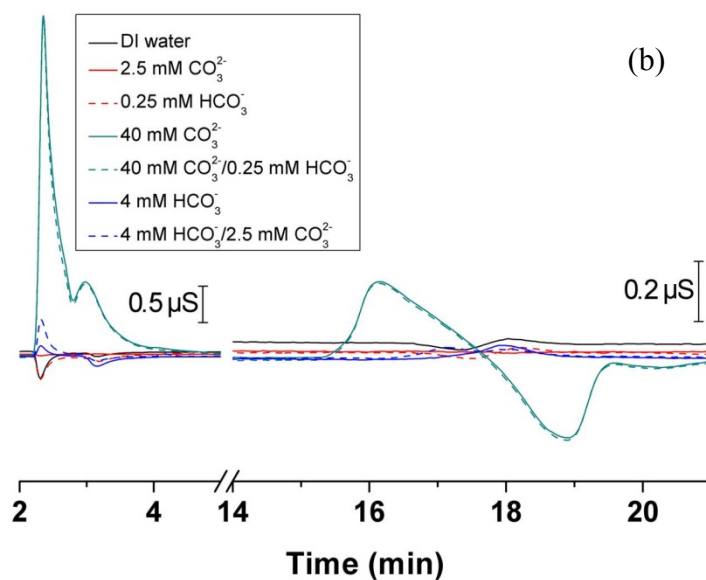
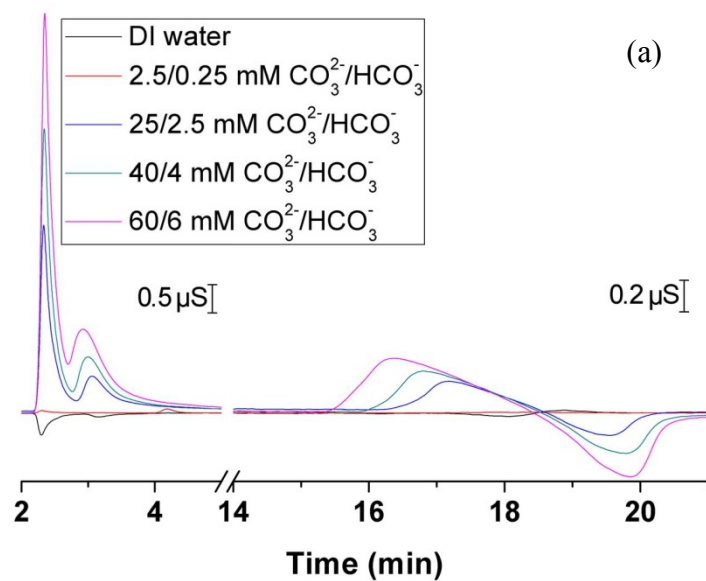


**Figure 2.10** Injection system peaks under different injection matrix concentration conditions. Conditions are the same as in **Fig. 2.5**.

when a strongly retained solvent such as tetrahydrofuran is injected [21].

The local retention factors analyte ions inside the column depends on the surrounding eluent composition (**Eq. 2.8**). Upon injection of high matrix concentration, the  $\text{CO}_3^{2-}/\text{HCO}_3^-$  which surrounds the analyte ions is different from that in the eluent. Since  $\text{CO}_3^{2-}$  is strongly retained by the column, the early eluted analyte ions ( $\text{F}^-$  and  $\text{Cl}^-$ ) quickly migrate out of the injection band and so are less affected. Analyte ions whose retention is similar ( $\text{Br}^-$  and  $\text{NO}_3^-$ ) to the second system peak remain in the vicinity of the high  $\text{CO}_3^{2-}/\text{HCO}_3^-$  band for a greater portion of the column length, and so are highly affected by the variance of local eluent composition. The late eluting  $\text{SO}_4^{2-}$  moves much slower than the second system peak and so co-elutes with the matrix for only a short portion of the column, and so is less affected.

Recent studies [42] have shown that mass overload of analyte on modern ion chromatography columns obeys a competitive Langmuir isotherm behavior, in which both analytes and strongly adsorbed mobile phase components compete for sorption sites [39,43]. For Langmuir isotherms, the competitive situation is described by:

$$\frac{q_k}{q_s} = \frac{b_k C_k}{1 + \sum_{k=1}^n b_k C_k} \quad (2.11)$$

where  $q_k$  is the amount of the analyte or mobile phase component in equilibrium

with the stationary phase,  $q_s$  is the capacity of the given compound.  $b_k$  is the Langmuir coefficient for the  $k^{\text{th}}$  component, and the denominator sums all species sorbing onto the stationary phase [39,43]. Both tailing and fronting of overloaded analyte peaks were observed. Fronting was observed when the eluent ion (e.g.,  $\text{CO}_3^{2-}$ ) was more strongly retained than the analyte peak (e.g.,  $\text{Br}^-$ ). Past theoretical [44] and experimental [13] studies have shown complex interactions between analyte peaks and system peaks due to a strongly adsorbed eluent component. Hence, it is believed that the peak fronting observed in this case is due to competitive adsorption behavior.

## 2.6 Conclusions

Most HPLC separations are performed in the reversed phase mode. Thus, many of the rules of thumb in HPLC come from RPLC behavior. In RPLC injection of a strong solvent such as acetonitrile results in distortion (peak fronting) of the early eluting peaks. Thus, chromatographers are advised to inject samples in the mobile phase or weaker, and are trained to monitor the early eluting peaks for evidence of injection solvent induced band broadening.

This chapter shows that such rules are inappropriate for ion chromatography. Rather than distorting the early eluting peaks, injection of sample in a high

carbonate matrix concentration most impacts the peaks eluting close to the  $\text{CO}_3^{2-}$  system peak (i.e.,  $\text{NO}_3^-$  and  $\text{Br}^-$ ). Also, IC is much more tolerant of the matrix concentration injected. This chapter proves its good tolerance by *sensitivity* analysis which was previously used in evaluating the response of RPLC column to injection solvent mismatch [9]. Thus use of the rule to inject no stronger than the eluent concentration results in unnecessary sample dilution in IC.

In conclusion, it is important to consider the specific chromatographic mode being used to properly evaluate the potential and nature of injection solvent induced band broadening.

## 2.7 References

- [1] F. Gritti, G. Guiochon, J. Chromatogr. A 1228 (2012) 2.
- [2] C.A. Lucy, M.F. Wahab, LC-GC North America 31 (2013) 38.
- [3] J.W. Dolan, LC-GC North America 23 (2005) 738.
- [4] F. Gritti, C.A. Sanchez, T. Farkas, G. Guiochon, J. Chromatogr. A 1217 (2010) 3000.
- [5] N. Wu, A.C. Bradley, C.J. Welch, L. Zhang, J. Sep. Sci. 35 (2012) 2018.
- [6] F. Gritti, G. Guiochon, J. Chromatogr. A 1218 (2011) 4632.
- [7] B.L. Karger, M. Martin, G. Guiochon, Anal. Chem. 46 (1974) 1640.

- [8] D. Vukmanic, M. Chiba, *J. Chromatogr. A* 483 (1989) 189.
- [9] B.J. VanMiddlesworth, J.G. Dorsey, *J. Chromatogr. A* 1236 (2012) 77.
- [10] C.B. Castells, R.C. Castells, *J. Chromatogr. A* 805 (1998) 55.
- [11] S. Keunchkarian, M. Reta, L. Romero, C. Castells, *J. Chromatogr. A* 1119 (2006) 20.
- [12] H.J. Catchpoole, R. Andrew Shalliker, G.R. Dennis, G. Guiochon, *J. Chromatogr. A* 1117 (2006) 137.
- [13] S. Golshan-Shirazi, G. Guiochon, *J. Chromatogr.* 461 (1989) 19.
- [14] T. Zhou, C.A. Lucy, *J. Chromatogr. A* 1187 (2008) 87.
- [15] G. Rousseaux, A. De Wit, M. Martin, *J. Chromatogr. A* 1149 (2007) 254.
- [16] G. Rousseaux, M. Martin, A. De Wit, *J. Chromatogr. A* 1218 (2011) 8353.
- [17] N.M. Vieno, T. Tuhkanen, L. Kronberg, *J. Chromatogr. A* 1134 (2006) 101.
- [18] G. van Vyncht, A. Janosi, G. Bordin, B. Toussaint, G. Maghuin-Rogister, E. De Pauw, A.R. Rodriguez, *J. Chromatogr. A* 952 (2002) 121.
- [19] P.W. Wrezel, I. Chion, R. Pakula, *LC-GC North America* 23 (2005) 682.
- [20] E. Loeser, S. Babiak, P. Drumm, *J. Chromatogr. A* 1216 (2009) 3409.
- [21] E. Loeser, P. Drumm, *J. Sep. Sci.* 29 (2006) 2847.
- [22] E.S. Kozlowski, R.A. Dalterio, *J. Sep. Sci.* 30 (2007) 2286.

- [23] K. Tian, P.K. Dasgupta, T.A. Anderson, *Anal. Chem.* 75 (2003) 701.
- [24] V. Ruiz-Calero, L. Puignou, M.T. Galceran, M. Diez, *J. Chromatogr. A* 775 (1997) 91.
- [25] X.-H. Chen, M.-Q. Cai, M.-C. Jin, *Chromatographia* 70 (2009) 1201.
- [26] P.R. Haddad, P. Doble, M. Macka, *J. Chromatogr. A* 856 (1999) 145.
- [27] C.F. Poole, *The Essence of Chromatography*, Elsevier, Amsterdam, 2003.
- [28] M.S. Jeansonne, J.P. Foley, *J. Chromatogr.* 461 (1989) 149.
- [29] D.H. Marchand, L.R. Snyder, J.W. Dolan, *J. Chromatogr. A* 1191 (2008) 2.
- [30] B. Alsehli, J.W. Dolan, *LC-GC North America* 30 (2012) 898.
- [31] M.A. Quarry, R.L. Grob, L.R. Snyder, *Anal. Chem.* 58 (1986) 907.
- [32] L.R. Snyder, J.W. Dolan, J.R. Gant, *J. Chromatogr.* 165 (1979) 3.
- [33] J.E. Madden, P.R. Haddad, *J. Chromatogr. A* 829 (1998) 65.
- [34] C. Liang, C.A. Lucy, *J. Chromatogr. A* 1217 (2010) 8154.
- [35] H. Sato, *Anal. Chem.* 62 (1990) 1567.
- [36] T. Okada, T. Kuwamoto, *Anal. Chem.* 56 (1984) 2073.
- [37] H. Watanabe, H. Sato, *Anal. Sci.* 11 (1995) 923.
- [38] T. Fornstedt, D. Westerlund, *J. Chromatogr.* 648 (1993) 315.
- [39] T. Fornstedt, G. Guiochon, *Anal. Chem.* 66 (1994) 2116.

- [40] Y. Michigami, Y. Yamamoto, *J. Chromatogr.* 623 (1992) 148.
- [41] F.G.P. Mullins, *Analyst* 112 (1987) 665.
- [42] M.F. Wahab, J.K. Anderson, M. Abdelrady, C.A. Lucy, *Anal. Chem.* 86 (2014) 559.
- [43] G. Guiochon, A. Felinger, D.G. Shirazi, A.M. Katti, *Fundamentals of Preparative and Nonlinear Chromatography*, Elsevier Academic Press, Amsterdam, 2006.
- [44] S. Golshan-Shirazi, G. Guiochon, *J. Chromatogr.* 461 (1989) 1.

## **CHAPTER THREE: Amide Carbon HILIC Stationary**

### **Phase**

#### **3.1 Introduction**

Porous graphitic carbon (PGC) particles for liquid chromatography were first introduced by Knox et al. in 1986 [1]. Unlike silica stationary phases, PGC shows wider pH stability range of 0 ~ 12. PGC also possesses good mechanical strength and high temperature tolerance (up to 200 °C) [2,3]. One commercially available PGC phase for HPLC is Hypercarb<sup>TM</sup> marketed by Thermo Scientific. The particles are highly porous with 250 Å pores and a surface area of 120 m<sup>2</sup>/g [4]. They are available in 3, 5, and 7 µm particle sizes). In this chapter, we report a new amide-modified porous graphitic carbon stationary phase for hydrophilic interaction liquid chromatography (HILIC) and attenuated reversed phase liquid chromatography (RPLC).

PGC columns show reversed phase behavior as bare carbon is very hydrophobic [3,5,6]. Indeed, a 20 ~ 40% higher ratio of organic modifier is required with PGC to give comparable retention to a conventional C<sub>18</sub> RPLC phase [6]. The high stability of PGC also makes it useful for some applications such as high temperature LC [7]. However, the strong retention on PGC can result in peak tailing and irreversible adsorption in RPLC separations of some analytes

[8]. Thus, one of the objectives of the amide modification of PGC described in this chapter is to reduce the hydrophobicity of the PGC surface to improve RPLC separations.

Surprisingly, PGC retains some polar analytes such as arsenic compounds [9], nucleotides, nucleotide sugars [8] and lipid-linked oligosaccharides [10]. The mechanism of retention is termed *Polar Retention Effect on Graphite* (PREG) [3,11,12]. The mechanism of PREG is unclear, but has been explained as an induced polarization on the graphite surface. Thus, in PREG the orientation of the analyte on the surface is very important [3,5]. As the retention of polar compounds on PGC is suppressed under organic rich aqueous phase [13], unmodified PGC is not a suitable stationary phase for hydrophilic interaction liquid chromatography (HILIC). Amide-functionalized silica is a popular HILIC stationary phase type. It is hoped that introduction of amide functionality to the PGC surface will yield a more effective PGC HILIC phase.

As discussed in Chapter 1, HILIC has three main advantages for liquid chromatographic separations: retention of polar compounds such as pharmaceuticals; good water compatibility; and compatibility with mass spectrometry [13-15]. In HILIC separations, the stationary phase is polar and hydrophilic, while the mobile phase contains a high %ACN within an aqueous

solution. A stagnant water-rich layer on the surface of the stationary phase is responsible for the retention of polar analytes [16]. Thus classically the major retention mechanism of HILIC is partitioning. However, hydrogen bonding, adsorption and ion exchange also play a role in the retention [17,18]. Based on the PGC properties discussed above, the hydrophobic PGC must be modified to become hydrophilic to be an effective HILIC phase.

The inertness and stability of PGC makes it very attractive for chromatography. However, the inertness is also a drawback. It is very difficult to do surface modification on PGC. Knox et al. coated PGC with adsorbed polyethyleneimine [19]. Strong oxidizing agents such as nitric acid [20] and potassium permanganate [2] form different types of oxides (e.g. hydroxyls and carbonyl groups) on the PGC surface, [21]. A popular method for PGC surface modification is to use diazonium chemistry [22-29]. On-column electroreduction of diazonium ion has been performed but requires custom apparatus and commercial diazonium solutions [22,23]. Chemical reduction of diazonium using  $\text{NaBH}_4$  [24-26] or  $\text{H}_3\text{PO}_2$  [27-29] has been reported as fast and easy. But  $\text{H}_3\text{PO}_2$  reduction requires pure diazonium solutions. Other radical PGC modifications such as peroxide [30] and alkyl halides [31] have long preparation times and require heating. In this chapter, I used the  $\text{NaBH}_4$  method because it is a one-pot

synthesis with *in situ* generated diazonium ion instead of pure diazonium solution [28].

In this chapter, 4-aminoacetanilide is used as the diazonium precursor. In the presence of nitrous acid, the precursor is converted *in situ* into the diazonium ion which is pre-adsorbed on the PGC surface. Then addition of NaBH<sub>4</sub> reduces the diazonium to form a radical. This radical scavenges an electron from the PGC particle to form a covalent bond. The acetanilide moieties introduced to the PGC make the surface hydrophilic, allowing the particles to disperse well in water. The new stationary phase was characterized and chromatographically investigated. The Amide-PGC phase showed a unique HILIC retention behavior that is intermediate between that of amide-silica and a bare PGC stationary phase.

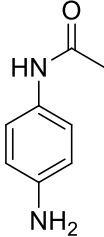
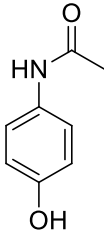
## **3.2 Experimental**

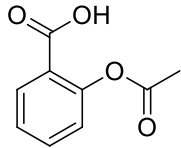
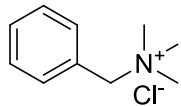
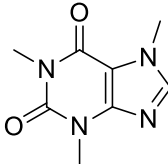
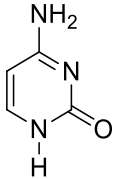
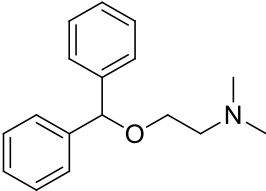
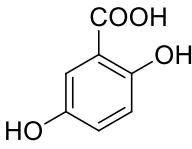
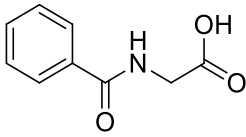
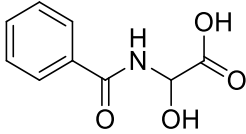
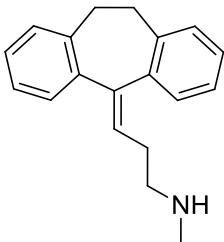
### **3.2.1 Chemicals**

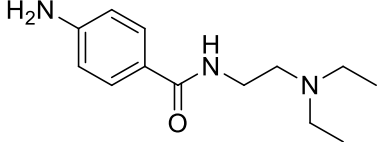
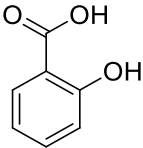
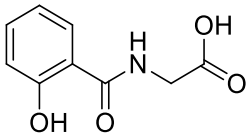
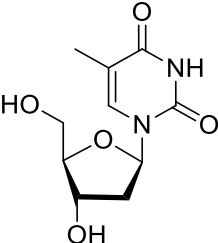
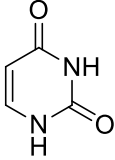
All water used was purified to  $\geq 17.8$  M $\Omega$ -cm using a Barnstead E-pure ultrapure water purification system (Dubuque, IA, USA). 4-Aminoacetanilide, sodium nitrite, sodium borohydride, diphenhydramine, acetaminophen, procainamide, nortriptyline, caffeine, acetylsalicylic acid, gentisic acid, hippuric acid, salicylic acid,  $\alpha$ -hydroxyhippuric acid, uracil, cytosine and thymidine were

from Sigma-Aldrich (99% grade or better, St. Louis, MO, USA). Salicylic acid, acetonitrile (ACN, Optima grade) and porous graphitic carbon (PGC, 5  $\mu\text{m}$ , lot no. PGC593) were from Thermo Fisher Scientific (Fair Lawn, NJ, USA). Benzyltrimethylammonium chloride (BTMA) was from Acros Organics (part of Thermo Fisher Scientific). Sodium hydroxide was from Anachemia Canada Inc. (Montréal, QC, Canada). Anhydrous ethyl alcohol was from Commercial Alcohols (Brampton, ON, Canada). Hydrochloric acid was from Caledon Laboratory Chemicals (Georgetown, ON, Canada). Ammonium acetate was from Alfa Aesar (Wardtown, MA, USA).

**Table 3.1** Structures of compounds used in **Chapter 3**.

Compound Name	Structure
4-aminoacetanilide	
acetaminophen	

acetylsalicylic acid	
benzyltrimethylammonium (BTMA)	
caffeine	
cytosine	
diphenhydramine	
gentisic acid	
hippuric acid	
α-hydroxyhippuric acid	
nortriptyline	

procainamide	
salicylic acid	
salicyluric acid	
thymidine	
uracil	

### 3.2.2 Apparatus

The HPLC system consisted of: a Prostar 210 pump (Varian, part of Agilent Technologies, Santa Clara, CA, USA); a Varian Prostar 410 autosampler equipped with a 40  $\mu$ L injection loop; and a Knauer UV detector 2500 (Berlin, Germany) set at 254 nm. Data was collected at 5 Hz using Star Chromatography Workstation Version 6.20 software running on an A-Tech Pentium III computer (Edmonton, AB, Canada). All separations were performed at ambient temperature.

X-ray photoelectron spectroscopy (XPS) analysis was performed on an AXIS 165 spectrometer (Kratos Analytical, Manchester, UK) in the Alberta Centre for Surface Engineering and Science (ACSES). The data was analyzed by CasaXPS 2.3.16 PR 1.6.

Elemental analysis (EA) analysis was performed on a Carlo Erba CHNS-O EA 1108 Elemental Analyzer (CE Elantech, Inc. Lakewood, NJ, USA).

### **3.2.3 Synthesis of Amide-PGC Stationary Phase**

The synthetic route for the amide carbon phase (**Fig. 3.1**) was inspired by the prior diazonium synthesis of the carboxylate carbon phase [26]. First, 1.8765 g (12.5 mmol) of 4-aminoacetanilide was dissolved in 100 mL of deionized water and added into a 1 L beaker. Next, 0.5988 g (49.9 mmol) of PGC powder was added into the 1 L beaker. PGC is highly hydrophobic and floats on top of water. Ten minutes of magnetic stirring partially disperses the PGC particles into small lumps, and then the 1 L beaker was placed in an ice bath with stirring. After 10 min, 0.858 g (12.4 mmol) of  $\text{NaNO}_2$  in 15 mL deionized water was added dropwise into the 1 L beaker. The solution was allowed to stir for 5 min, and then 3.75 mL of 36.5 % HCl (37.5 mmol) was added dropwise over 5 min. The mixture was stirred for 30 min to allow adequate formation of the diazonium salt and its

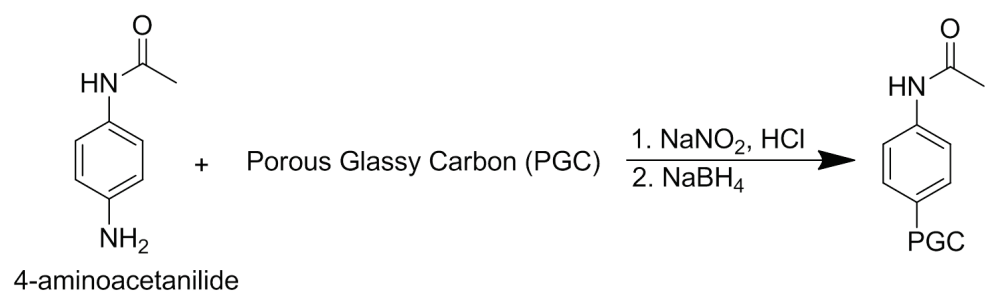


**Figure 3.1** Synthetic route for Amide-PGC stationary phase.

adsorption on the surface [26]. Next, 1.216 g (31.3 mmol) of NaBH<sub>4</sub> in 30 mL deionized water was added drop wise using a dropping funnel (about 1 drop per 2 s) under vigorous stirring. **Caution:** This step was very vigorous because hydrogen and nitrogen gas were produced, giving lots of bubbles. After completion of the NaBH<sub>4</sub> addition, the 1 L beaker was removed from the ice bath, and allowed to sit at room temperature for 30 min.

The suspension was filtered using 0.22 μm nylon membrane filters from Millipore (Bedford, MA, USA). Residues were also transferred to the filter using deionized water washes of the beaker. The modified particles on the filter were then washed thoroughly with deionized water, 1% NaOH, deionized water and anhydrous ethyl alcohol.

A previous study by Wahab et al. showed that the surface loading via diazonium chemistry increased after repeating the same reaction [24,26]. The synthetic procedure was then repeated a second time to yield a higher surface coverage [24,26].

After the second modification and washing, the particles were dispersed in 1 L of deionized water with sonication, and then allowed to settle for 24 h. The thin film of floating un-modified PGC particles was removed by sucking the solution surface via tubing which is connected to reduced pressure (**Fig. 3.2**). The

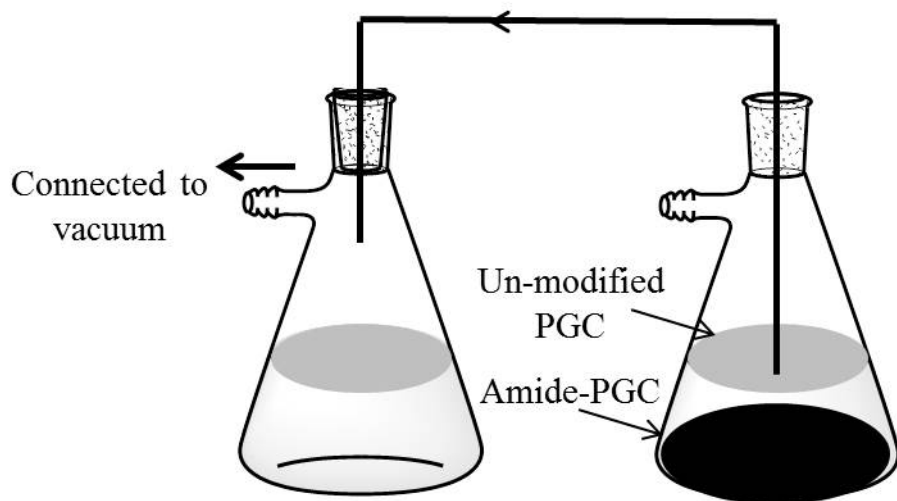


**Figure 3.2** Apparatus for removing un-modified PGC particles.

remained particles were filtered using the 0.22  $\mu\text{m}$  nylon membrane filter and vacuum dried overnight at room temperature. In three batches of synthesis, an average 60% yield was achieved.

### 3.2.4 Column Packing and Treatment

The packing procedure was adapted from Wahab et al. [32]. Unless stated otherwise, all of the packing parts were from Dionex (Thermo Scientific, Sunnyvale, CA, USA). The packing system (**Fig. 3.3**) consisted of a Haskel pump (DSF-122-87153, Burbank, CA, USA) attached to a nitrogen gas cylinder (Praxair Inc., Edmonton, AB, Canada). A 40 mL stainless cylindrical slurry reservoir from Lab Alliance (1.4 cm i.d., State College, PA, USA) was connected the pump to a stainless steel connecting column (5 cm  $\times$  0.4 cm i.d.). The outlet end of connecting column was attached to a polyether ether ketone column (PEEK, 15 cm  $\times$  3 mm i.d.) which is to be packed. The end of the PEEK column was capped by a PEEK screw cap with Zitex membrane (0.2  $\mu\text{m}$ , G-108, for outlet frit only) and 2  $\mu\text{m}$  Ti and stainless steel frit. The modified PGC (1.7 g, as per **Section 3.2.3**) was well suspended in 35 mL deionized water using 5 min of sonication in a 75HT AQUASONIC sonicator (VWR Scientific, Radnor, PA, USA). The slurry was immediately transferred into the 40 mL packing cylindrical reservoir.

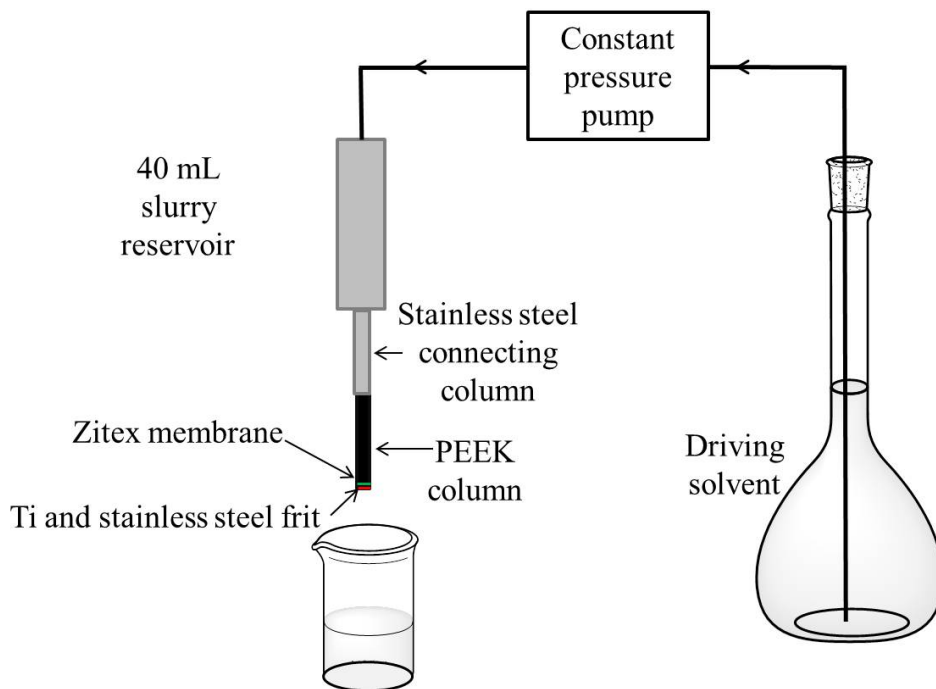


**Figure 3.3** Column packing apparatus.

Five mL of deionized water was used to ensure complete transfer of the particles into the reservoir. The column (PEEK, 15 cm × 0.3 cm i.d.) was packed under 5,000 psi constant pressure for 1.5 h using deionized water as the driving solvent. After the packing process was finished, the pump was stopped and the packing apparatus was allowed to sit until the pressure dropped to around 100 psi (about 30 min). The column was removed from the packing apparatus, both ends of the packed bed were flattened with spatula to remove the extruded portion of the bed and then capped with Zitex membranes (G-108, for outlet frit only), UHMWPE (Ultra high molecular weight polyethylene) frits and PEEK screw caps (gifts from Dionex) as soon as possible. The packed column was flushed with 70% ACN using the HPLC system in **Section 3.2.2** at 1.0 mL/min for the first hour and then 0.6 mL/min. Once the baseline at 254 nm was stable, the column was ready for separations.

### **3.2.5 Standard, Sample and Eluent Preparation**

The 25 mM ammonium acetate (pH=5.00) buffer was prepared by dissolving 0.4832 g of ammonium acetate in 240 mL deionized water. The pH was adjusted to 5.00 using 1% (diluted from 36.5% HCl), sonicated, diluted to 250 mL in a volumetric flask and filtered through a 0.22 µm nylon membrane filter.

The 20 mM ammonium acetate pH 6.80 buffer was prepared by dissolving 0.3078 g of ammonium acetate in 190 mL deionized water, pH adjusted with 1% HCl and/or 1% NaOH, sonicated, diluted to 200 mL in a volumetric flask and filtered through 0.22  $\mu\text{m}$  filters. The 10 mM and 25 mM ammonium acetate (pH 6.80) buffer solution was prepared in the same manner.

The mobile phase was prepared by mixing ACN and buffer solution according to the percentage of ACN and buffer solution type required. For instance, 90 % ACN with 20 mM ammonium acetate buffer solution (pH=6.80) was prepared by mixing 180 mL ACN and 20 mL of 20 mM ammonium acetate buffer (pH=6.80) together. Then the prepared eluent was sonicated for 5 min and vacuum degassed for another 5 min.

Stock (0.05 M) RPLC analyte solutions were prepared individually by dissolving diphenhydramine, acetaminophen and caffeine in 10 mL ACN. Procainamide and nortriptyline are dissolved in 10 mL ACN and 1 mL deionized water to 0.04 M. Analyte solutions were prepared by mixing various volumes of the respective stock analyte solutions and bringing to volume (1 mL) with ACN.

Stock (0.05 M) organic acid analytes solutions were prepared individually by dissolving hippuric acid,  $\alpha$ -hydroxyhippuric acid, salicylic acid, acetylsalicylic acid, salicyluric acid and gentisic acid in 90% ACN. Analyte solutions were

prepared by mixing various volumes of the respective stock analyte solutions and bringing to volume (1 mL) with ACN.

Uracil, cytosine, BTMA, adenine, thymidine (0.02 M of each) and adenosine (0.008 M) stock solutions were prepared by dissolving each individually in deionized water. Analyte solutions were prepared by mixing various volumes of the respective stock analyte solutions and bringing to volume (1 mL) with ACN.

### 3.3 Results and Discussion

The porous graphitic carbon (PGC) modification herein was inspired by the work of Wahab et al. [24,26]. **Figure 3.4** shows the scheme for attaching acetanilide functionality onto the porous PGC surface. In step 1, nitrous acid was generated *in situ* from sodium nitrite and hydrochloric acid. The formed weak nitrous acid can be further protonated. Further, it loses one water molecule to form the nitrosonium ion ( $^+N\equiv O$ ). The lone pair on the nitrogen of the amine group of 4-aminoacetanilide nucleophilically attacks the positively charged nitrosonium ion and further form the diazonium ion [33]. The freshly formed diazonium ion adsorbed onto the PGC surface. This pre-adsorption yields increased surface coverage [34-36]. In step 2, sodium borohydride was added to reduce the diazonium ion, release  $N_2$  and generate the aryl radical. The unstable radical

forms



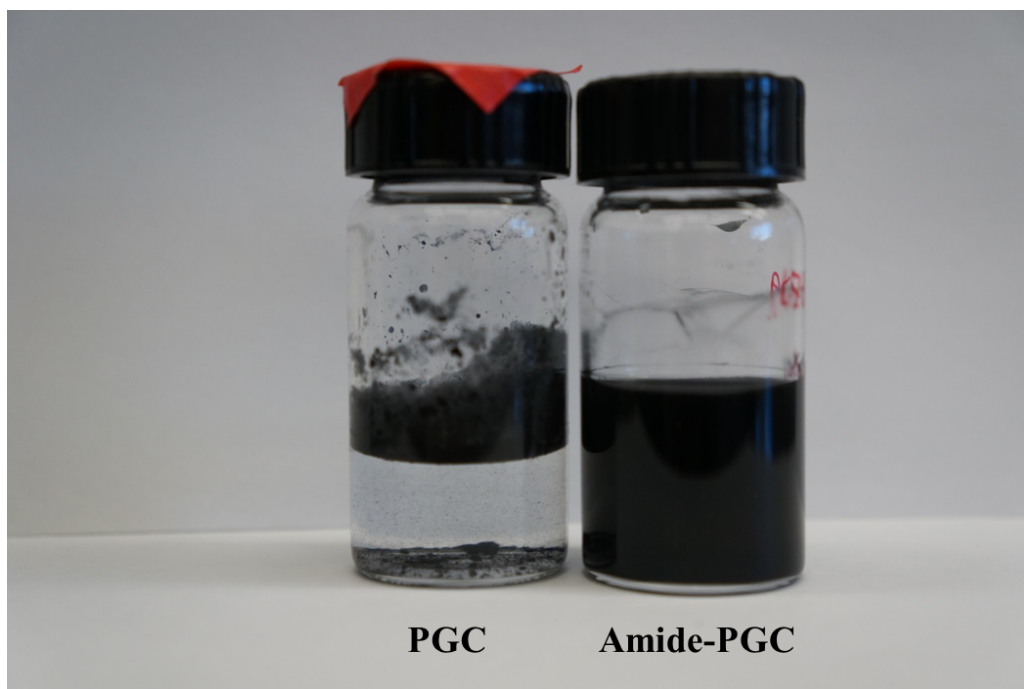


**Figure 3.5** Comparison of PGC and Amide-PGC wettability. Both vials were sonicated in deionized water for 3 min and then allowed to sit for 1 min before the photograph was taken.

in the vicinity of the PGC surface because of the diazonium ion adsorption in step 1. The arene radicals formed a covalent bond to the carbon surface [22]. Sodium borohydride does not reduce esters, amides or carboxylic acids [37], which means this reduction is very specific.

After modification, the PGC particles became much more hydrophilic than un-modified PGC particles. As shown in **Fig. 3.5** the un-modified PGC particles are highly hydrophobic, floating in an agglomerated form on the surface of deionized water, even after several months. The modification step increased the wettability of PGC significantly. Amide-PGC particles dispersed well in deionized water, indicating a hydrophilic character. The Amide-PGC particles did settle to the bottom of the vial if allowed to sit for 12 h. However they were easily re-dispersed by stirring, shaking the vial or sonication.

### **3.3.1 Surface Characterization of Amide-PGC**

**Table 3.2** shows the CHNX elemental analysis. The bare PGC contains 99.8% carbon (within 0.2% calibration error) with no detectable nitrogen. The synthesis (**Fig. 3.4**) reduced the %C to 94.82% and introduced 0.80% of nitrogen. In the synthesis of carboxylate-PGC, the bulk oxygen increased from 0.2% to 1.2% [26]. Assuming the increased oxygen and nitrogen only arises from the surface modification, one added  $-\text{COOH}$  contributes two oxygens whereas one amide

only contributes one nitrogen. Taking the mass of nitrogen and oxygen into consideration, the Amide-PGC contains  $5.7 \times 10^{-4}$  mol/g of amide while the Carboxylate-PGC only contains  $3.1 \times 10^{-4}$  mol/g carboxylic acid. Carboxylic acid is more electron withdrawing than the amide functional group. So in Carboxylate-PGC synthesis, the positively charged diazonium salt formed is less stable than the amide diazonium intermediate. Thus, the higher yield for the Amide-PGC is not unexpected.

**Table 3.2** Elemental analysis of PGC and Amide-PGC<sup>a</sup>

Analyte	Carbon	Nitrogen	Hydrogen	Total
Porous Graphitic Carbon (PGC)	99.8	0	0	99.8
Amide - PGC <sup>b</sup>	94.8	0.8	0.4 <sup>c</sup>	96.0

- Mass fractions of carbon, hydrogen, nitrogen and heteroatoms.
- After two diazonium modifications, as per **Section 3.2.3**.
- Below the low calibration standard.

X-ray photoelectron spectroscopy (XPS) provides surface specific compositional information. As shown in **Table 3.3**, the Amide-PGC surface contains 2.43% of nitrogen, which supports the presence of the amide functional group. The high resolution de-convoluted XPS spectrum (**Fig. 3.6**) of the O<sub>1s</sub> band

indicates both C-O and C=O bonding are present. In bare PGC, the edges of the graphene sheets may contain non-specific oxides such as hydroxyl, carbonyl and carboxylate groups due to oxidation by air [21,38,39]. De-convolution of the O<sub>1s</sub> peak in **Fig. 3.6** indicates that about half of the oxygen was in the C=O bond form. High resolution XPS analysis of unmodified PGC found 2.00% oxygen exclusively due to C-O bonding [26]. Therefore, the C=O observed in **Fig. 3.6** after modification can be attributed to the amide functionality. Based on **Table 3.3**, 2.31% of oxygen is bonded to the surface via C=O bond. Thus the observed N:O<sub>C=O</sub> ratio of 2.43:2.31 is close to the 1:1 N:O ratio expected for an amide.

**Table 3.3** X-Ray Photoelectron Spectroscopy of Amide-PGC

Elements	Position (eV)	Atomic%
O (1s)	531.60	4.31 <sup>a</sup>
C (1s)	284.00	93.26
N (1s)	399.60	2.43

a. The O<sub>1s</sub> % of PGC is 2.00% [26].

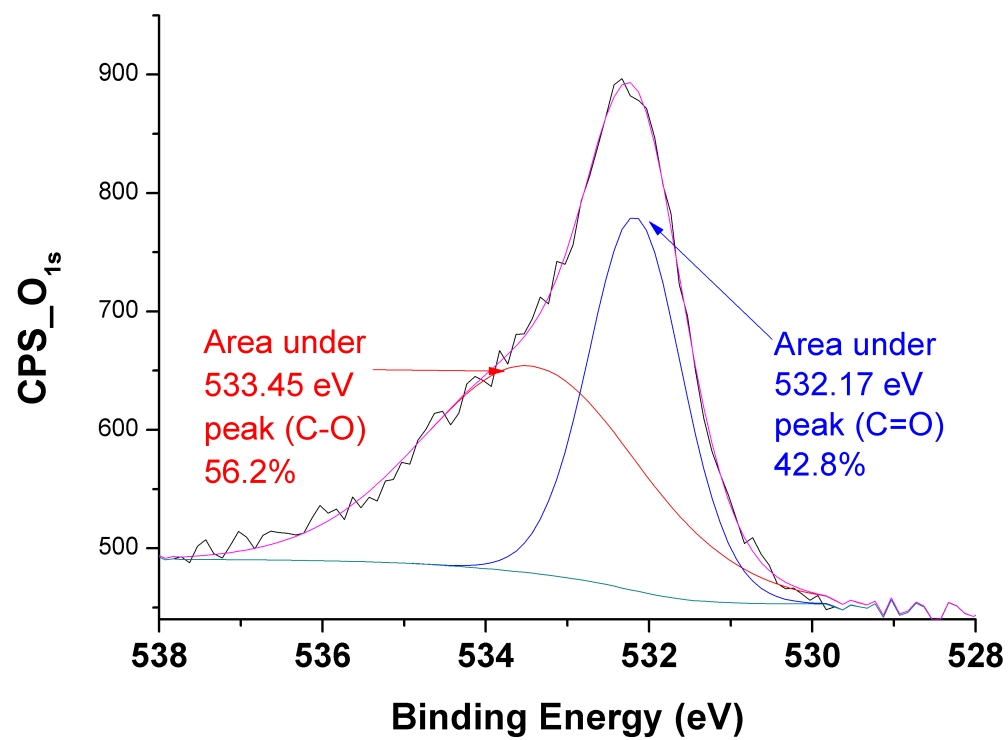
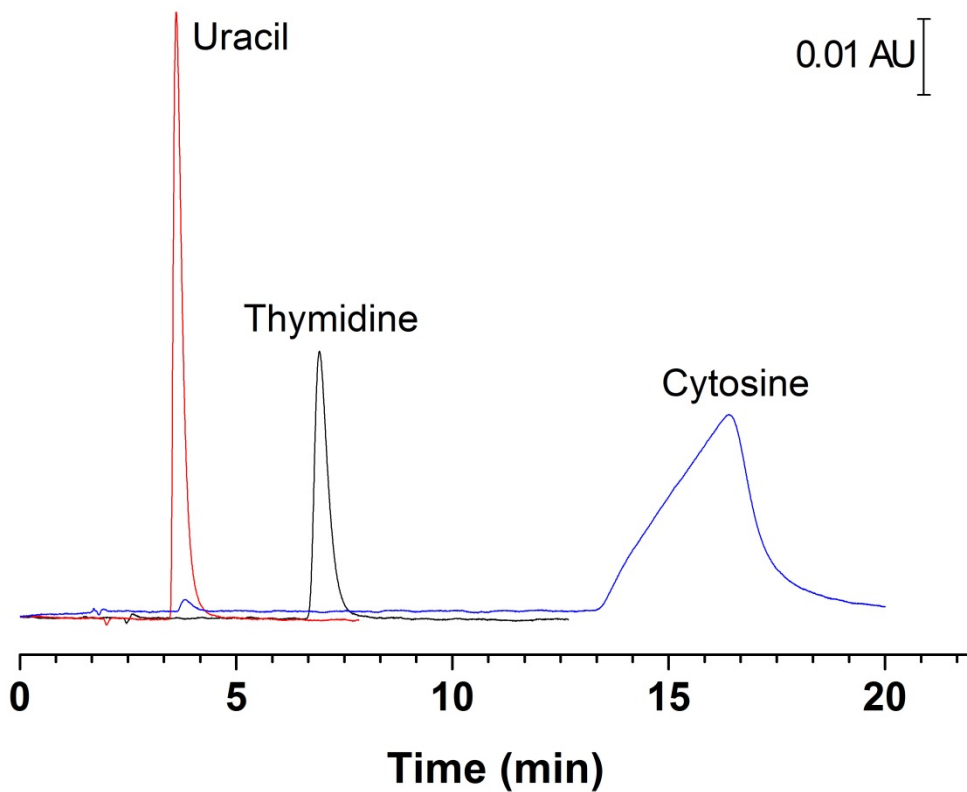


**Figure 3.6** High resolution O<sub>1s</sub> XPS spectrum of the Amide-PGC phase. The de-convolution of optimized fit was performed using CasaXPS 2.3.16 PR 1.6 software.

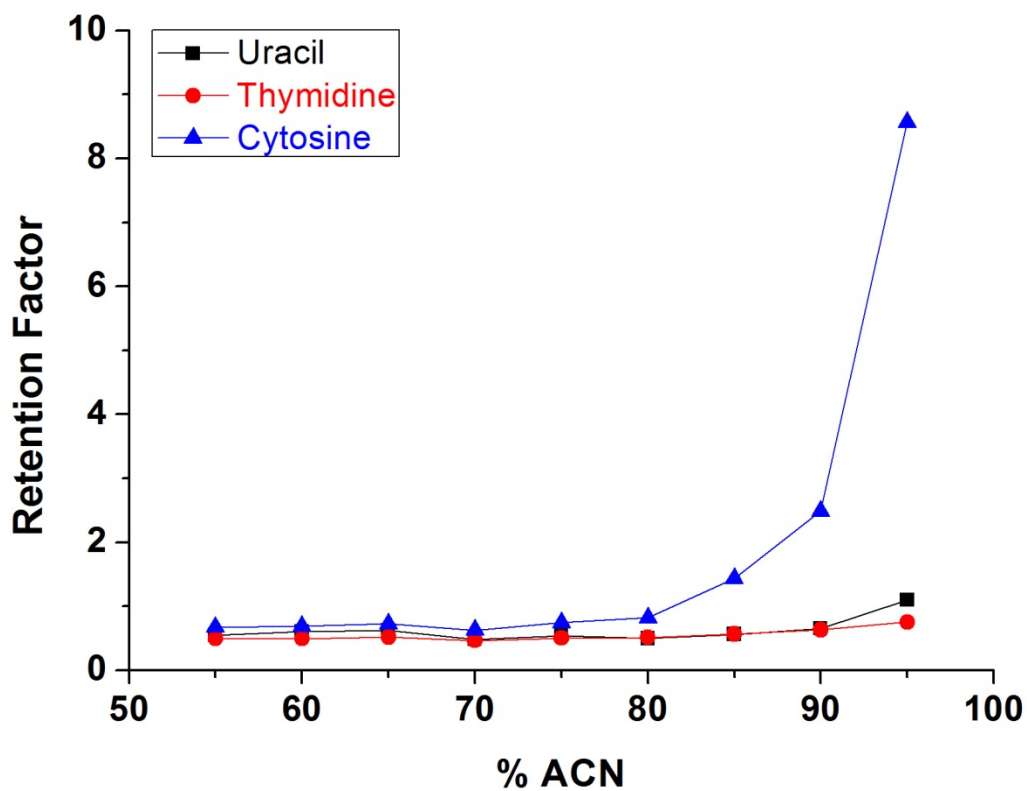
### 3.3.2 HILIC Behavior of Amide-PGC

Preliminary studies of the HILIC behavior of the Amide-PGC phase used uracil, thymidine, and cytosine. The octanol/water partition coefficients for cytosine is much smaller than that of uracil or thymidine [40,41]. Thus, the order of elution at high %ACN is consistent with HILIC behavior [17]. The relative retention at 95% ACN (**Fig. 3.7**) is also consistent with that observed on a TSKgel-Amide 80 HILIC column (uracil 7.3 min; thymidine 9.0 min; and cytosine 34.0 min) [42].

**Fig. 3.8** shows the effect of %ACN on retention on the Amide-PGC column. The retention factors for all analytes were small ( $k=0.5 \sim 0.8$ ) from 55% ACN to 80% ACN. However, as the %ACN increased from 80 to 95%, the retention factor of most hydrophilic cytosine increased greatly ( $k = 0.8$  in 80% ACN to  $k = 8.6$  in 95% ACN), whereas that of the less hydrophilic uracil and thymidine increased only slightly (uracil, 0.5 to 1.1; thymidine, 0.5 to 0.8). The upward trend in retention with %ACN in **Fig. 3.8** is also consistent with HILIC behavior [43].



**Figure 3.7** Separation of uracil, cytosine and thymidine on Amide-PGC. Conditions: Amide-PGC (15 cm  $\times$  3 mm i.d., 5  $\mu$ m); 0.5 mL/min of 95%ACN; 10 mM ammonium acetate (pH = 6.74); 20  $\mu$ L injection of 0.4-0.5 mM of uracil, thymidine and cytosine in ACN; 254 nm detection; 0.2 s data acquisition speed.

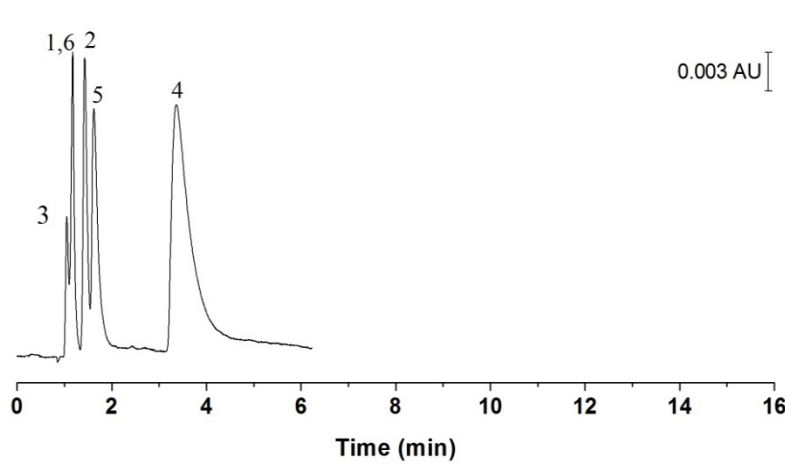


**Figure 3.8** Retention factor of uracil, cytosine and thymidine on the Amide-PGC as a function of %ACN. Experimental conditions: Amide-PGC (15 cm × 3 mm i.d., 5 μm); 0.5 mL/min; 10 mM ammonium acetate (pH = 6.74); 20 μL injection of 0.4-0.5 mM of uracil, thymidine and cytosine in ACN; 254 nm detection; 0.2 s data acquisition speed.

### 3.3.3 Organic Acids Separation

**Fig. 3.9** shows the separation of six organic acids (see **Table 3.1** for structures) on eight commercial columns and two homemade HILIC carbon columns [26,44,45]. The positions of the analyte numbers reflect their retention times on the various columns under the eluent conditions detailed in the figure caption. Analytes separated by a comma indicate co-eluting peaks. A wide variety of elution orders are observed, indicating the involvement of the column functionality in the selectivity of HILIC columns.

On the TSKgel Amide-80 HILIC column, the elution order is 1 to 6, with  $\alpha$ -hydroxyhippuric acid (peak 6) being the most retained compound. In contrast, bare PGC only shows significant retention for salicyluric acid (peak 4). The carboxylate-PGC shows a greater retention of hippuric acid (peak 5) and particularly of salicyluric acid (peak 4). On the Amide-PGC, the early eluting organic acids are better separated than on bare PGC, with salicyluric acid (peak 4) again showing strongest retention. Thus, the Amide-PGC column exhibits retention that is a combination of that of bare PGC and the amide functional group. Its selectivity is unique among the ten tested columns.

Column Chemistry	Retention Times of Analytes
Alkyl silica with -COOH terminus	1,2,3 4,6,5
Carboxylate-PGC	12,3 6 5 4
Sulfobetaine	1 2 3 4 6 5
Silica	1 3 4 2,6 5
Cross-linked diol	1 2,3 4 5,6
Polyvinyl alcohol	1 2 3 4 6 5
Bare PGC	6,3,2,1,5 4
Amide	1 2 3 4 5 6
Polyhydroxyethyl-Aspartamide	1 2 3 4 5 6
Amide-PGC	

**Figure 3.9** Comparison of the separation of six aromatic carboxylic acids on eight commercial columns and two homemade HILIC carbon columns. The positions of analyte numbers reflect the actual retention times. Co-eluted analytes are separated by comma. Experimental conditions: 0.5 – 4.5 mM of (1) salicylic acid,

(2) gentisic acid, (3) acetylsalicylic acid, (4) salicyluric acid, (5) hippuric acid and (6)  $\alpha$ -hydroxyhippuric acid (structures in **Table 3.1**); 1.0 mL/min of 85% ACN; 20 mM ammonium acetate (pH = 6.80) buffer; detection at 254 nm with 20  $\mu$ L injection. Other retention results are adapted from [45] except for carboxylate-PGC [26].

### 3.3.4 Selectivity Plot

Another way to look at the selectivity of HILIC columns is based on the behavior of model analyte pairs. **Figure 3.10** represents the selectivity properties of various types of columns, e.g. bare silica, amide, diol, etc. The retention factor ratio of cytosine/uracil is used as the x-axis. Cytosine and uracil are both highly hydrophilic and strongly retained in HILIC phases (e.g., **Fig. 3.7**). After analysis of 22 probes, Dinh et al. recommended the retention ratio of cytosine to uracil as a measure of the “hydrophilicity” of a HILIC stationary phase [17]. Cytosine is more hydrophilic than uracil. Thus, a larger retention ratio indicates a more hydrophilic phase [17,18]. The stationary phases which are plotted in the right side of the selectivity column (e.g., silica) are more hydrophilic than the phases in the left side (e.g., silica with a C<sub>18</sub> bonded phase). The retention factor ratio of benzyltrimethylammonium (BTMA)/cytosine is set as the y-axis to reflect any ion exchange properties of the HILIC columns [17,18]. BTMA is a quaternary amine, carrying a positive charge while cytosine has a similar structure but no positive charge on it. Thus, BTMA and cytosine experience similar hydrophilic interactions but BTMA will also experience cation exchange interactions [17]. Cation exchange interactions result in a BTMA/cytosine retention ratio that is greater than 1. BTMA is sufficiently strongly retained in HILIC that reductions in

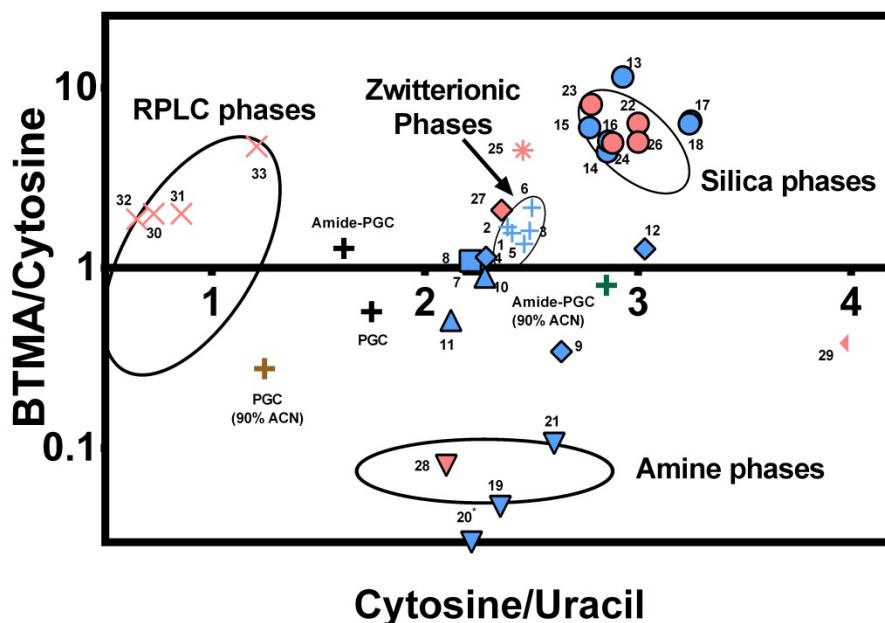


**Figure 3.10** Hydrophilicity vs. ion exchange selectivity plot. The individual columns are detailed in Table 3.4. The classes of HILIC columns included are: Bare silica (●), amide (■), diol (▲), amine and/or triazole (▼), polymer substrate and/or polymer coated silica (◆), zwitterionic (+), RPLC (×), latex coated silica (\*), proprietary polar phase (▶). Blue markers indicate data from Dinh et al. [17], pink markers from Ibrahim et al. [18], and black markers are our columns (Amide-PGC and PGC). The green marker is Amide-PGC under 90% ACN mobile phase. Experimental conditions: 25 mM ammonium acetate (pH=6.8) in 80% ACN; 0.5 mL/min; 1.6  $\mu$ L injection of 0.44 – 9 mM of BTMA, cytosine and uracil; ambient temperature; 254 nm. Pure ACN was injected to measure the baseline deflection as the dead time marker.

its retention can be used to reflected electrostatic repulsion from the stationary phase. Thus, if the HILIC column has an anion exchange nature (i.e., positive charge), this is indicated by a BTMA/cytosine retention ratio smaller than 1. The usage of retention ratios in the selectivity plot eliminates the effect from other factors such as surface area, column length which could also affect the retention time.

**Table 3.4** Characteristics of HILIC columns characterized in reference [17,18]

#	Name (Company)	Particle Diameter (Support)	Functional Group	Pore size (Å)	Surface area (m <sup>2</sup> /g)	Column Dimensions (mm × mm)
1	ZIC-HILIC (Merck)	5 µm (Silica)	Polymeric sulfoalkylbetaine  zwitterionic	200	135	100 x 4.6
2	ZIC-HILIC (Merck)	3.5 µm (Silica)	Polymeric sulfoalkylbetaine  zwitterionic	200	135	150 x 4.6
3	ZIC-HILIC (Merck)	3.5 µm (Silica)	Polymeric sulfoalkylbetaine  zwitterionic	100	180	150 x 4.6
4	ZIC-HILIC (Merck)	5 µm (Porous polymer)	Polymeric sulfoalkylbetaine  zwitterionic	N/A	N/A	50 x 4.6

5	Nucleodur HILIC (Macherey-Nagel)	5 µm (Silica)	Sulfoalkylbetaine zwitterionic	110	340	100 x 4.6
6	PC HILIC (Shiseido)	5 µm (Silica)	Phosphorylcholine zwitterionic	100	450	100 x 4.6
7	TSKgel Amide 80 (Tosoh Bioscience)	5 µm (Silica)	Amide (polymericcarbamoyl)	80	450	100 x 4.6
8	TSKgel Amide 80 (Tosoh Bioscience)	3 µm (Silica)	Amide (polymericcarbamoyl)	80	450	50 x 4.6
9	PolyHydroxyethylA (PolyLC)	5 µm (Silica)	Poly(2-hydroxy-ethyl aspartamide)	200	188	100 x 4.6
10	LiChrospher 100 Diol (Merck)	5 µm (Silica)	2,3-Dihydroxypropyl	100	350	125 x 4.0
11	Luna HILIC (Phenomenex)	5 µm (Silica)	Cross-linked diol	200	185	100 x 4.6
12	PolySulfoethyl-A (PolyLC)	5 µm (Silica)	Poly(2-sulfoethylaspartamide)	200	188	100 x 4.6
13	Chromolith Si (Merck)	Silica monolith	Underivatized	130	300	100 x 4.6
14	Atlantis HILIC Si (Waters)	5 µm (Silica)	Underivatized	100	330	100 x 4.6
15	Purospher STAR Si	5 µm	Underivatized	120	330	125 x 4.0

	(Merck)	(Silica)				
16	LiChrospher Si 100 (Merck)	5 µm (Silica)	Underivatized	100	400	125 x 4.0
17	LiChrospher Si 60 (Merck)	5 µm (Silica)	Underivatized	60	700	125 x 4.0
18	Cogent Type C Silica (Microsolv)	4 µm (Silica)	Silica hydride (“Type C” silica)	100	350	100 x 4.6
19	LiChrospher 100 NH2 (Merck)	5 µm (Silica)	3-Aminopropyl	100	350	125 x 4.0
20	Purospher STAR NH2 (Merck)	5 µm (Silica)	3-Aminopropyl	120	330	125 x 4.0
21	TSKgel NH2-100 (Tosoh Bioscience)	3 µm (Silica)	Aminoalkyl	100	450	50 x 4.6
22	Atlantis HILIC (Waters)	3 µm (Silica)	Underivatized	100	330	50 x 1.0
23	Onyx silica monolith (Phenomenex)	Silica monolith	Underivatized	130	300	100 x 4.6
24	Zorbax HILIC plus (Agilent)	3.5 µm (Silica)	Underivatized	95	160	100 x 4.6
25	Silica monolith	Silica	Silica – cationic	130	300	80 x 4.6

	coated with AS9-SC (Homemade)	monolith	nanoparticle			
26	Zorbax RRHD HILIC plus (Agilent)	1.8 µm (Silica)	Underivatized	95	160	100 x 3.0
27	Acclaim Trinity P1 (Dionex)	3 µm (Silica)	Silica-cationic nanoparticle	N/A	N/A	150 x 3.0
28	Cosmosil HILIC (Nacalai)	5 µm (Silica)	Triazole	120	300	150 x 4.6
29	Acclaim HILIC-10 (Dionex Thermo Scientific)	3 µm (Silica)	Proprietary neutral polar functionality	120	300	150 x 4.6
30	Zorbax Eclipse XDBC18 (Agilent)	5 µm (Silica)	Octadecyl	80	180	150 x 4.6
31	XBridge C18 (Waters)	5 µm (Silica BEH)	Octadecyl	130	185	150 x 4.6
32	YMC Pro C18 (YMC)	3 µm (Silica)	Octadecyl	120	340	150 x 2.0
33	Zorbax SB-aq (Agilent)	3.5 µm (Silica)	Octadecyl	80	180	150 x 2.1
34	Hypercarb™ (Thermo)	5 µm	Underivatized	250	120	100 x 4.6

	Fisher)	(Carbon)				
35	Acclaim- WCX-1  (Dionex)	5 $\mu$ m  (Silica)	Carboxylic acid	120	300	150 x 4.6

In **Fig. 3.10**, Ibrahim et al. used 75% confidence ellipses to categorize the groups of tested columns [18]. Silica phases (underivatized silica, e.g. 22-24) are in the right side of the plot, indicating strongly hydrophilic HILIC phases. The hydrophobic RPLC phases (octadecyl functional groups, e.g. 30-33) are at the left side of the plot. Strong cation exchange phases such as silica are near the top. While strong anion exchange phases such as amine phases are at the bottom.

The hydrophobicity of neutral phases such as amide (7, 8) and diol (10, 11) phases was moderate (cytosine/uracil  $\sim$  2.2). Amide stationary phases showed little ion exchange character (BTMA/cytosine  $\sim$ 1) and the diol stationary phase shows no or slightly anion exchange character.

The hydrophilicity of un-modified PGC (+ in **Fig. 3.10**) fell between neutral HILIC columns (amide, diol etc.) and traditional RPLC phases. The un-modified PGC also shows slight anion exchange character, presumably due to a small portion of oxide on the surface [21,38,39]. Surprisingly, after the surface modification, the Amide-PGC (+ in **Fig. 3.10**) still shows comparable hydrophilic

character to bare PGC. However, dispersion tests (**Fig. 3.5**) showed that PGC is highly hydrophobic (i.e., floated on the water) while Amide-PGC was well dispersed in aqueous solution. This Amide-PGC is also less hydrophilic than silica based amide columns (10, 11), consistent with the retention observed in **Fig. 3.9**.

It should be noted that the eluent conditions used in Fig. 3.9 and 3.10 were developed for silica based columns, for which 80% ACN yields strong HILIC retention. As shown in Fig. 3.8, HILIC behavior on Amide-PGC only shows an onset at 80% ACN. Thus, these non-optimized conditions may not properly reflect the behavior of PGC based HILIC phases.

To investigate the Amide-PGC phase selectivity under conditions where HILIC behavior was stronger, we measured the retention of BTMA, cytosine and uracil under 90% ACN with 20 mM ammonium acetate (pH = 6.80). Under 90% ACN, bare PGC column became more hydrophobic (**Fig. 3.10**, black and brown cross), whereas the Amide-PGC showed greater hydrophilicity (**Fig. 3.10**, black and dark green cross). Increasing the %ACN in the eluent also appears to strengthen the anion exchange ability of both PGC and Amide-PGC columns. However, it should be noted that the effect of %ACN on the selectivity plot has not previously been studied. Thus the changes noted in **Fig. 3.10** upon changing the %ACN from 80% to 90% should be viewed with some caution. Studies on the

effect of eluent conditions on the selectivity plot are currently underway in our laboratory.

### 3.3.5 Mechanism of HILIC Retention on Amide-PGC

In Alpert's original model of HILIC, retention was attributed to partitioning of the polar analyte into the adsorbed water layer as discussed in **Section 1.5.1** [43]. Under this mechanism,  $\log k$  should be related to the %water (Eq. 1.26). Helmström and Irgum [14] have shown that many "HILIC" separations are not truly partitioning in nature, but rather also have adsorptive character. Their test for which type of retention was dominant was to plot both  $\log k$  vs. %water (partitioning mechanism) and  $\log k$  vs.  $\log$  %water (adsorption). Whichever plot was more linear was viewed to be the dominant retention mechanism.

**Fig. 3.11** plots the retention data of uracil, thymidine and cytosine from **Fig. 3.8** to test whether retention is via partitioning (**Fig. 3.11a**) or adsorption (**Fig. 3.11b**). For all three analytes, the  $\log k$  vs.  $\log$  %water plot is more linear. This indicates that retention on the Amide-PGC is predominantly adsorptive in nature.

This conclusion is consistent with the selectivity observed for the organic acids on Amide-PGC (**Fig. 3.9**). A partitioning mechanism would not be expected to be able to separate isomers, where adsorption on a planar surface is well known

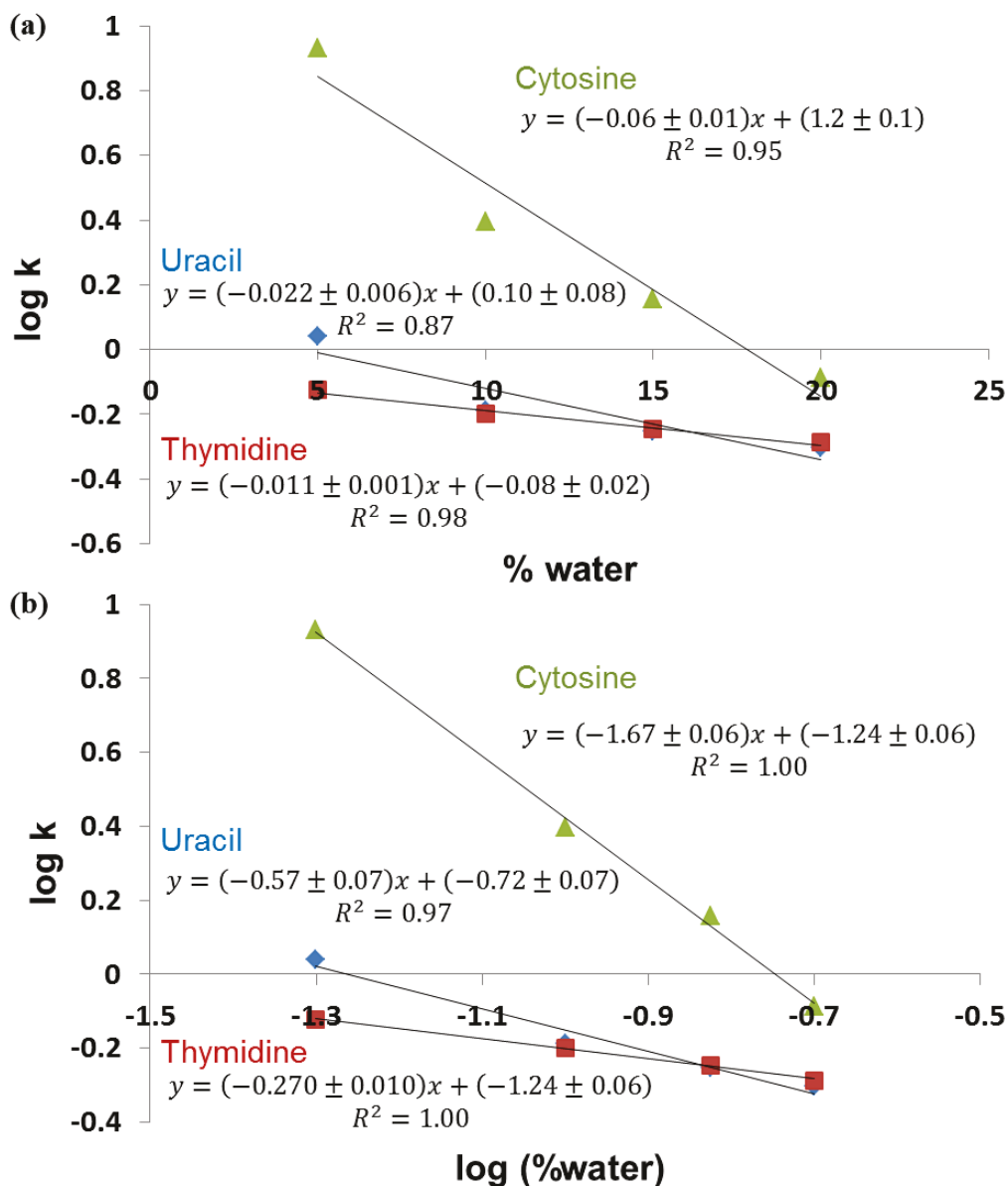


**Figure 3.11** Retention mechanism study (a) log k vs % water; (b) log k vs log %water. Experimental conditions: Amide-PGC (15 cm × 3 mm i.d., 5 μm); 0.5 mL/min; 10 mM ammonium acetate (pH = 6.74); 20 μL injection of 0.4-0.5 mM of uracil, thymidine and cytosine in ACN; 254 nm detection; 0.2 s data acquisition speed.

to yield isomeric separations [46]. In **Fig. 3.9**, salicylic acid (peak 4) is much stronger retained than  $\alpha$ -hydroxyhippuric acid (peak 6). As shown in **Table 3.1**, for salicylic acid, the hydroxyl group is in the ortho position on the benzene ring whereas for  $\alpha$ -hydroxyhippuric acid, the hydroxyl group is in the  $\alpha$  position of the side chain carboxylic acid. The ability of PGC phases to separate these isomers indicates adsorption on PGC surface is a significant contributor to retention on these columns [46].

Thus, as with many “HILIC” columns the retention on Amide-PGC is mixed mode in nature. The contributions of both the stagnant water layer and the PGC surface result in Amide-PGC offering unique selectivity.

### 3.3.6 Attenuated RPLC Separation

PGC is retentive under RPLC conditions [3,5,6]. It was believed that the introduction of the hydrophilic amide functionality to the PGC surface would reduce the hydrophobicity of the phase. **Fig. 3.12** shows the separation of five model pharmaceutical components on Amide-PGC using a low %ACN where RPLC would be the dominant retention mode. Using 63% ACN as eluent, all components eluted within 8 min. On bare PGC under the same eluent conditions over 90 min were required to elute the components with the order 1&2, 3, 5, 4

[47]. On PGC, procainamide and nortryptiline were very broad and tailing peaks, 8 min and 28 min wide respectively [47]. In contrast the amide modification changed the selectivity and allowed the separation to be completed quickly.

Decreasing the %ACN from 63% to 50% increased the retention times (red plot in **Fig. 3.12**), as would be expected for RPLC retention. It should be noted that in these preliminary experiments, the analytes were dissolved in 63% ACN. As shown in **Chapter 2**, injecting in a stronger solvent in RPLC reduces separation efficiency of early eluting peaks, but not retention time [48]. Thus the wider early peaks in the 50% ACN chromatogram are believed to be caused by injection broadening.

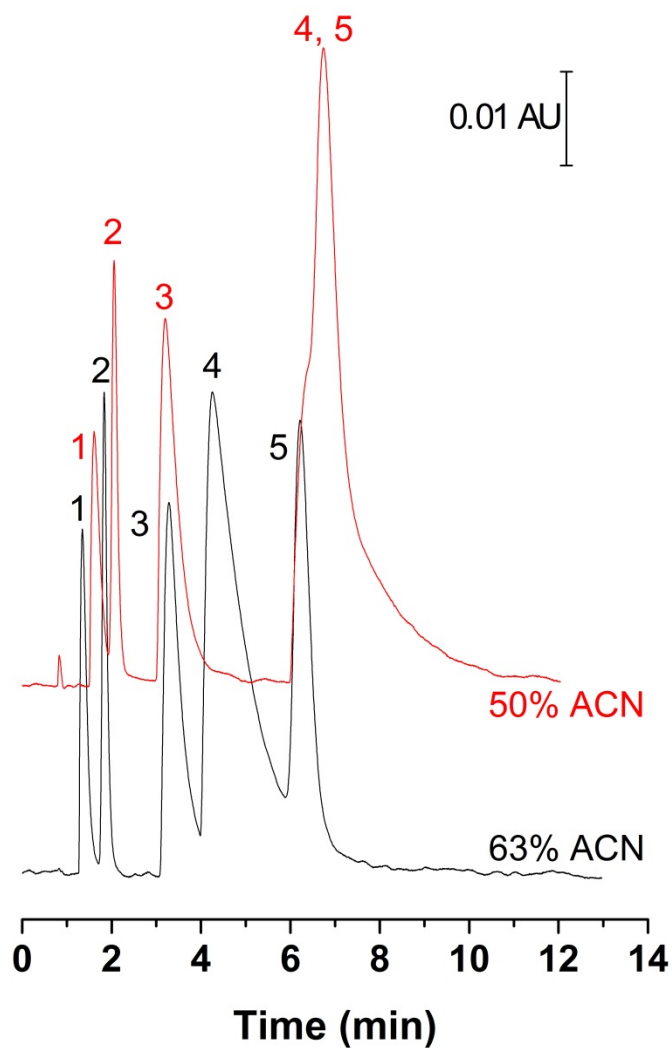


**Figure 3.12** Attenuated RPLC separations. Conditions: Amide-PGC (15 cm × 3 mm i.d., 5 μm); 0.6 mL/min; 20 mM ammonium acetate (pH = 5.00) buffer with 63% ACN (black trace) or 50% ACN (red trace); 20 μL injection of 0.2-5 mM of (1) diphenhydramine, (2) acetaminophen, (3) procainamide, (4) nortriptyline and (5) caffeine (structures shown in **Table 3.1**) in 63% ACN; 254 nm detection; 0.2 s data acquisition speed.

### 3.4 Conclusions

Porous graphitic carbon (PGC) has good pH stability (0 – 12), mechanical strength, high temperature stability and unique selectivity. This has made it a useful phase in RPLC. These features of PGC also make it attractive for HILIC separations. However, bare PGC is highly hydrophobic. An acetanilide moiety was introduced onto the PGC surface via diazonium chemistry.

The synthesized Amide-PGC phase showed increased hydrophilicity relative to bare PGC, but less hydrophilic than amide silica phases. Nonetheless Amide-PGC showed a unique selectivity compared with other commercial HILIC columns, due to the combined contributions of HILIC partitioning and adsorption onto the underlying carbon phase. The Amide-PGC phase also showed attenuated RPLC behavior relative to bare PGC

### 3.5 References

- [1] J.H. Knox, B. Kaur, G.R. Millward, *J. Chromatogr.* 352 (1986) 3.
- [2] A. Tornkvist, K.E. Markides, L. Nyholm, *Analyst* 128 (2003) 844.
- [3] C. West, C. Elfakir, M. Lafosse, *J. Chromatogr. A* 1217 (2010) 3201.
- [4] ThermoScientific, available online at <http://info.thermoscientific.com/content/PGC-physicalproperties> accessed

on June 18, 2014.

- [5] M.C. Hennion, V. Coquart, S. Guenu, C. Sella, *J. Chromatogr. A* 712 (1995) 287.
- [6] E. Forgacs, *J. Chromatogr. A* 975 (2002) 229.
- [7] D.R. Stoll, X.P. Li, X.O. Wang, P.W. Carr, S.E.G. Porter, S.C. Rutan, *J. Chromatogr. A* 1168 (2007) 3.
- [8] M. Pabst, J. Grass, R. Fischl, R. Leonard, C.S. Jin, G. Hinterkorn, N. Borth, F. Altmann, *Anal. Chem.* 82 (2010) 9782.
- [9] S. Mazan, G. Cretier, N. Gilon, J.M. Mermet, J.L. Rocca, *Anal. Chem.* 74 (2002) 1281.
- [10] C.W. Reid, J. Stupak, C.M. Szymanski, J.J. Li, *Anal. Chem.* 81 (2009) 8472.
- [11] J.H. Knox, P. Ross, in P.R. Brown, E. Grushka (Editors), *Advances in Chromatography*, Vol 37, Marcel Dekker, New York, 1997.
- [12] B.J. Bassler, R. Kaliszan, R.A. Hartwick, *J. Chromatogr.* 461 (1989) 139.
- [13] L. Pereira, *LC-GC North America* 29 (2011) 262.
- [14] P. Hemstrom, K. Irgum, *J. Sep. Sci.* 29 (2006) 1784.
- [15] B. Buszewski, S. Noga, *Anal. Bioanal. Chem.* 402 (2012) 231.
- [16] M.E.A. Ibrahim, C.A. Lucy, in B.A. Olsen, B.W. Pack (Editors),

Hydrophilic Interaction Chromatography: a Guide for Practitioners, John Wiley & Sons Inc., Hoboken, 2013.

- [17] N.P. Dinh, T. Jonsson, K. Irgum, *J. Chromatogr. A* 1218 (2011) 5880.
- [18] M.E.A. Ibrahim, Y. Liu, C.A. Lucy, *J. Chromatogr. A* 1260 (2012) 126.
- [19] J.H. Knox, Q.H. Wan, *Chromatographia* 42 (1996) 83.
- [20] N. Zhang, L.Y. Wang, H. Liu, Q.K. Cai, *Surf. Interface Anal.* 40 (2008) 1190.
- [21] H.P. Boehm, W. Heck, R. Sappok, E. Diehl, *Angew. Chem. Int. Ed.* 3 (1964) 669.
- [22] J.A. Harnisch, D.B. Gazda, J.W. Anderegg, M.D. Porter, *Anal. Chem.* 73 (2001) 3954.
- [23] J.L. Bahr, J.P. Yang, D.V. Kosynkin, M.J. Bronikowski, R.E. Smalley, J.M. Tour, *J. Am. Chem. Soc.* 123 (2001) 6536.
- [24] M.F. Wahab, C.A. Pohl, C.A. Lucy, *Analyst* 136 (2011) 3113.
- [25] S.D. Chambers, M.T. McDermott, C.A. Lucy, *Analyst* 134 (2009) 2273.
- [26] M.F. Wahab, M.E.A. Ibrahim, C.A. Lucy, *Anal. Chem.* 85 (2013) 5684.
- [27] G.G. Wildgoose, N.S. Lawrence, H.C. Leventis, L. Jiang, T.G.J. Jones, R.G. Compton, *J. Mater. Chem.* 15 (2005) 953.
- [28] M. Pandurangappa, N.S. Lawrence, R.G. Compton, *Analyst* 127 (2002)

1568.

- [29] G.G. Wildgoose, H.C. Leventis, I.J. Davies, A. Crossley, N.S. Lawrence, L. Jiang, T.G.J. Jones, R.G. Compton, *J. Mater. Chem.* 15 (2005) 2375.
- [30] D.S. Jensen, V. Gupta, R.E. Olsen, A.T. Miller, R.C. Davis, D.H. Ess, Z.H. Zhu, M.A. Vail, A.E. Dadson, M.R. Linford, *J. Chromatogr. A* 1218 (2011) 8362.
- [31] H. Ganegoda, D.S. Jensen, D. Olive, L.D. Cheng, C.U. Segre, M.R. Linford, J. Terry, *J. Appl. Phys.* 111 (2012) 6.
- [32] M.F. Wahab, C.A. Pohl, C.A. Lucy, *J. Chromatogr. A* 1270 (2012) 139.
- [33] J. Clayden, N. Greeves, S. Warren, *Organic Chemistry*, Oxford University Press, New York 2001.
- [34] A. Rieker, *Industrie Chimique Belge-Belgische Chemische Industrie* 36 (1971) 1078.
- [35] M. Delamar, R. Hitmi, J. Pinson, J.M. Saveant, *J. Am. Chem. Soc.* 114 (1992) 5883.
- [36] P. Allongue, M. Delamar, B. Desbat, O. Fagebaume, R. Hitmi, J. Pinson, J.M. Saveant, *J. Am. Chem. Soc.* 119 (1997) 201.
- [37] L. Banfi, E. Narisano, R. Riva, in *Encyclopedia of Reagents for Organic Synthesis*, John Wiley & Sons, Ltd, New York, 2001.

- [38] R.L. McCreery, *Chemical Reviews* 108 (2008) 2646.
- [39] Y.C. Liu, R.L. McCreery, *J. Am. Chem. Soc.* 117 (1995) 11254.
- [40] C. Hansch, A. Leo, D.H. Hoekman, *Exploring QSAR*, American Chemical Society, , Washington, DC, 1995.
- [41] D. Mackay, W. Shiu, K. Ma, *Illustrated Handbook of Physical-Chemical Properties and Environmental Fate for Organic Chemicals*, Lewis Publishers, Boca Raton, 1995.
- [42] P. Chen, W. Li, Q. Li, Y.H. Wang, Z.G. Li, Y.F. Ni, K. Koike, *Talanta* 85 (2011) 1634.
- [43] A.J. Alpert, *J. Chromatogr.* 499 (1990) 177.
- [44] Y. Guo, S. Gaiki, *J. Chromatogr. A* 1074 (2005) 71.
- [45] G. Yong, in *Hydrophilic Interaction Liquid Chromatography (HILIC) and Advanced Applications*, CRC Press, Boca Raton, 2011.
- [46] J.C. Reepmeyer, J.F. Brower, H.P. Ye, *J. Chromatogr. A* 1083 (2005) 42.
- [47] C.D. Iverson, C.A. Lucy, Personal communication.
- [48] B.J. VanMiddlesworth, J.G. Dorsey, *J. Chromatogr. A* 1236 (2012) 77.

## **CHAPTER FOUR: Conclusions**

### **4.1 Conclusions and Perspectives**

This thesis explored methods for improving liquid chromatographic separations. Improvements may be made by developing a new stationary phase with unique selectivity or by optimizing steps in the separation method such as injection or sample preparation.

Chapter Two studied injection matrix effects on Ion Chromatography (IC). Previously systematic investigations on injection solvent effect on peak shapes and efficiencies in Reversed Phase Liquid Chromatography have been done [1-4]. Conventionally in IC, it has recommended to dilute samples which contain high concentrations of matrix ions [5]. However, this dilution comes at the cost of increased sample preparation time and decreased analyte signal. In Chapter Two, I systematically studied the effect of injection of a suppressible carbonate/bicarbonate matrix on common inorganic anions. Peak broadening and distortions were examined using a variety of chromatographic (number of plates) and statistical (center of gravity, variance, asymmetry) metrics. The injection sensitivity parameter of VanMiddlesworth and Dorsey [2] was also applied to analysis of the IC injection broadening.

Ion chromatography was found to be much more tolerant to the injected

matrix than RPLC. This means that much less dilution of concentrated matrices are needed in IC than would be expected based on the RPLC literature. Also, the nature of the peak distortions in IC was different than in RPLC. In RPLC, peak fronting of early eluting peaks is the diagnostic of injection induced broadening. In IC, the peaks nearest to the system peak due to the strong eluent component are most affected.

Chapter Three reports a new carbon based HILIC stationary phase. 4-Acetanilide was covalently attached to hydrophobic porous graphitic carbon (PGC) surface via diazonium chemistry. The synthesized and characterized Amide-PGC stationary phase is highly hydrophilic, meeting the essential requirement for HILIC. The Amide-PGC packed column showed unique separation properties among 37 columns (35 commercial, PGC and carboxylate PGC) [6,7]. The Amide-PGC might be precursor for other new HILIC columns. Introduction of the amide functionality also attenuated the strong RPLC nature of the PGC surface.

On-going work, not included in this thesis, is focusing on injection induced broadening in Hydrophilic Interaction Liquid Chromatography (HILIC). HILIC is often referred to as an “aqueous normal phase” due to its compatibility with water containing eluents. However, HILIC is highly sensitive towards the water contents in the mobile phase [8]. Injecting samples which are dissolved in different %ACN

from that of the eluent causes peak broadening and retention time changes [9]. Greater insight into the injection induced broadening in HILIC would be achieved using a similar systematic study on injection solvent as applied in Chapter Two. Currently, a student (R. Manaloor) in our group is working on this under my supervision.

#### 4.2 References

- [1] J.W. Dolan, LC-GC North America 23 (2005) 738.
- [2] B.J. VanMiddlesworth, J.G. Dorsey, J. Chromatogr. A 1236 (2012) 77.
- [3] C.B. Castells, R.C. Castells, J. Chromatogr. A 805 (1998) 55.
- [4] S. Keunchkarian, M. Reta, L. Romero, C. Castells, J. Chromatogr. A 1119 (2006) 20.
- [5] P.R. Haddad, P. Doble, M. Macka, J. Chromatogr. A 856 (1999) 145.
- [6] M.F. Wahab, M.E.A. Ibrahim, C.A. Lucy, Anal. Chem. 85 (2013) 5684.
- [7] M.E.A. Ibrahim, Y. Liu, C.A. Lucy, J. Chromatogr. A 1260 (2012) 126.
- [8] P. Hemstrom, K. Irgum, J. Sep. Sci. 29 (2006) 1784.
- [9] T. Zhou, C.A. Lucy, J. Chromatogr. A 1187 (2008) 87.

## **BIBLIOGRAPHY**

- B. Buszewski, S. Noga, *Anal. Bioanal. Chem.* 402 (2012) 231.
- S. Golshan-Shirazi, G. Guiochon, *J. Chromatogr.* 461 (1989) 19.
- S. Golshan-Shirazi, G. Guiochon, *J. Chromatogr.* 461 (1989) 1.
- F. Gritti, G. Guiochon, *J. Chromatogr. A* 1218 (2011) 4632.
- F. Gritti, G. Guiochon, *J. Chromatogr. A* 1228 (2012) 2.
- F. Gritti, G. Guiochon, *J. Chromatogr. A* 1302 (2013) 1.
- F. Gritti, C.A. Sanchez, T. Farkas, G. Guiochon, *J. Chromatogr. A* 1217 (2010) 3000.
- G. Guiochon, A. Felinger, D.G. Shirazi, A.M. Katti, *Fundamentals of Preparative and Nonlinear Chromatography*, Elsevier Academic Press, Amsterdam, 2006.
- Y. Guo, S. Gaiki, *J. Chromatogr. A* 1074 (2005) 71.
- Z.M. Guo, Y. Jin, T. Liang, Y.F. Liu, Q. Xu, X.M. Liang, A.W. Lei, *J. Chromatogr. A* 1216 (2009) 257.
- P.R. Haddad, P. Doble, M. Macka, *J. Chromatogr. A* 856 (1999) 145.
- P.R. Haddad, P.N. Nesterenko, W. Buchberger, *J. Chromatogr. A* 1184 (2008) 456.
- T. Hanai, *HPLC, a practical guide*, Royal Society of Chemistry, Cambridge, 1999.
- C. Hansch, A. Leo, D.H. Hoekman, *Exploring QSAR*, American Chemical

Society, , Washington, DC, 1995.

J.A. Harnisch, D.B. Gazda, J.W. Anderegg, M.D. Porter, *Anal. Chem.* 73 (2001) 3954.

D.C. Harris, *Quantitative Chemical Analysis*, 7th ed., W.H. Freeman and Co., New York, 2007.

S.J. Hawkes, *J. Chem. Educ.* 60 (1983) 393.

P. Hemstrom, K. Irgum, *J. Sep. Sci.* 29 (2006) 1784.

M.C. Hennion, V. Coquart, S. Guenu, C. Sella, *J. Chromatogr. A* 712 (1995) 287.

C.G. Horvath, S.R. Lipsky, *Nature* 211 (1966) 748.

M.E.A. Ibrahim, in PhD thesis, Department of Chemistry, University of Alberta, Edmonton, Alberta, Canada, 2014.

M.E.A. Ibrahim, Y. Liu, C.A. Lucy, *J. Chromatogr. A* 1260 (2012) 126.

M.E.A. Ibrahim, C.A. Lucy, in B.A. Olsen, B.W. Pack (Editors), *Hydrophilic Interaction Chromatography: a Guide for Practitioners*, John Wiley & Sons Inc., Hoboken, 2013.

M.E.A. Ibrahim, T. Zhou, C.A. Lucy, *J. Sep. Sci.* 33 (2010) 773.

C.D. Iverson, C.A. Lucy, Personal communication.

P. Jandera, *Analytica Chimica Acta* 692 (2011) 1.

P. Jandera, T. Hajek, V. Skerikova, J. Soukup, *J. Sep. Sci.* 33 (2010) 841.

M.S. Jeansonne, J.P. Foley, *J. Chromatogr.* 461 (1989) 149.

D.S. Jensen, V. Gupta, R.E. Olsen, A.T. Miller, R.C. Davis, D.H. Ess, Z.H. Zhu, M.A. Vail, A.E. Dadson, M.R. Linford, *J. Chromatogr. A* 1218 (2011) 8362.

W. Jiang, K. Irgum, *Anal. Chem.* 71 (1999) 333.

W. Jiang, K. Irgum, *Anal. Chem.* 73 (2001) 1993.

B.L. Karger, M. Martin, G. Guiochon, *Anal. Chem.* 46 (1974) 1640.

H. Kazoka, *J. Chromatogr. A* 942 (2002) 1.

S. Keunchkarian, M. Reta, L. Romero, C. Castells, *J. Chromatogr. A* 1119 (2006) 20.

J.H. Knox, B. Kaur, G.R. Millward, *J. Chromatogr.* 352 (1986) 3.

J.H. Knox, P. Ross, in P.R. Brown, E. Grushka (Editors), *Advances in Chromatography*, Vol 37, Marcel Dekker, New York, 1997.

J.H. Knox, Q.H. Wan, *Chromatographia* 42 (1996) 83.

E.S. Kozlowski, R.A. Dalterio, *J. Sep. Sci.* 30 (2007) 2286.

M. Lafosse, B. Herbreteau, M. Dreux, L. Morinallory, *J. Chromatogr.* 472 (1989) 209.

C. Liang, C.A. Lucy, *J. Chromatogr. A* 1217 (2010) 8154.

Y.C. Liu, R.L. McCreery, *J. Am. Chem. Soc.* 117 (1995) 11254.

E. Loeser, S. Babiak, P. Drumm, *J. Chromatogr. A* 1216 (2009) 3409.

E. Loeser, P. Drumm, *J. Sep. Sci.* 29 (2006) 2847.

C.A. Lucy, M.F. Wahab, *LC-GC North America* 31 (2013) 38.

C.A. Lucy, K.K.C. Yeung, X.J. Peng, D.D.Y. Chen, *LC GC* 16 (1998) 26.

D. Mackay, W. Shiu, K. Ma, *Illustrated Handbook of Physical-Chemical Properties and Environmental Fate for Organic Chemicals*, Lewis Publishers, Boca Raton, 1995.

J.E. Madden, P.R. Haddad, *J. Chromatogr. A* 829 (1998) 65.

D.H. Marchand, L.R. Snyder, J.W. Dolan, *J. Chromatogr. A* 1191 (2008) 2.

S. Mazan, G. Cretier, N. Gilon, J.M. Mermet, J.L. Rocca, *Anal. Chem.* 74 (2002) 1281.

D.V. McCalley, *J. Chromatogr. A* 793 (1998) 31.

D.V. McCalley, *J. Chromatogr. A* 1171 (2007) 46.

D.V. McCalley, *J. Chromatogr. A* 1217 (2010) 858.

R.L. McCreery, *Chemical Reviews* 108 (2008) 2646.

Y. Michigami, Y. Yamamoto, *J. Chromatogr.* 623 (1992) 148.

J.M. Miller, *Chromatography: Concepts and Contrasts*, Wiley, Hoboken, 2005.

M.J. Motilva, A. Serra, A. Macia, *J. Chromatogr. A* 1292 (2013) 66.

F.G.P. Mullins, *Analyst* 112 (1987) 665.

U.D. Neue, *HPLC Columns: Theory, Technology, and Practice*, Wiley-VCH,

New York, 1997.

T. Okada, T. Kuwamoto, *Anal. Chem.* 56 (1984) 2073.

B.A. Olsen, *J. Chromatogr. A* 913 (2001) 113.

M. Pabst, J. Grass, R. Fischl, R. Leonard, C.S. Jin, G. Hinterkorn, N. Borth, F. Altmann, *Anal. Chem.* 82 (2010) 9782.

M. Pandurangappa, N.S. Lawrence, R.G. Compton, *Analyst* 127 (2002) 1568.

J.M. Peng, J.E. Elias, C.C. Thoreen, L.J. Licklider, S.P. Gygi, *Journal of Proteome Research* 2 (2003) 43.

L. Pereira, *LC-GC North America* 29 (2011) 262.

C.A. Pohl, J.R. Stillian, P.E. Jackson, *J. Chromatogr. A* 789 (1997) 29.

C.F. Poole, *The Essence of Chromatography*, Elsevier, Amsterdam, 2003.

M.A. Quarry, R.L. Grob, L.R. Snyder, *Anal. Chem.* 58 (1986) 907.

J.L. Rafferty, L. Zhang, J.I. Siepmann, M.R. Schure, *Anal. Chem.* 79 (2007) 6551.

J.C. Reepmeyer, J.F. Brower, H.P. Ye, *J. Chromatogr. A* 1083 (2005) 42.

C.W. Reid, J. Stupak, C.M. Szymanski, J.J. Li, *Anal. Chem.* 81 (2009) 8472.

A. Rieker, *Industrie Chimique Belge-Belgische Chemische Industrie* 36 (1971) 1078.

G. Rousseaux, A. De Wit, M. Martin, *J. Chromatogr. A* 1149 (2007) 254.

G. Rousseaux, M. Martin, A. De Wit, *J. Chromatogr. A* 1218 (2011) 8353.

V. Ruiz-Calero, L. Puignou, M.T. Galceran, M. Diez, *J. Chromatogr. A* 775 (1997)

91.

K. Sakodyns, *J. Chromatogr.* 73 (1972) 303.

H. Sato, *Anal. Chem.* 62 (1990) 1567.

M.R. Schure, R.S. Maier, D.M. Kroll, H.T. Davis, *J. Chromatogr. A* 1031 (2004)

79.

R.P.W. Scott, *Liquid Chromatography Detectors*, Elsevier, Amsterdam, 1986.

D. Singer, J. Kuhlmann, M. Muschket, R. Hoffmann, *Anal. Chem.* 82 (2010)

6409.

H. Small, T.S. Stevens, W.C. Bauman, *Anal. Chem.* 47 (1975) 1801.

L.R. Snyder, J.W. Dolan, J.R. Gant, *J. Chromatogr.* 165 (1979) 3.

L.R. Snyder, J.J. Kirkland, J.W. Dolan, *Introduction to Modern Liquid Chromatography*, 3rd ed., Wiley, Hoboken, 2010.

D.R. Stoll, X.P. Li, X.O. Wang, P.W. Carr, S.E.G. Porter, S.C. Rutan, *J. Chromatogr. A* 1168 (2007) 3.

M. Swartz, *LC-GC North America* 28 (2010) 530.

ThermoScientific, available online at

<http://info.thermoscientific.com/content/PGC-physicalproperties> accessed on June

18, 2014.

K. Tian, P.K. Dasgupta, T.A. Anderson, *Anal. Chem.* 75 (2003) 701.

A. Tornkvist, K.E. Markides, L. Nyholm, *Analyst* 128 (2003) 844.

J.C. Valette, C. Demesmay, J.L. Rocca, E. Verdon, *Chromatographia* 59 (2004) 55.

J.J. van Deemter, F.J. Zuiderweg, A. Klinkenberg, *Chemical Engineering Science* 5 (1956) 271.

G. van Vyncht, A. Janosi, G. Bordin, B. Toussaint, G. Maghuin-Rogister, E. De Pauw, A.R. Rodriguez, *J. Chromatogr. A* 952 (2002) 121.

B.J. VanMiddlesworth, J.G. Dorsey, *J. Chromatogr. A* 1236 (2012) 77.

N.M. Vieno, T. Tuhkanen, L. Kronberg, *J. Chromatogr. A* 1134 (2006) 101.

D. Vukmanic, M. Chiba, *J. Chromatogr. A* 483 (1989) 189.

M.F. Wahab, J.K. Anderson, M. Abdelrady, C.A. Lucy, *Anal. Chem.* 86 (2014) 559.

M.F. Wahab, M.E.A. Ibrahim, C.A. Lucy, *Anal. Chem.* 85 (2013) 5684.

M.F. Wahab, C.A. Pohl, C.A. Lucy, *Analyst* 136 (2011) 3113.

M.F. Wahab, C.A. Pohl, C.A. Lucy, *J. Chromatogr. A* 1270 (2012) 139.

H. Watanabe, H. Sato, *Anal. Sci.* 11 (1995) 923.

J. Weiss, *Handbook of Ion Chromatography*, Wiley-VCH, Weinheim, 2004.

C. West, C. Elfakir, M. Lafosse, *J. Chromatogr. A* 1217 (2010) 3201.

G.G. Wildgoose, N.S. Lawrence, H.C. Leventis, L. Jiang, T.G.J. Jones, R.G. Compton, *J. Mater. Chem.* 15 (2005) 953.

G.G. Wildgoose, H.C. Leventis, I.J. Davies, A. Crossley, N.S. Lawrence, L. Jiang, T.G.J. Jones, R.G. Compton, *J. Mater. Chem.* 15 (2005) 2375.

P.W. Wrezel, I. Chion, R. Pakula, *LC-GC North America* 23 (2005) 682.

G. Yong, in *Hydrophilic Interaction Liquid Chromatography (HILIC) and Advanced Applications*, CRC Press, Boca Raton, 2011.

N. Zhang, L.Y. Wang, H. Liu, Q.K. Cai, *Surf. Interface Anal.* 40 (2008) 1190.

T. Zhou, C.A. Lucy, *J. Chromatogr. A* 1187 (2008) 87.